DIELESS INCREMENTAL FORMING USING 3-AXIS CNC MILLING MACHINE FOR ALUMINIUM SHEET

SHEA CHENG KUANG

B. ENG. (HONS.) MANUFACTURING ENGINEERING

UNIVERSITI MALAYSIA PAHANG

SHEA CHENG KUANG B. ENG. (HONS.) MANUFACTRURING ENGINEERING 2016 UMP

DIELESS INCREMENTAL FORMING USING 3-AXIS CNC MILLING MACHINE FOR ALUMINIUM SHEET

SHEA CHENG KUANG

Report submitted in partial fulfilment of the requirements
for the award of the degree of
Bachelor of Engineering in Manufacturing Engineering

Faculty of Manufacturing Engineering
UNIVERSITI MALAYSIA PAHANG

JUNE 2016

UNIVERSITI MALAYSIA PAHANG

DECLARATION OF THESIS AND COPYRIGHT

Author's Full Name	:	____________________
Identification Card No	:	____________________
Title	:	____________________
		____________________
Academic Session	:	____________________

I declare that this thesis is classified as:

☐	**CONFIDENTIAL**	(Contains confidential information under the Official Secret Act 1972)
☐	**RESTRICTED**	(Contains restricted information as specified by the organization where research was done)*
☐	**OPEN ACCESS**	I agree that my thesis to be published as online open access (Full text)

I acknowledge that Universiti Malaysia Pahang reserve the right as follows:

1. The Thesis is the Property of University Malaysia Pahang.
2. The Library of University Malaysia Pahang has the right to make copies for the purpose of research only.
3. The Library has the right to make copies of the thesis for academic exchange.

Certified by:

_______________________________ _______________________________

(Author's Signature) (Supervisor's Signature)

____

Name of Supervisor

Date: ________________ Date: ________________

SUPERVISOR'S DECLARATION

I hereby declare that I have checked this thesis and in my opinion, this thesis is adequate in terms of scope and quality for the award of the degree of Bachelor of Engineering in Manufacturing.

Signature :
Name of supervisor : DR ZAMZURI BIN HAMEDON
Position : SENIOR LECTURER / DEPUTY DEAN
Date :

STUDENT'S DECLARATION

I hereby declare that the work in this thesis is my own except for quotation and summaries which have been duly acknowledged. The thesis has not been accepted for any degree and is not concurrently submitted for award of other degree.

Signature :
Name : SHEA CHENG KUANG
ID Number : FA12052
Date :

ACKNOWLEDGEMENTS

I would like to express my sincere gratitude to my final year project supervisor, Dr Zamzuri bin Hamedon for his technical guidance, innovative ideas, invaluable advices and suggestions, continuous encouragement and constant support in making this project successful. I appreciate his consistent supervision from the first day I worked on this project to these final moments. Special thanks to all the technical staff of the Faculty of Manufacturing Engineering and my team members for helping me in operating various machines and equipment. I would also like to express my gratefulness to the Faculty of Manufacturing Engineering for providing the opportunity in utilising the facilities to complete my project.

I acknowledge my sincere appreciation and gratitude to my parents for their love, dream and sacrifice throughout my life. I cannot find the appropriate words that could properly describe my appreciation for their devotion, support and faith in my ability to attain my goals.

ABSTRACT

Incremental sheet forming is a versatile sheet metal forming process where a sheet metal is formed into its final shape by a series of localized deformation without a specialised die. However, it still has many shortcomings that need to be overcome such as geometric accuracy, surface roughness, formability, forming speed, and so on. This project focus on minimising the surface roughness of aluminium sheet and improving its thickness uniformity in incremental sheet forming via optimisation of wall angle, feed rate, and step size. Besides, the effect of wall angle, feed rate, and step size to the surface roughness and thickness uniformity of aluminium sheet was investigated in this project. First of all, part design and tool path generation were done in CATIA software to form the shape of pyramid frustum. Then, the blank holder and the forming tool made of mild steel were fabricated afterwards. Through the selected design of experiments, the incremental sheet forming experiments were carried out on a 3-axis CNC milling machine. From the results, it was observed that surface roughness and thickness uniformity were inversely varied due to the formation of surface waviness. Increase in feed rate and decrease in step size will produce a lower surface roughness, while uniform thickness reduction was obtained by reducing the wall angle and step size. By using Taguchi analysis, the optimum parameters for minimum surface roughness and uniform thickness reduction of aluminium sheet were determined. Meanwhile, analysis of variance concluded that step size is the most significant parameter to both the surface roughness and thickness uniformity of aluminium sheet in incremental sheet forming. The finding of this project helps to reduce the time in optimising the surface roughness and thickness uniformity in incremental sheet forming.

ABSTRAK

Pembentukan berperingkat merupakan suatu proses pembentukan kepingan logam yang serba boleh di mana kepingan logam dibentuk kepada bentuk yang dikehendaki melalui perubahan bentuk setempat tanpa acuan yang khusus. Namum, proses tersebut masih mempunyai banyak kelemahan yang perlu diatasi seperti ketepatan geometri, kekasaran permukaan, kebolehbentukan, kelajuan membentuk, dan sebagainya. Projek ini menumpukan kepada pengurangan kekasaran permukaan kepingan aluminium dan meningkatkan keseragaman ketebalannya dalam pembentukan berperingkat melalui pengoptimumam sudut, kadar pembentukan, dan kedalaman pembentukan . Selain itu, kesan sudut, kadar pembentukan, dan kedalaman penbentukan terhadap kekasaran permukaan dan keseragaman ketebalan kepingan aluminium telah disiasati dalam projek ini. Pertama sekali, perekaan bentuk dan penjanaan perjalanan alat telah dilakukan dalam perisian CATIA untuk menghasilkan bentuk piramid frustum. Selepas itu, pemegang kepingan aluminium dan alat membentuk diperbuat daripada keluli lembut telah difabrikasikan. Melalui reka bentuk eksprimen yang terpilih, eksperimen pembentukan berperingkat telah dilakukan dengan menggunakan mesin pengilangan CNC 3 paksi. Keputusan menunjukkan kekasaran permukaan dan keseragaman ketebalan mempunyai perbezaan yang songsang disebabkan oleh pembentukan permukaan gelombang. Peningkatan kadar membentuk dan pengurangan pendalaman membentuk akan menghasilkan kekasaran permukaan yang rendah, manakala ketebalan seragam boleh didapatkan dengan mengurangkan sudut dan kedalaman membentuk. Dengan menggunakan analisis Taguchi, parameter optimum bagi kekasaran permukaan minimum dan ketebalan yang seragam telah ditentukan. Di samping itu, analisis varians menyimpulkan bahawa kedalaman membentuk merupakan parameter yang paling ketara terhadap kekasaran permukaan dan keseragaman ketebalan dalam pembentukan berperingkat. Keputusan yang diperoleh dalam projek ini akan membantu menjimatkan masa dalam pengoptimuman kekasaran permukaan dan keseragaman ketebalan kepingan aluminium dalam pembentukan berperingkat.

TABLE OF CONTENTS

LIST OF TABLES

LIST OF FIGURES

LIST OF SYMBOLS

n	Number of observations
t_0	Initial thickness of sheet
t_1	Final thickness of sheet
y	Response
α	Wall angle

LIST OF ABBREVIATIONS

A	Angle
ANOVA	Analysis of Variance
CAD	Computer-aided design
CAM	Computer-aided manufacturing
CNC	Computer Numerical Control
DF	Degree of freedom
DOE	Design of experiment
F	Ratio of variance of a source to the variance of error
FR	Feed rate
FYP	Final year project
ISF	Incremental sheet forming
MS	Mean squares
NC	Numerical control
RPM	Revolution per minute
S/N	Signal-to-noise
SPIF	Single point incremental forming
SR	Surface roughness
SS	Step size
SS	Sum of squares
TPIF	Two point incremental forming
TU	Thickness uniformity

CHAPTER 1

INTRODUCTION

1.1 Introduction

Chapter 1 will discuss about the background of the project, problem statement, objectives to be achieved in this project, as well as the project scopes.

1.2 Project Background

Incremental sheet forming (ISF) is a versatile sheet metal forming process where a sheet metal is formed into its final shape by a series of localized deformation. Generally, the process can be carried out on a CNC machine, where the perimeter of the sheet metal is clamped in a special blank holder. While the forming tool is attached to the CNC machine, it is usually round-ended with a diameter of 5 to 20mm, moving along a designed tool path and continuously indent the sheet following the contour until the final part is formed.

The ISF process has been introduced to the manufacturing industry since the last decades, although patents showed that ISF existed before the year 1993, but it did not contribute to the development of the modern ISF. Major growth of the modern ISF began in the 1990's, where the works were initiated by Iseki and his partners in Japan. The process started to vary from single point incremental forming (SPIF) to two point incremental forming (TPIF). Researches on ISF begins to expand to the western countries in this century (Emmens et al , 2010).

SPIF and TPIF are the most widely used methods of incremental sheet forming. SPIF uses a single indenter to form the sheet metal which was clamped around its edges, whereas in TPIF a male or female die is involved, together with a second indenter (Jackson & Allwood, 2009). However, SPIF is more favourable in batch production due to the elimination of die which leads to low production costs and reduced production time. SPIF also found increasing of demands in rapid prototyping. Although ISF is considered a promising and feasible technology in forming sheet metal products, many researches are still undergoing to improvise the process such as improving the formability, improving the accuracy, eliminating springback, optimizing surface roughness etc. Figure 1.1 and Figure 1.2 shows the example of SPIF and TPIF.

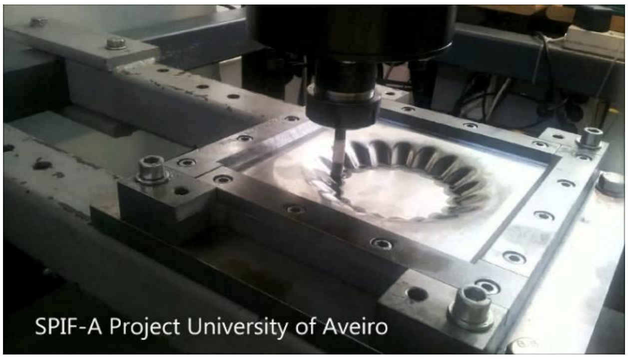

Figure 1.1: Example of Single Point Incremental Forming (SPIF)

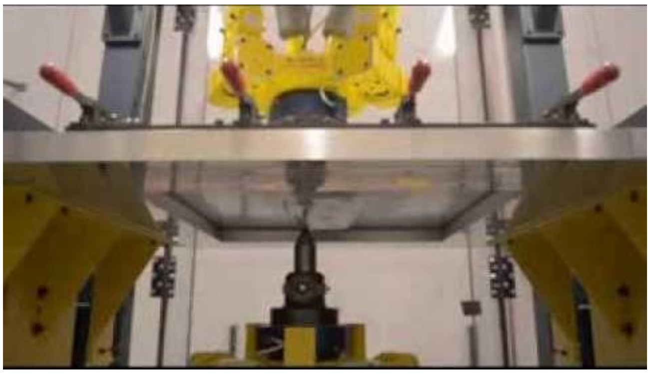

Figure 1.2: Example of Two Point Incremental Forming (TPIF)

1.3 Problem Statement

In the recent manufacturing industries, the demands for sheet metal forming is increasing rapidly. Although mass production remained dominated in the industry, batch production also facing strong competitions in terms of production cost and time. For high volume production, traditional sheet metal forming methods such as drawing and stamping are still the most effective ways to produce a large number of parts in a short period of time, it is because the high cost of initial capital investment can be shared among a large amount of products. However, for batch production, which usually involved customized products, traditional forming methods are not suitable as the highly specialized tools and dies are expensive and time consuming to produce, which will cause higher costs of products. Therefore, ISF is gaining its important role in the sheet metal forming industry, which is to reduce the set-up cost and production time.

Even though ISF is considered as a capable and promising technology in forming sheet metal parts, the process still has many shortcomings that need to be overcome. Among the drawbacks include geometric accuracy, surface roughness, formability, and forming speed. Many studies have been done in order to optimize the process by varying the process parameters, such as tool diameter, wall angle, tool path, step size, sheet thickness, spindle speed, and feed rate, but the mechanism is still not fully understood. Hence, better understanding of the mechanism of ISF is required to improve the part precision in order to achieve higher quality of products.

1.4 Objectives

The objectives to be achieved in this project are:

i. To optimise the wall angle, feed rate, and step size in the ISF process for aluminium sheet to obtain minimum surface roughness and uniform thickness reduction.
ii. To analyse the effect of wall angle, feed rate, and step size in the ISF process to the thickness reduction of aluminium sheet.
iii. To determine the influence of wall angle, feed rate, and step size in the ISF process to the surface roughness of aluminium sheet.

1.5 Project Scopes

This project aims to obtain a sheet metal part with an asymmetric shape which is formed by dieless incremental forming using optimum process parameters, where it will be carried out on a 3-axis CNC milling machine. Single Point Incremental Forming (SPIF) technique is used in this project. The tool path can be generated by the CAM software. The material of the sheet metal is aluminium with the size of 350mm x 350mm x 1mm. The blank holder is made by four hollow bars where it is welded into the shape of square, the material used is mild steel. Besides that, the forming tools are made from 3-axis CNC turning machine in which a hemisphere end is needed. The optimum process parameters for ISF to be investigated in this project are wall angle, feed rate, and step size, where various designs of experiment (DOE) will be carried out, including Taguchi method and ANOVA. While the outputs used to determine the optimum process parameters are thickness reduction and surface roughness of aluminium sheet.

CHAPTER 2

LITERATURE REVIEW

2.1 Introduction

This chapter covered about the researches related to this project. Previously, there are many studies about the analysis of incremental sheet forming, such as analysis of the formability of sheet metal, force measurement, energy efficiency, surface roughness, and influence of process parameters. Various effects of process parameters towards the geometrical accuracy are also discussed in this chapter.

2.2 Mechanics of Incremental Sheet Forming

Incremental sheet forming (ISF) is a flexible process used in sheet metal prototyping and batch production applications. It is flexible because a specialized die is not required, in which the process is also called dieless incremental sheet forming. The sheet is usually fixed horizontally, where all the edges are clamped in a special blank holder.

In a typical ISF process, a general round-ended forming tool is moved along the NC controlled tool path, the tool moves downwards, indents the sheet by a specific depth, causing localized deformation in the sheet, then draws a contour on a horizontal plane, and then makes a step downwards, draws the next contour, makes the next step downwards, and so on (Pohlak et al, 2007). The process is illustrated in Figure 2.1 below.

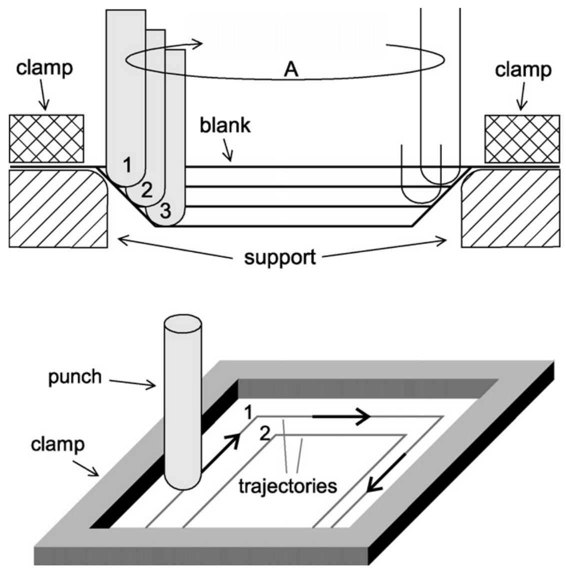

Figure 2.1: Working principle of incremental sheet forming

Source: Emmens et al. (2010)

There are two types of forming technique in ISF, negative forming and positive forming as shown in Figure 2.2. The main difference between them is the presence of die in positive forming. Most of the times, positive incremental forming always capable to produce parts with better accuracy and increased formability, therefore it is possible to make complicated shapes such as sharp corners and edges. However, in negative incremental forming, formability is not as good as positive incremental forming due to lack of die as a support tool. Park and Kim's work (2003) showed that crack is easily occurred due to biaxial mode of deformation. Therefore, many researchers are trying to increase the formability of sheet metal in negative incremental forming by performing various analysis on ISF. One of the most common research is the optimization of process parameters.

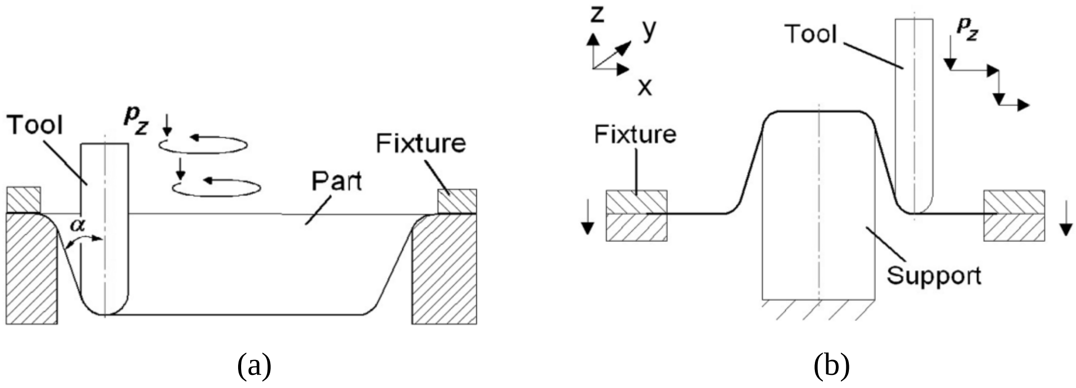

Figure 2.2: (a) Negative forming and (b) Positive forming

Source: Pohlak et al. (2007)

2.3 Influence of Tool Diameter

Tool diameter is one of the significant process parameters in ISF as it will not only affects the formability but also the surface finish of the sheet. Duflou et al showed that increase in tool diameter will increase the required force for forming (Duflou et al, 2007). Kim and Park found that increasing of tool diameter will increase the forming depth due to increase of contact zone (Kim & Park, 2002). Oleksik's work revealed that smaller tool diameter along with larger vertical step size will increase the maximum thickness reduction of the sheet metal (Oleksik, 2014).

Malwad and Nandedkar's work showed that the smaller tool diameter produced more vibrations, but the force generated is lesser. Smaller tool diameter also has better formability because of concentration of force and strain. However, penetration occurred instead of deformation when the tool diameter is less than 6mm (Malwad & Nandedkar, 2014). Jeswiet et al concluded that the smaller tool diameter provides greater formability along transverse direction, while the larger tool diameter provides better formability along rolling direction (Jeswiet et al., 2005).

Han et al showed that the larger tool diameter will increase the springback because more residual stress was released when uninstalling the load (Han et al., 2013). While Ambrogio et al proved that the tool diameter has a great influence on the pillow effect of sheet metal which resulted from springback (Ambrogio et al, 2007).

Echrif and Hrairi found that the surface roughness and microstructure of sheet metal is improved along with the increase of tool diameter, but the part accuracy is decreased (Echrif & Hrairi, 2014).

2.4 Influence of Wall Angle

Malwad and Nandedkar (2014) did some experiments and observed that larger wall angle will result in a higher thickness reduction. However, uniform thickness distribution can only be achieved when the wall angle is less than 65 degrees. Deformation occurred when the wall angle increases because of stretching and local shearing, where stretching causes more thickness reduction near the top than near the bottom. Besides that, no crack was found near the bottom of a depth of 50 mm for every wall angle tested in the experiment, which is 55 degrees, 65 degrees, and 75 degrees. They also concluded that greater formability can be done for wall angle less than 75 degrees. The results of the experiment were clearly shown in Figure 2.3.

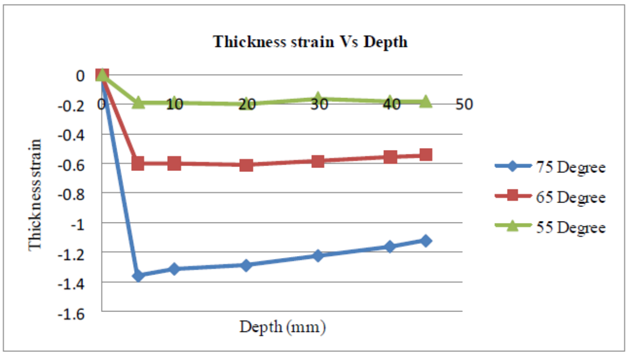

Figure 2.3: Thickness strain vs depth at different wall angle

Source: Malwad and Nandedkar (2014)

Duflou et al (2007) showed that the required forming force increased along with the magnitude of the wall angle. However, there is a remarkable peak of force followed by a notable drop and gradually increasing again for wall angle of 60 degrees as shown in Figure 2.4. This phenomenon is an indication of the maximum achievable wall angle and was explained as a sign of failure. According to the authors' experience, the decrease of the required forming force can be described as localized necking, where it was commonly found in the part near the maximum achievable wall angle in SPIF. Hence, part failure can be predicted by observing the significant peak of forming force which followed by a rapid drop for various wall angles.

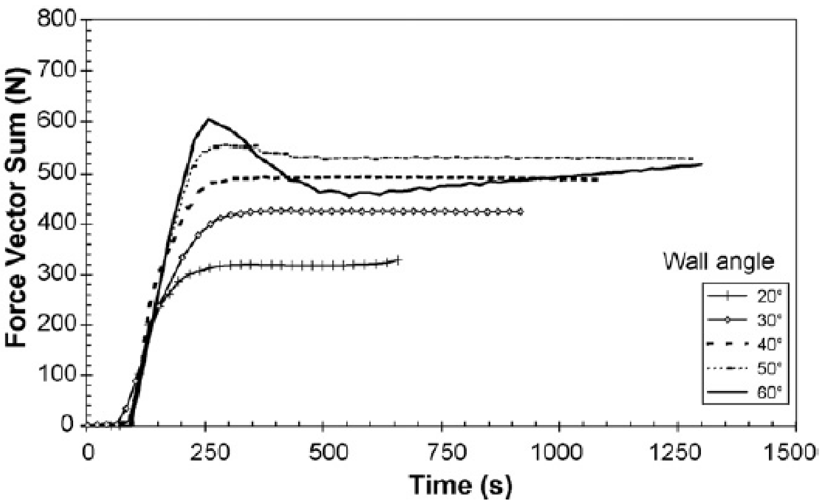

Figure 2.4: Force curve for wall angles of 20º to 60º

Source: Duflou et al (2007)

2.4.1 Sine Law

Sine law is a formula used to estimate the deformation of sheet metal in the spinning process, but it was also used in the ISF process to predict the thickness of the sheet after the forming process, where the wall angles are the main variable. The sine law was defined in Eq. (2.1):

$$t_1 = t_0 \sin (90^o - \alpha) \tag{2.1}$$

Where t_1 is the final thickness of the sheet, t_0 is the sheet's initial thickness, and α is the wall angle, which is defined as the angle between the deformed sheet and un-deformed sheet, as shown in Figure 2.5.

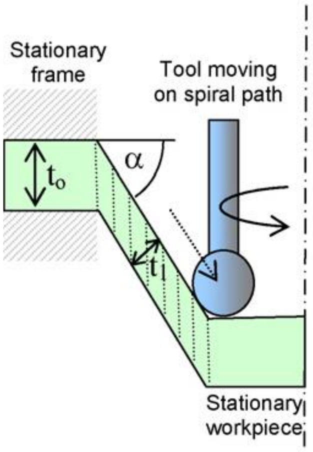

Figure 2.5: Deformation of sheet in ISF and parameters of sine law

Source: Jackson & Allwood (2009)

Oleksik's work in 2014 which investigates the influence of wall angle on the thickness reduction of SPIF showed that the maximum deformation was close to the value obtained from the sine law only at about ¾ of the forming depth, where the wall angle and height were fixed at 45° and 24 mm respectively. However, after the author decrease the height of the pyramid frustum to 16 mm while other parameters kept constant, the sine law was no longer respected, even for different angles, which were 45º, 55º, and 65º. Especially for the latter two angles, the strain was strongly localized. Oleksik suggested that this is because the "critical height" of the part to stabilise the maximum thickness reduction has not reached. Yet, the accuracy of the sine law increased as the degree of complexity of the part increased.

Ham and Jeswiet (2006) performed two Design of Experiments (DOE) in order to study the forming criteria for aluminium in SPIF, where each parameters consist of two levels including wall angle. In the first DOE, it was observed that the wall angle greatly affected the formability. Based on sine law, larger angle will produce thinner cross section, and cracks are most likely to occur in this area. But the chosen material must be thin in order to maintain its constant volume.

2.5 Influence of Feed Rate

Hamilton and Jeswiet (2010) studied about effects of high feed rates on the surface and structure of sheet metal in SPIF. When the feed rate was 2540 mm/min or lower, characteristic thinning occurred and then stabilization of thickness. After that, when the feed rate was increased to around 5080 to 8890 mm/min, similar thickness distributions were found in the sheet. The characteristic initial thinning, thickness stabilization and recovery were amplified as the wall angle increased. The results proved that SPIF can be carried out at high feed rate.

Kim and Park (2002) showed that as the feed rate increased from 0.1 to 0.5 mm, the formability decreased in both rolling direction and transverse direction. Although the slower feed rate produced greater formability, the forming time was longer as well. On the other hand, Strano (2005) proved that higher feed rate will decrease the probability of having a sound part. Jeswiet et al (2005) also suggested that feed rate in forming process is much higher than the normal machining process because the material removal rate is not a concern in the forming process.

2.6 Influence of Step Size

Echrif and Hrairi (2014) showed that vertical step size in ISF was a very significant factor to the surface roughness of the sheet along with the tool size. Smaller step size will cause less surface waviness and very smooth surface. Besides, Jeswiet et al (2005) also found that larger step size will not only produced higher surface roughness, but will also affect the size of orange peel effect. Hamilton and Jeswiet (2010) proved that step size has a great influence on the change of grain size which is the most significant difference in their study. Malwad and Nandedkar's (2014) studies on the deformation mechanism analysis of SPIF also concluded that surface roughness increased along with the step size. While for smaller step size, local deformation plays an important role instead of stretching. Figure 2.6 showed the surface finish for step size of 0.2 mm and 0.5 mm respectively.

(a) (b)

Figure 2.6: Surface finish for step size: (a) 0.2 mm and (b) 0.5 mm

Source: Malwad & Nandedkar (2014)

CHAPTER 3

METHODOLOGY

3.1 Introduction

Chapter 3 will discuss about the methods used in this project in order to achieve the objectives. Generally, design of experiment (DOE) is the main approach to carry out the experiment, Taguchi method is used to determine the optimum process parameters in ISF, and ANOVA method is used to find out the most significant process parameters in ISF.

3.2 Flow Chart of the Project

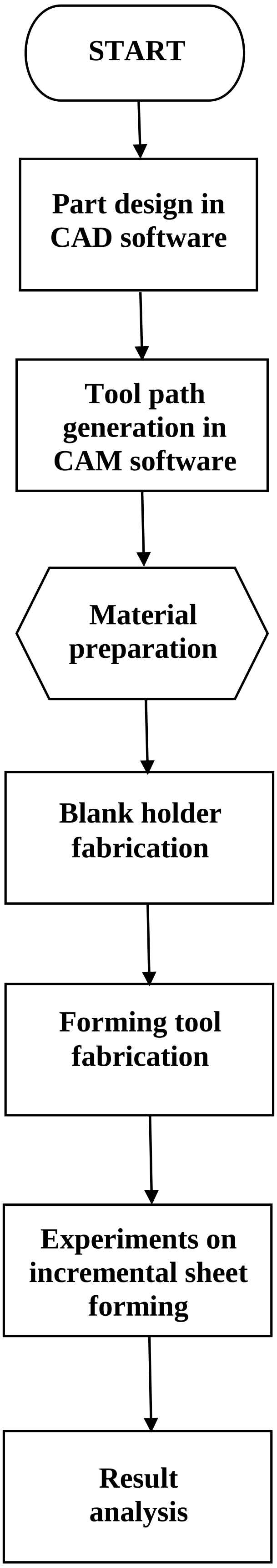

3.3 Design of Experiment

Firstly, the part to be formed in ISF process is designed in CAD software (CATIA), with the variance of wall angles in which the optimum one will be determined after the experiment. Then, the tool path will be generated on a CAM platform (CATIA), which is fixed throughout the experiment. The generated G-code for the ISF process will then ready to transfer to the 3-axis CNC milling machine.

The forming tool for ISF process is a mild steel rod, it will be fabricated with a 3-axis CNC turning machine in the FKP Machining Lab to create a ball end with a diameter of 10 mm which is kept constant for all experiments. Figure 3.1 shows the turning machine used in fabricating the forming tool and Figure 3.2 shows the end product of the forming tool.

Figure 3.1: Turning machine

Figure 3.2: Forming tool for ISF

On the other hand, the blank holder for the ISF process is assembled using mild steel hollow bars by welding each of it into a square shape. Figure 3.3 shows the complete structure of the blank holder. While the entire ISF experiment was carried out on a CNC milling machine as shown in Figure 3.4.

Figure 3.3: Complete structure of blank holder for ISF

Figure 3.4: CNC milling machine

In this experiment, wall angle, feed rate, and step size are going to be investigated with 3 levels each. Table 3.1 shows the experimental setting for each process parameter, and Table 3.2 shows the different combinations of every process parameters carry out in this experiment. Figure 3.4 shows the shape of aluminium sheet going to form in ISF, which is a pyramid frustum. The forming depth is fixed at 24 mm throughout the experiment. While Figure 3.5 shows the tool path of ISF generated in CATIA which is inward helical along the contour only. Spindle speed was kept constant at 0 rpm. The experiment setup for ISF including the aluminium sheet and blank holder on the CNC milling machine was clearly shown in Figure 3.6.

Table 3.1: Process parameters and level descriptions

Parameters	Level 1	Level 2	Level 3
Wall Angle	35º	45º	55º
Feed Rate (mm/min)	700	900	1100
Step Size (mm)	0.25	0.50	1.00

Table 3.2: Design of experiment plan

Experiment	Wall Angle	Feed Rate (mm/min)	Step Size (mm)
1	35º	700	0.25
2	35º	900	0.50
3	35º	1100	1.00
4	45º	700	0.50
5	45º	900	1.00
6	45º	1100	0.25
7	55º	700	1.00
8	55º	900	0.25
9	55º	1100	0.50

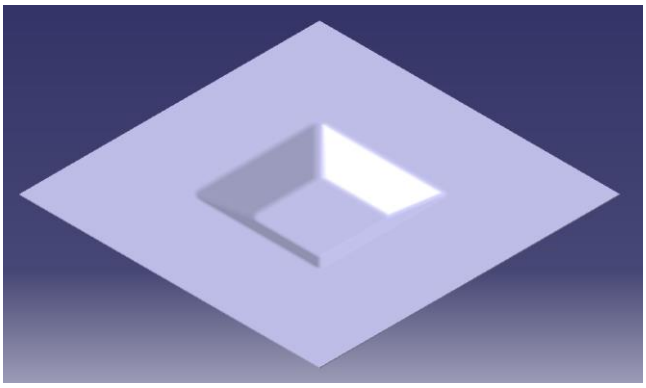

Figure 3.5: Sketch of pyramid frustum shape of aluminium sheet in CATIA

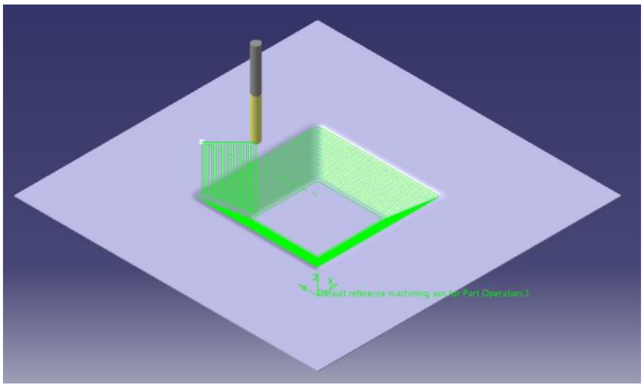

Figure 3.6: Tool path generation in CATIA

Figure 3.7: Experiment setup for ISF on CNC milling machine

3.4 Materials and Equipment

3.4.1 Bill of Materials

Table 3.3 showed the list of materials used in this experiment.

Table 3.3: Bill of Materials

No.	Item	Size (mm)	Qty.
1	Aluminium sheet	350 x 350 x 1	15
2	Mild steel rod	Ø10 x 85	1
3	Mild steel hollow bar	50 x 50 x 400	4

3.4.2 Machines and Equipment

Table 3.4 listed the machines and equipment used in this project and their respective locations.

Table 3.4: Equipment used and their respective locations

No.	Equipment	Location
1	Makino KE55 Vertical Machining Centre	Machining Lab, FKP.
2	ROMI C 420 CNC Lathe	
3	T-Jaw 360 Vertical Band Saw	
4	SURFCOM 130A Surface Roughness Tester	Materials Lab, FKP.
5	Microscope Profile Video Measuring System	

Figure 3.8 shows the vertical band saw which was used to cut the formed aluminium sheets into smaller pieces for analysis purpose. While the surface roughness tester and the video measuring system showed in Figure 3.9 and Figure 3.10 was used to measure the surface roughness and thickness reduction of the formed aluminium sheets respectively.

Figure 3.8: Vertical band saw

Figure 3.9: Surface roughness tester

Figure 3.10: Microscope profile video measuring system

CHAPTER 4

RESULTS ANALYSIS AND DISCUSSIONS

4.1 Introduction

The formed aluminium sheets were analysed for average surface roughness on four sides of internal slopes and four different radius size of internal corner. Meanwhile, the average thickness reduction of the sheet was measured and compare with the result obtained from the sine law, the uniformity of thickness reduction was investigated as well. The respective areas to be analysed were labelled as shown in Figure 4.1.

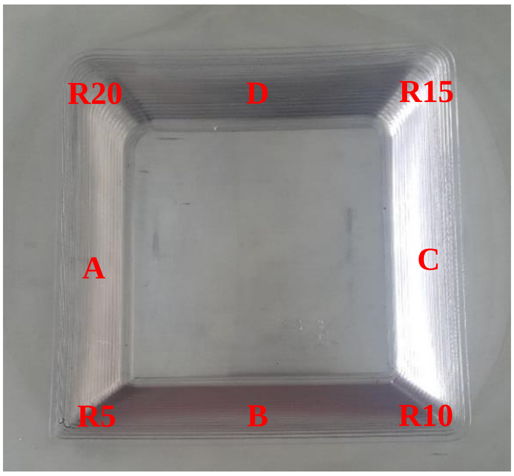

Figure 4.1: Top view of an aluminium sheet after ISF

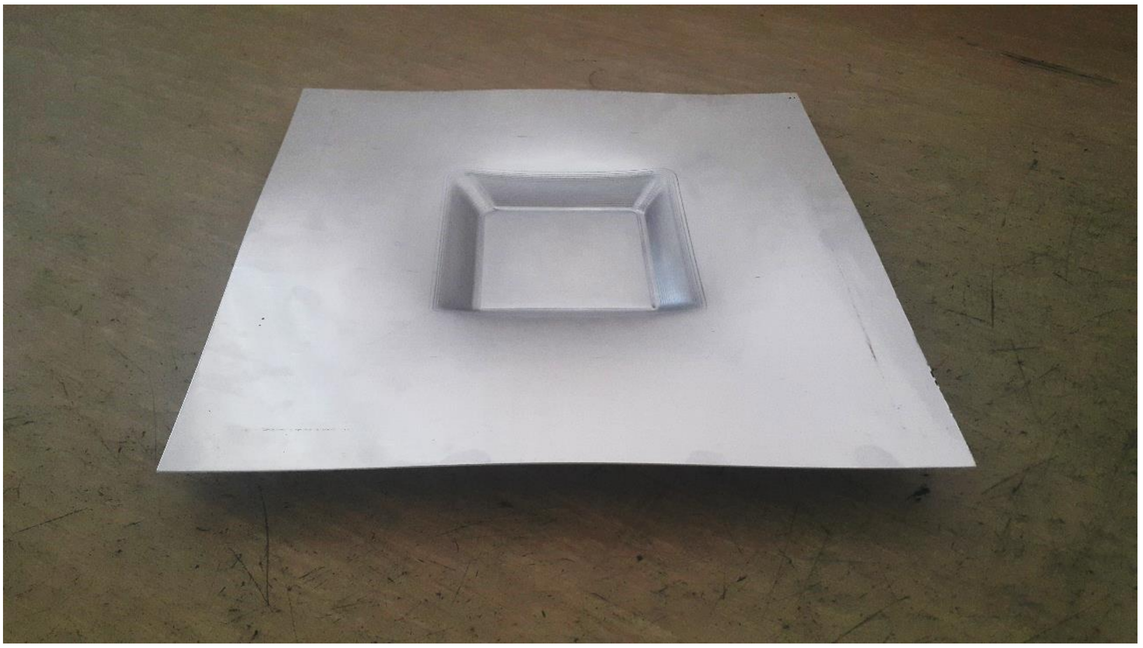

Figure 4.2: Overview of the aluminium sheet after ISF

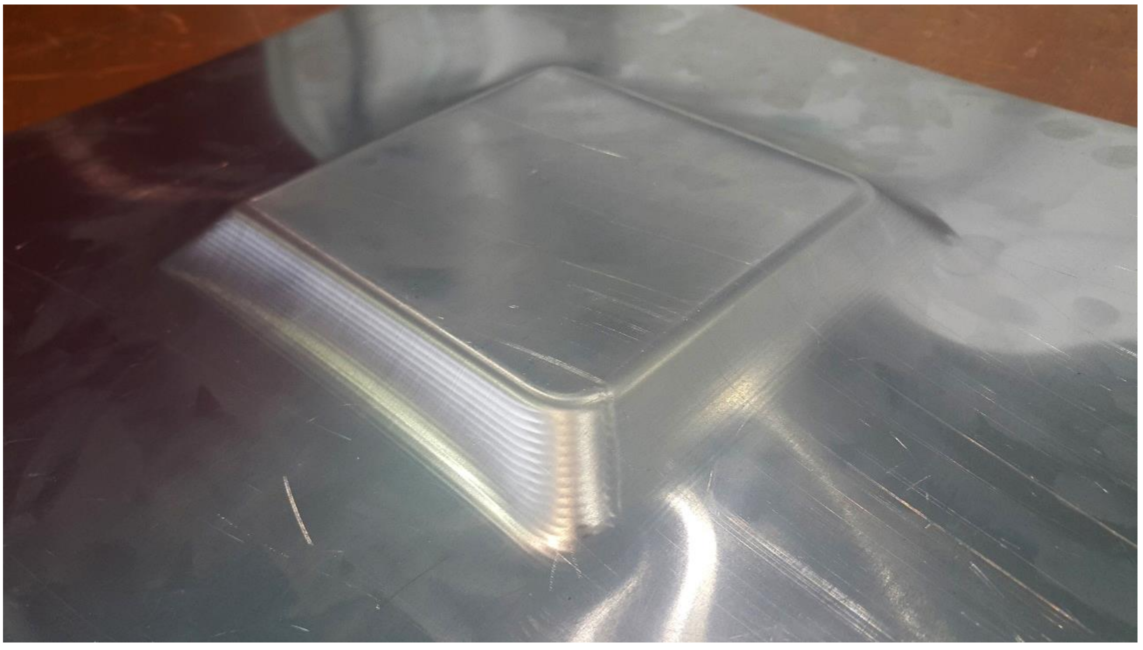

Figure 4.3: Bottom view of the aluminium sheet after ISF

4.2 Data Collection

4.2.1 Surface Roughness

The surface roughness on each area of the aluminium sheet including the four corners as shown in Figure 4.1 was measured using surface roughness tester. The readings were taken on three different regions on each area and the average value was calculated. The final value was the mean of all the average readings from each area. The results were shown in the following tables.

Table 4.1: Average surface roughness of aluminium sheet in ISF for Experiment 1

	Surface Roughness (μm)			
	Trial 1	**Trial 2**	**Trial 3**	**Average**
Area A	9.867	4.985	6.864	7.239
Area B	4.953	3.447	2.677	3.692
Area C	7.894	4.401	6.174	6.156
Area D	10.915	6.646	5.219	7.593
R5	3.674	7.754	9.394	6.941
R10	6.677	6.769	5.731	6.392
R15	4.529	6.491	5.699	5.573
R20	10.434	11.577	14.412	12.141
			Overall	6.966

Figure 4.4: Surface of aluminium sheet for Experiment 1

Table 4.2: Average surface roughness of aluminium sheet in ISF for Experiment 2

	Surface Roughness (µm)			
	Trial 1	**Trial 2**	**Trial 3**	**Average**
Area A	4.763	4.808	5.114	4.895
Area B	6.930	5.923	5.321	6.058
Area C	3.063	4.670	4.946	4.226
Area D	8.147	5.734	9.580	7.820
R5	3.075	7.093	4.691	4.953
R10	5.807	6.370	6.983	6.387
R15	3.092	11.993	8.158	7.748
R20	5.675	9.930	9.680	8.428
			Overall	6.314

Figure 4.5: Surface of aluminium sheet for Experiment 2

Table 4.3: Average surface roughness of aluminium sheet in ISF for Experiment 3

	Surface Roughness (µm)			
	Trial 1	**Trial 2**	**Trial 3**	**Average**
Area A	3.538	4.939	2.364	3.614
Area B	8.194	5.489	7.459	7.047
Area C	5.346	5.596	7.900	6.281
Area D	4.943	8.206	6.080	6.410
R5	5.584	5.355	8.655	6.531
R10	3.155	4.963	4.081	4.066
R15	4.346	3.213	3.732	3.764
R20	3.069	3.084	3.740	3.298
			Overall	5.126

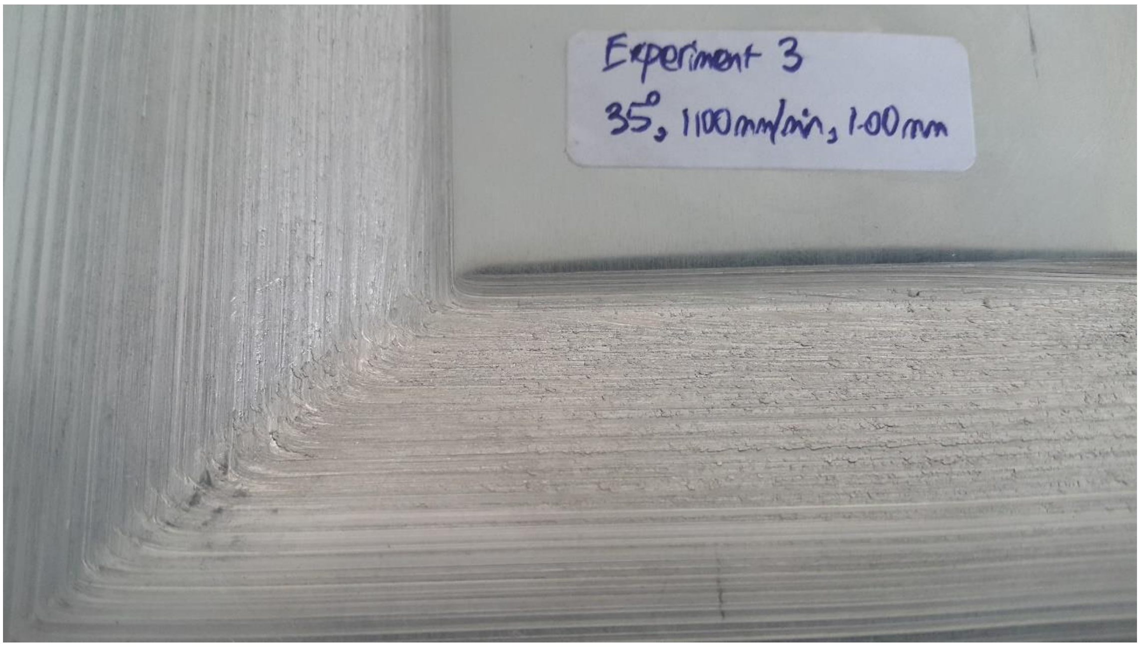

Figure 4.6: Surface of aluminium sheet for Experiment 3

Table 4.4: Average surface roughness of aluminium sheet in ISF for Experiment 4

	Surface Roughness (µm)			
	Trial 1	**Trial 2**	**Trial 3**	**Average**
Area A	3.896	3.420	3.214	3.510
Area B	2.783	2.214	2.268	2.422
Area C	3.207	3.364	3.073	3.215
Area D	4.078	3.142	2.585	3.268
R5	3.780	0.954	1.066	1.933
R10	1.143	1.184	1.984	1.437
R15	1.570	1.708	2.010	1.763
R20	1.163	1.272	0.910	1.115
			Overall	2.333

Figure 4.7: Surface of aluminium sheet for Experiment 4

Table 4.5: Average surface roughness of aluminium sheet in ISF for Experiment 5

	Surface Roughness (µm)			
	Trial 1	**Trial 2**	**Trial 3**	**Average**
Area A	2.494	1.153	1.862	1.836
Area B	4.619	3.317	3.934	3.957
Area C	3.675	3.467	3.015	3.386
Area D	3.798	2.513	4.496	3.602
R5	4.248	3.769	1.280	3.099
R10	2.514	1.276	1.675	1.822
R15	4.737	4.164	1.275	3.392
R20	1.860	3.762	4.578	3.400
			Overall	3.062

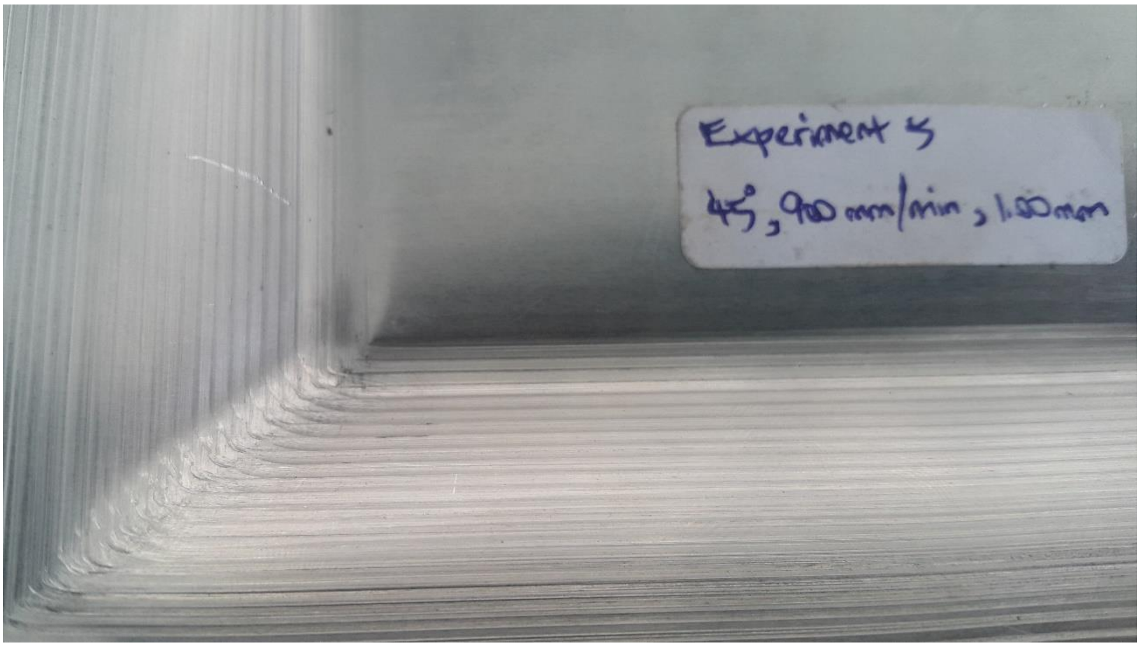

Figure 4.8: Surface of aluminium sheet for Experiment 5

Table 4.6: Average surface roughness of aluminium sheet in ISF for Experiment 6

	Surface Roughness (µm)			
	Trial 1	**Trial 2**	**Trial 3**	**Average**
Area A	5.033	5.118	5.989	5.380
Area B	9.034	4.648	6.347	6.676
Area C	4.993	5.930	4.755	5.226
Area D	6.737	6.235	2.965	5.312
R5	10.170	5.111	8.822	8.034
R10	8.685	8.261	9.242	8.729
R15	10.094	6.221	7.860	8.058
R20	4.822	6.582	4.214	5.206
			Overall	6.578

Figure 4.9: Surface of aluminium sheet for Experiment 6

Table 4.7: Average surface roughness of aluminium sheet in ISF for Experiment 7

	Surface Roughness (μm)			
	Trial 1	**Trial 2**	**Trial 3**	**Average**
Area A	2.301	3.507	2.350	2.719
Area B	3.548	3.551	4.020	3.706
Area C	3.256	3.360	2.888	3.168
Area D	1.893	1.981	2.089	1.988
R5	2.557	2.250	2.938	2.582
R10	3.595	3.328	2.396	3.106
R15	2.059	1.889	2.894	2.281
R20	2.789	2.293	2.798	2.627
			Overall	2.772

Figure 4.10: Surface of aluminium sheet for Experiment 7

Table 4.8: Average surface roughness of aluminium sheet in ISF for Experiment 8

	Surface Roughness (µm)			
	Trial 1	**Trial 2**	**Trial 3**	**Average**
Area A	2.958	3.318	2.058	2.778
Area B	2.226	2.819	1.982	2.342
Area C	2.228	3.957	2.966	3.050
Area D	3.501	3.414	3.883	3.599
R5	10.164	15.736	13.612	13.171
R10	7.743	6.604	5.754	6.700
R15	6.685	6.963	6.566	6.738
R20	8.818	6.787	7.435	7.680
			Overall	5.757

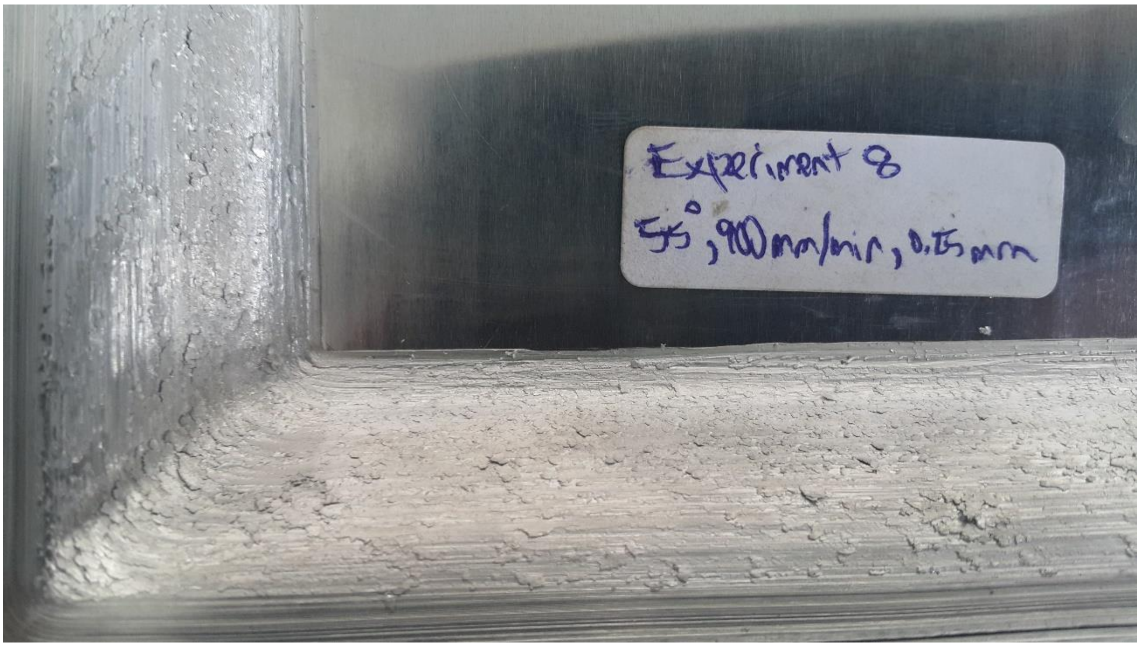

Figure 4.11: Surface of aluminium sheet for Experiment 8

Table 4.9: Average surface roughness of aluminium sheet in ISF for Experiment 9

	Surface Roughness (μm)			
	Trial 1	**Trial 2**	**Trial 3**	**Average**
Area A	5.863	9.476	5.296	6.878
Area B	5.739	5.590	6.139	5.823
Area C	5.355	5.284	8.486	6.375
Area D	6.125	5.008	8.044	6.392
R5	10.768	13.001	10.289	11.353
R10	4.322	6.282	4.145	4.916
R15	9.880	7.230	5.979	7.696
R20	5.530	7.653	10.783	7.989
			Overall	7.178

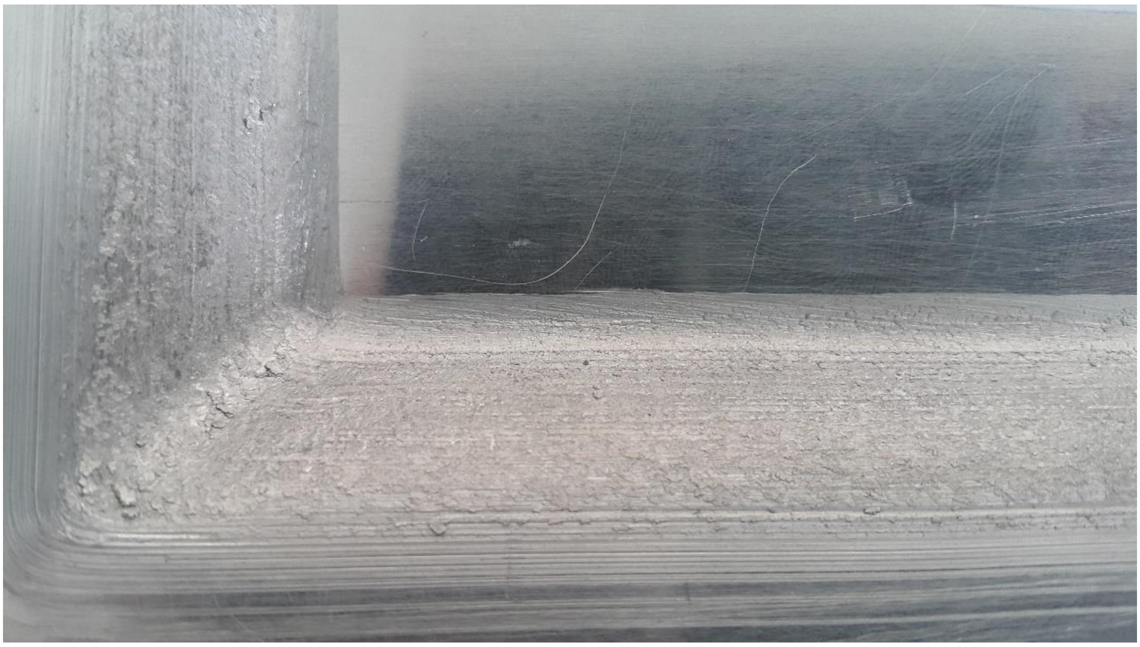

Figure 4.12: Surface of aluminium sheet for Experiment 9

Table 4.10: Summary of average surface roughness of aluminium sheet in ISF

Experiment	Angle	Feed Rate (mm/min)	Step Size (mm)	Average Surface Roughness (µm)
1	35º	700	0.25	6.966
2	35º	900	0.50	6.315
3	35º	1100	1.00	5.126
4	45º	700	0.50	2.333
5	45º	900	1.00	3.062
6	45º	1100	0.25	6.578
7	55º	700	1.00	2.772
8	55º	900	0.25	5.757
9	55º	1100	0.50	7.178

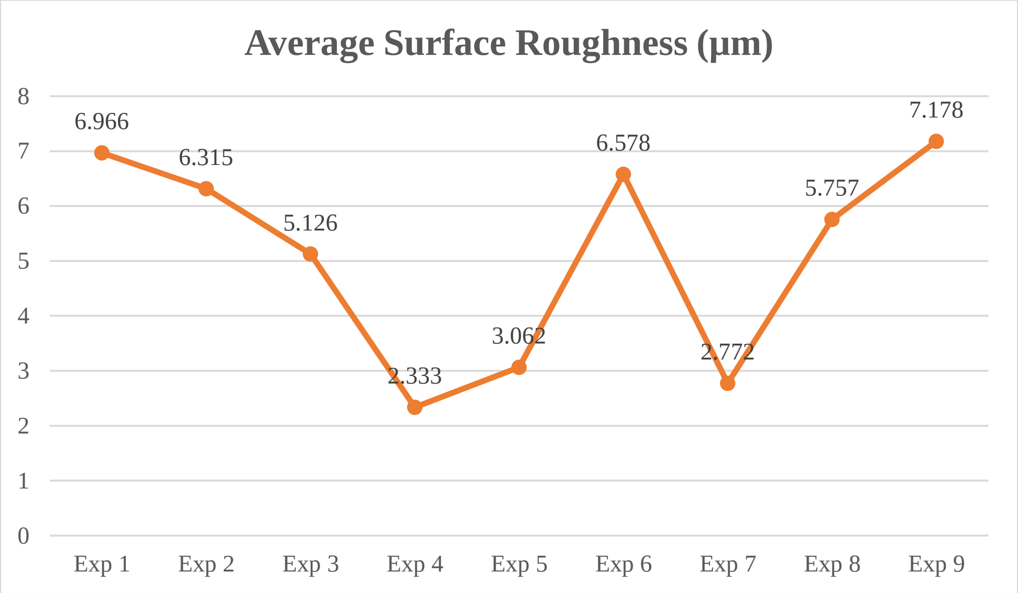

Figure 4.13: Comparison of average surface roughness of aluminium sheet in ISF

Figure above shows that Experiment 4 has the lowest average surface roughness while Experiment 9 produced the highest average surface roughness. For wall angle of 35º, surface roughness decreased when the feed rate and step size increased. However, the surface roughness increased when the feed rate increased for 45º and 55º of wall angle.

Table 4.11 shows the average surface roughness of each corner of the pyramid frustum on aluminium sheet labelled after Figure 4.1 for each experiment. The radius of each corner for R5, R10, R15, and R20 was 5mm, 10mm, 15mm, and 20mm respectively.

Table 4.11: Average surface roughness of each corner of pyramid frustum in ISF

Experiment	**Surface Roughness (µm)**			
	R5	**R10**	**R15**	**R20**
1	6.941	6.392	5.573	12.141
2	4.953	6.387	7.748	8.428
3	6.531	4.066	3.764	3.298
4	1.933	1.437	1.601	1.115
5	3.099	1.822	3.392	3.400
6	8.034	8.729	8.058	5.206
7	2.582	3.106	2.281	2.627
8	13.171	6.700	6.738	7.680
9	11.353	4.916	7.696	7.989
Average	6.511	4.839	5.206	5.765

From the results, it was observed that the surface roughness did not have a specific trend along with increasing corner radius for each experiment. Moreover, Experiment 2 and Experiment 3 even have an opposite trend of surface roughness when the corner radius was increased. On the other hand, Experiment 1, 8, and 9 shows the most significant difference of surface roughness between the different corner radiuses. For the rest of the experiments, the surface roughness was fluctuating within a small range when the corner radius was increasing. However in average, the surface roughness in R5 was the highest, followed by R20, R15, and lastly R10. The graph of average surface roughness of each corner for each experiment was shown in Figure 4.14.

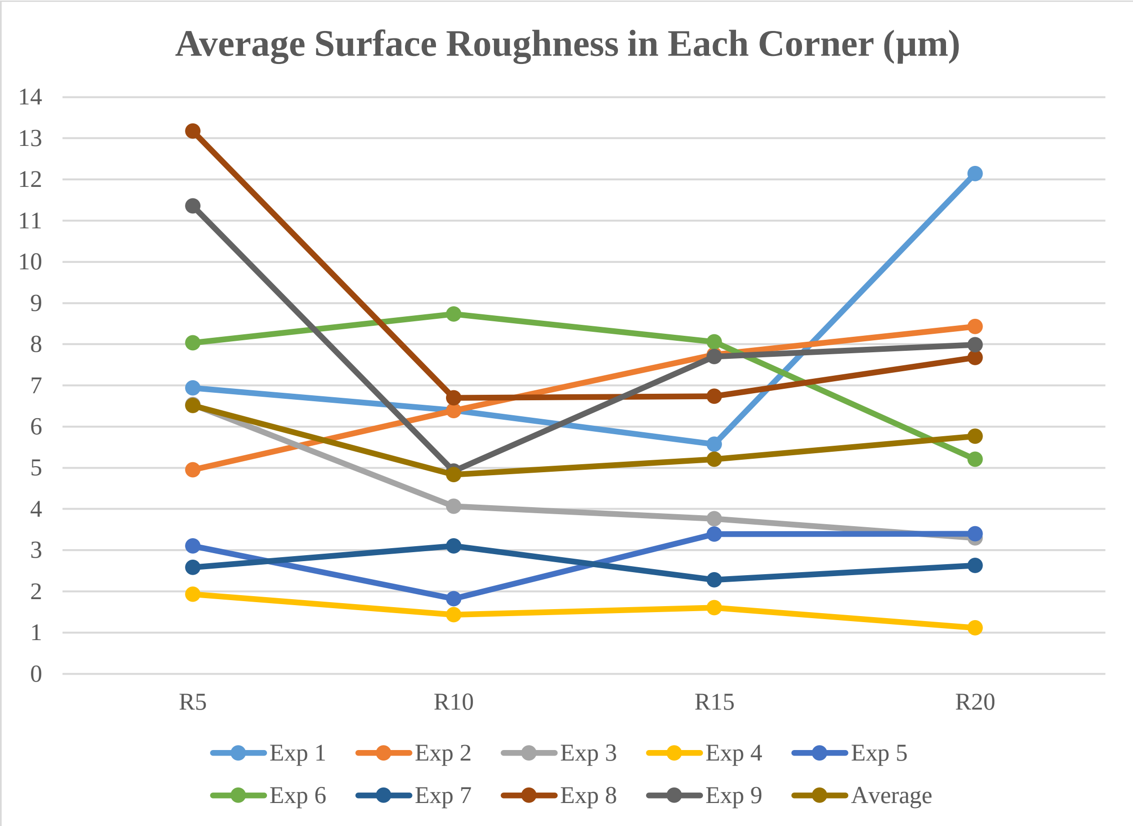

Figure 4.14: Average surface roughness of each corner of pyramid frustum in ISF

4.2.2 Thickness Reduction

Table 4.12 to 4.20 shows the theoretical and experimental value of thickness reduction of aluminium sheet after incremental forming. The theoretical value was obtained from Eq. (2.1) while the result acquired from ISF was measured from each side from Area A, B, C, and D using microscope video measuring system and the average value was taken.

Table 4.12: Thickness reduction of aluminium sheet for Experiment 1

	Thickness Reduction (mm)			
	Trial 1	**Trial 2**	**Trial 3**	**Average**
Area A	0.8744	0.8015	0.8206	0.8322
Area B	0.8320	0.8827	0.7647	0.8265
Area C	0.8504	0.8285	0.8110	0.8300
Area D	0.8615	0.7757	0.8390	0.8254
			Overall	0.8285

Table 4.13: Thickness reduction of aluminium sheet for Experiment 2

	Thickness Reduction (mm)			
	Trial 1	**Trial 2**	**Trial 3**	**Average**
Area A	0.8852	0.7976	0.8236	0.8355
Area B	0.8703	0.7967	0.8816	0.8495
Area C	0.8076	0.8860	0.8912	0.8616
Area D	0.8695	0.8737	0.8320	0.8584
			Overall	0.8513

Table 4.14: Thickness reduction of aluminium sheet for Experiment 3

	Thickness Reduction (mm)			
	Trial 1	**Trial 2**	**Trial 3**	**Average**
Area A	0.9110	0.8344	0.9455	0.8970
Area B	0.9140	0.8727	0.8206	0.8691
Area C	0.8382	0.8539	0.8997	0.8639
Area D	0.9048	0.7921	0.8183	0.8384
			Overall	0.8671

Table 4.15: Thickness reduction of aluminium sheet for Experiment 4

	Thickness Reduction (mm)			
	Trial 1	**Trial 2**	**Trial 3**	**Average**
Area A	0.7656	0.7343	0.7011	0.7337
Area B	0.7328	0.6799	0.6574	0.6900
Area C	0.7242	0.7476	0.7178	0.7299
Area D	0.6332	0.7656	0.6906	0.6965
			Overall	0.7125

Table 4.16: Thickness reduction of aluminium sheet for Experiment 5

	Thickness Reduction (mm)			
	Trial 1	**Trial 2**	**Trial 3**	**Average**
Area A	0.7541	0.6799	0.7860	0.7400
Area B	0.6920	0.6691	0.7265	0.6959
Area C	0.7309	0.7841	0.7171	0.7440
Area D	0.7572	0.6993	0.7555	0.7373
			Overall	0.7293

Table 4.17: Thickness reduction of aluminium sheet for Experiment 6

	Thickness Reduction (mm)			
	Trial 1	**Trial 2**	**Trial 3**	**Average**
Area A	0.7202	0.7790	0.6907	0.7300
Area B	0.6908	0.7450	0.7779	0.7379
Area C	0.7583	0.6976	0.7125	0.7228
Area D	0.6504	0.7662	0.7371	0.7179
			Overall	0.7272

Table 4.18: Thickness reduction of aluminium sheet for Experiment 7

	Thickness Reduction (mm)			
	Trial 1	**Trial 2**	**Trial 3**	**Average**
Area A	0.6055	0.6406	0.5791	0.6084
Area B	0.6383	0.5594	0.6480	0.6152
Area C	0.5525	0.5817	0.5994	0.5779
Area D	0.5840	0.5716	0.5730	0.5762
			Overall	0.5944

Table 4.19: Thickness reduction of aluminium sheet for Experiment 8

	Thickness Reduction (mm)			
	Trial 1	**Trial 2**	**Trial 3**	**Average**
Area A	0.5986	0.6197	0.6372	0.6185
Area B	0.5966	0.5594	0.5632	0.5731
Area C	0.5672	0.5563	0.5709	0.5648
Area D	0.5677	0.5564	0.5894	0.5712
			Overall	0.5819

Table 4.20: Thickness reduction of aluminium sheet for Experiment 9

	Thickness Reduction (mm)			
	Trial 1	**Trial 2**	**Trial 3**	**Average**
Area A	0.5840	0.5525	0.5730	0.5698
Area B	0.5394	0.5473	0.6066	0.5644
Area C	0.5284	0.6511	0.5899	0.5898
Area D	0.5986	0.6081	0.6268	0.6112
			Overall	0.5838

Table 4.21 shows the standard deviation of average thickness reduction of aluminium sheet for each experiment. A smaller value of standard deviation indicates that the thickness from each area are closer to the mean, which means that the thickness reduction is more uniform. The graph of results was demonstrated in Figure 4.15 where the thickness uniformity represents the standard deviation of thickness reduction.

Table 4.21: Summary of thickness reduction of aluminium sheet in ISF

Experiment	**Thickness Reduction (mm)**					**Standard Deviation**
	Area A	**Area B**	**Area C**	**Area D**	**Average**	
1	0.8322	0.8265	0.8300	0.8254	0.8285	0.0031
2	0.8355	0.8495	0.8616	0.8584	0.8513	0.0117
3	0.8970	0.8691	0.8639	0.8384	0.8671	0.0240
4	0.7337	0.6900	0.7299	0.6965	0.7125	0.0225
5	0.7400	0.6959	0.7440	0.7373	0.7293	0.0224
6	0.7300	0.7379	0.7228	0.7179	0.7272	0.0087
7	0.6084	0.6152	0.5779	0.5762	0.5944	0.0203
8	0.6185	0.5731	0.5648	0.5712	0.5819	0.0247
9	0.5698	0.5644	0.5898	0.6112	0.5838	0.0213

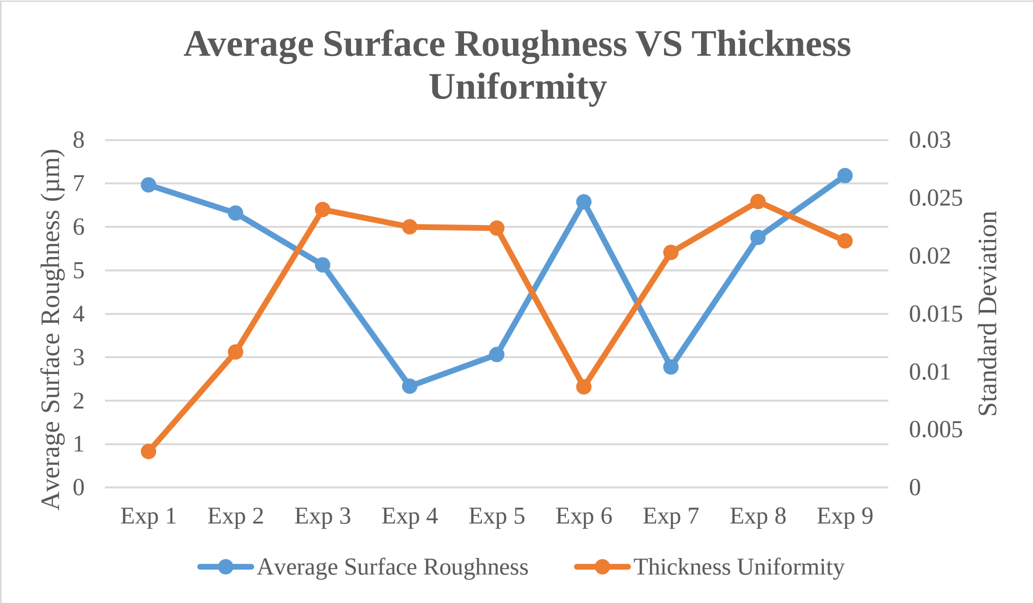

Figure 4.15: Average surface roughness and thickness uniformity of aluminium sheet

The previous results revealed that Experiment 1 has the most uniform thickness reduction due to lowest value of standard deviation, while Experiment 8 has the least uniform thickness reduction. It was also observed that the wall angle of 55º (Experiment 7 – Experiment 9) has a relatively low thickness uniformity compared to other angles. Besides that, it can be concluded from Figure 4.15 that the average surface roughness was in contrast with the thickness uniformity of aluminium sheet in ISF. In other words, a higher surface roughness generated more uniform thickness reduction of aluminium sheet, and vice versa.

Table 4.22 shows the actual thickness reduction of aluminium sheet compared to the theoretical thickness reduction obtained from Eq. (2.1) which varies for different angles. The error percentage between the actual and theoretical values was calculated and the graph was plotted in Figure 4.16.

Table 4.22: Experimental and theoretical thickness reduction of aluminium sheet in ISF

Experiment	Thickness Reduction (mm)		Error (%)
	Actual	Theory	
1	0.8285	0.8192	1.1353
2	0.8513	0.8192	3.9185
3	0.8671	0.8192	5.8472
4	0.7125	0.7071	0.7778
5	0.7293	0.7071	3.1537
6	0.7272	0.7071	2.8567
7	0.5944	0.5736	3.6262
8	0.5819	0.5736	1.4470
9	0.5838	0.5736	1.7782

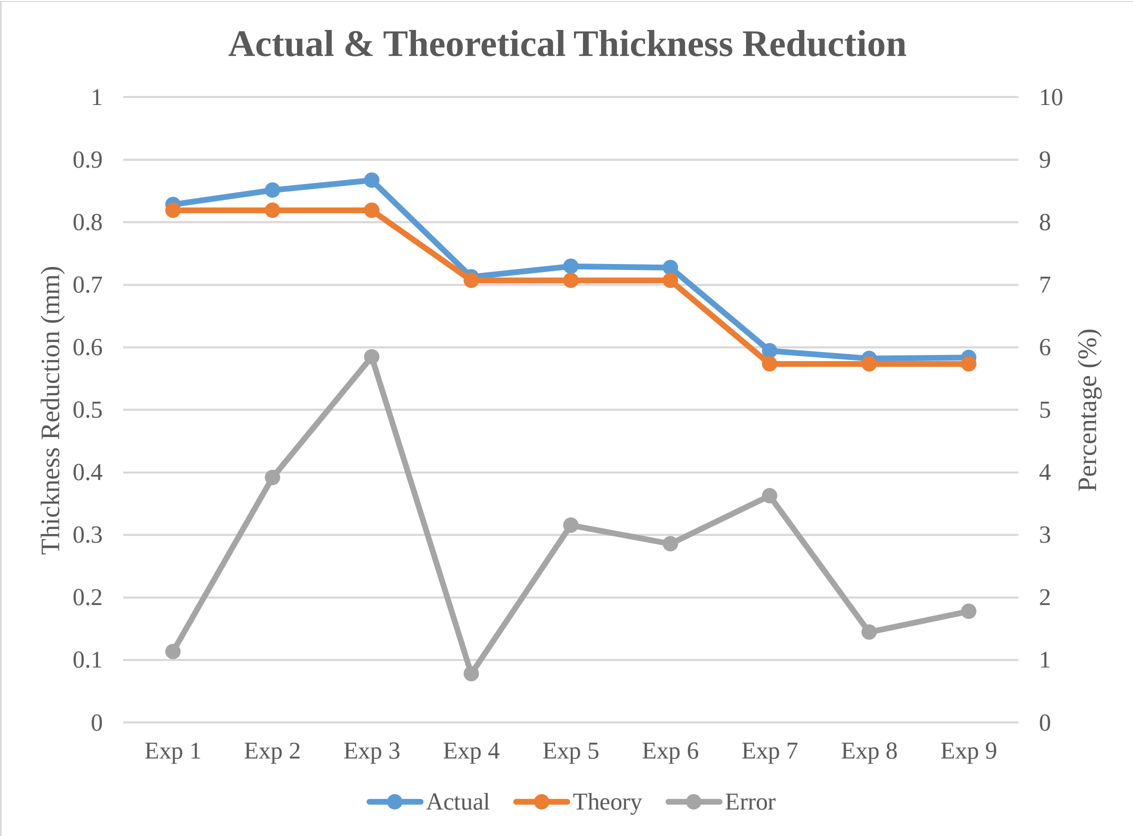

Figure 4.16: Actual and theoretical thickness reduction of aluminium sheet in ISF

The results above shows that Experiment 4 has the closest value of thickness reduction to the theoretical value with the error of 0.7778%, while the highest thickness reduction error was found in Experiment 3 (5.8472%). At wall angle of 35º, the thickness reduction error increased when the feed rate and the step size increased. It was also observed that at 55º, error increased along with increasing step size. However, the error of thickness reduction at 45º wall angle did not showed any specific pattern. In a nutshell, the low value of error percentage indicates that the equation of sine law can be implemented in ISF for prediction of sheet thickness.

4.3 Data Analysis

In this project, analysis of variance (ANOVA) was used to distinguish the most significant parameter from the insignificant parameters that affected the outcomes of surface roughness and thickness uniformity of aluminium sheets in ISF. The results of ANOVA F-test generated in Minitab software for both means and S/N ratios has revealed the most influential parameters for surface roughness and thickness uniformity. Where DF denotes degree of freedom, SS is sum of squares, MS is mean squares, and F is the ratio of variance of a source to the variance of error. The highest value of F means that the certain parameter is the most significant to the respective responses.

In order to minimise the output response, it is preferable to have a smaller value of signal-to-noise (S/N) ratio, where it measure how the response varies relative to the target value of zero under different noise conditions. The formula for smaller is better S/N ratio was shown in Eq. (4.1) where y is the response and n is the number of observations per parameter. In this case, the mean responses were already calculated, therefore y is the mean and n=1.

$$S/N = -10\ log \sum \left[\frac{y^2}{n}\right] \tag{4.1}$$

Furthermore, regression analysis was used to estimate the relationship between the parameters and the response, so that predictions of response can be done on a new set of parameters with the estimated regression equation. In addition, the percentage of regression represents the predictability of the responses, therefore the higher the better. The resulting regression equations were in linear form instead of a higher power form that would fit in the results better, thus the regression percentage was not at a very satisfactory level. The regression analysis was also carried out in the Minitab software. The following tables displayed the results of ANOVA, Taguchi, and regression analysis for surface roughness and thickness uniformity.

4.3.1 ANOVA for Surface Roughness

Table 4.23: Means and S/N ratios for surface roughness

Experiment	Mean	S/N Ratio
1	6.966	-16.8597
2	6.315	-16.0075
3	5.126	-14.1956
4	2.333	-7.3583
5	3.062	-9.7201
6	6.578	-16.3619
7	2.772	-8.8559
8	5.757	-15.2039
9	7.178	-17.1201

Table 4.23 presented the S/N ratio for overall surface roughness (SR) of aluminium sheet in ISF. The regression equation was shown in Eq. (4.2). Angle was represented by A, FR for feed rate, and SS for step size. The R-squared value was 70.6%.

$$SR = 4.16 - 0.0450\,A + 0.00568\,FR - 3.64\,SS \qquad (4.2)$$

Table 4.24: ANOVA for means (surface roughness)

Source	DF	Seq SS	Adj SS	Adj MS	F	P
Angle	2	6.959	3.479	3.479	2.58	0.279
Feed Rate	2	7.758	7.758	3.879	2.87	0.258
Step Size	2	11.703	11.703	5.851	4.34	0.187
Error	2	2.699	2.699	1.350	-	-
Total	8	29.119	-	-	-	-

Table 4.25: ANOVA for S/N ratios (surface roughness)

Source	DF	Seq SS	Adj SS	Adj MS	F	P
Angle	2	31.120	31.120	15.560	3.77	0.210
Feed Rate	2	35.613	35.613	17.807	4.32	0.188
Step Size	2	40.844	40.844	20.422	4.95	0.168
Error	2	8.253	8.253	4.126	-	-
Total	8	115.830	-	-	-	-

Table 4.24 and Table 4.25 showed the ANOVA for mean surface roughness and the respective S/N ratios. It was observed that the step size has the highest F value, which means that it is the most significant parameter affecting the surface roughness and the S/N ratio compared to wall angle and step size.

In order to have a better understanding on the surface roughness of aluminium sheet in ISF, the corners of pyramid frustum with different radius (R5, R10, R15, and R20) were investigated to compare with the overall surface roughness. Table 4.26, 4.27, and 4.28 showed the results for S/N ratio and ANOVA for R5.

Table 4.26: Means and S/N ratios for surface roughness of R5

Experiment	Mean	S/N Ratio
1	6.941	-16.8284
2	4.953	-13.8974
3	6.531	-16.2996
4	1.933	-5.7246
5	3.099	-9.8244
6	8.034	-18.0986
7	2.582	-8.2391
8	13.171	-22.3924
9	11.353	-21.1022

The regression equation for surface roughness of R5 was displayed in Eq. (4.3). The R-squared value was 71.2%.

$$SR = -\,6.97 + 0.145\,A + 0.0121\,FR - 6.64\,SS \qquad (4.3)$$

Table 4.27: ANOVA for means (SR of R5)

Source	DF	Seq SS	Adj SS	Adj MS	F	P
Angle	2	33.467	33.467	16.733	4.26	0.190
Feed Rate	2	36.287	36.287	18.144	4.61	0.178
Step Size	2	43.152	43.152	21.576	5.49	0.154
Error	2	7.864	7.864	3.932	-	-
Total	8	120.770	-	-	-	-

Table 4.28: ANOVA for S/N ratios (SR of R5)

Source	DF	Seq SS	Adj SS	Adj MS	F	P
Angle	2	58.693	58.693	29.346	6.20	0.139
Feed Rate	2	103.707	103.707	51.853	10.96	0.084
Step Size	2	93.651	93.651	46.825	9.90	0.092
Error	2	9.464	9.464	4.732	-	-
Total	8	265.515	-	-	-	-

By looking at the highest F value, Table 4.27 suggested that step size was the most significant parameter affecting the surface roughness of R5 compared to wall angle and feed rate. However, Table 4.28 proved that the S/N ratio for surface roughness of R5 was affected the most by feed rate.

Table 4.29: Means and S/N ratios for surface roughness of R10

Experiment	Mean	S/N Ratio
1	6.392	-16.1127
2	6.387	-16.1059
3	4.066	-12.1833
4	1.437	-3.1491
5	1.822	-5.2110
6	8.729	-18.8193
7	3.106	-9.8440
8	6.700	-16.5215
9	4.916	-13.8322

Table 4.29 showed the S/N ratio for surface roughness of R10. The regression equation for surface roughness of R10 was shown in Eq. (4.4). The R-squared value was 68.1%.

$$SR = 4.41 - 0.0354\,A + 0.00565\,FR - 5.24\,SS \qquad (4.4)$$

Table 4.30: ANOVA for means (SR of R10)

Source	DF	Seq SS	Adj SS	Adj MS	F	P
Angle	2	3.952	3.952	1.976	0.56	0.639
Feed Rate	2	7.729	7.729	3.864	1.10	0.475
Step Size	2	29.003	29.003	14.502	4.14	0.194
Error	2	7.002	7.002	3.501	-	-
Total	8	47.686	-	-	-	-

Table 4.31: ANOVA for S/N ratios (SR of R10)

Source	DF	Seq SS	Adj SS	Adj MS	F	P
Angle	2	53.75	53.75	26.88	1.79	0.358
Feed Rate	2	41.40	41.40	20.70	1.38	0.420
Step Size	2	106.43	106.43	53.22	3.55	0.220
Error	2	30.01	30.01	15.01	-	-
Total	8	231.60	-	-	-	-

In Table 4.30, the most influential parameter for surface roughness of R10 was step size. Moreover, step size also affected its S/N ratio the most according to Table 4.31.

Table 4.32: Means and S/N ratios for surface roughness of R15

Experiment	Mean	S/N Ratio
1	5.573	-14.9218
2	7.748	-17.7838
3	3.764	-11.5130
4	1.601	-4.0878
5	3.392	-10.6091
6	8.058	-18.1245
7	2.281	-7.1625
8	6.738	-16.5706
9	7.696	-17.7253

Table 4.32 revealed the S/N ratio for surface roughness of R15. The regression equation for surface roughness of R15 was stated in Eq. (4.5) with an R-squared value of 75.3%.

$$SR = 0.79 - 0.0062\,A + 0.00839\,FR - 4.89\,SS \tag{4.5}$$

Table 4.33: ANOVA for means (SR of R15)

Source	DF	Seq SS	Adj SS	Adj MS	F	P
Angle	2	3.315	3.315	1.657	0.51	0.663
Feed Rate	2	19.433	19.433	9.717	2.98	0.251
Step Size	2	20.938	20.938	10.469	3.21	0.237
Error	2	6.513	6.513	3.257	-	-
Total	8	50.199	-	-	-	-

Table 4.34: ANOVA for S/N ratios (SR of R15)

Source	DF	Seq SS	Adj SS	Adj MS	F	P
Angle	2	23.57	23.57	11.78	0.88	0.533
Feed Rate	2	89.77	89.77	44.88	3.34	0.230
Step Size	2	68.91	68.91	34.45	2.57	0.280
Error	2	26.86	26.86	13.43	-	-
Total	8	209.10	-	-	-	-

Table 4.33 proved that step size affected the surface roughness of R15 the most, while Table 4.34 showed that feed rate was the most significant parameter to the S/N ratio of surface roughness of R15.

Table 4.35: Means and S/N ratios for surface roughness of R20

Experiment	Mean	S/N Ratio
1	12.141	-21.6851
2	8.428	-18.5145
3	3.298	-10.3650
4	1.115	-0.9455
5	3.400	-10.6296
6	5.206	-14.3301
7	2.627	-8.3892
8	7.680	-17.7072
9	7.989	-18.0498

Table 4.35 showed the S/N ratio for surface roughness of R20. The regression equation for surface roughness of R20 was displayed in Eq. (4.6). The R-squared value was as low as 45.3%.

$$SR = 13.4 - 0.093\ A + 0.00051\ FR - 6.76\ SS \quad (4.6)$$

Table 4.36: ANOVA for means (SR of R20)

Source	DF	Seq SS	Adj SS	Adj MS	F	P
Angle	2	33.85	33.85	16.93	1.52	0.398
Feed Rate	2	2.51	2.51	1.26	0.11	0.899
Step Size	2	41.12	41.12	20.56	1.84	0.352
Error	2	22.34	22.34	11.17	-	-
Total	8	99.82	-	-	-	-

Table 4.37: ANOVA for S/N ratios (SR of R20)

Source	DF	Seq SS	Adj SS	Adj MS	F	P
Angle	2	109.11	109.11	54.56	1.43	0.412
Feed Rate	2	45.00	45.00	22.50	0.59	0.630
Step Size	2	102.36	102.36	51.18	1.34	0.428
Error	2	76.48	76.48	38.24	-	-
Total	8	332.95	-	-	-	-

Table 4.36 revealed that step size is the most significant parameter affecting the surface roughness of R20, while wall angle affected its S/N ratio the most according to Table 4.37.

4.3.2 ANOVA for Thickness Uniformity

Table 4.38 showed the means and S/N ratios for thickness uniformity of aluminium sheet in ISF.

Table 4.38: Means and S/N ratios for thickness uniformity

Experiment	Mean	S/N Ratio
1	0.0031	50.1728
2	0.0117	38.6363
3	0.0240	32.3958
4	0.0225	32.9563
5	0.0224	32.9950
6	0.0087	41.2096
7	0.0203	33.8501
8	0.0247	32.1461
9	0.0213	33.4324

The regression equation for thickness uniformity (TU) was showed in Eq. (4.7). The predictability was not really considerable as the R-squared value was only 56.9%.

$$TU = - 0.0164 + 0.000458\ A + 0.000007\ FR + 0.0126\ SS \qquad (4.7)$$

Table 4.39: ANOVA for means (thickness uniformity)

Source	DF	Seq SS	Adj SS	Adj MS	F	P
Angle	2	0.0001263	0.0001263	0.0000631	0.73	0.579
Feed Rate	2	0.0000283	0.0000283	0.0000142	0.16	0.860
Step Size	2	0.0001554	0.0001554	0.0000777	0.89	0.528
Error	2	0.0001736	0.0001736	0.0000868	-	-
Total	8	0.0004837	-	-	-	-

Table 4.40: ANOVA for S/N ratios (thickness uniformity)

Source	DF	Seq SS	Adj SS	Adj MS	F	P
Angle	2	81.25	81.25	40.62	1.15	0.465
Feed Rate	2	31.53	31.53	15.76	0.45	0.691
Step Size	2	107.30	107.30	53.65	1.52	0.397
Error	2	70.63	70.63	35.32	-	-
Total	8	290.71	-	-	-	-

Table 4.39 showed that step size was the most significant parameter to the thickness uniformity of aluminium sheet in ISF, while its S/N ratio was also affected the most by step size according to Table 4.40.

4.3.4 Parameters Optimisation for Surface Roughness

In order to minimise the surface roughness of aluminium sheet in ISF, optimisation of parameters was done from the results of the 9 experiments. By using Minitab software, response graphs for means and S/N ratios were generated. Figure 4.17 showed the response graphs for surface roughness. Generally, a smaller-is-better S/N ratio that is closer to zero is preferable in this case. On the other hand, the means of surface roughness for each parameters was plotted in the response graph.

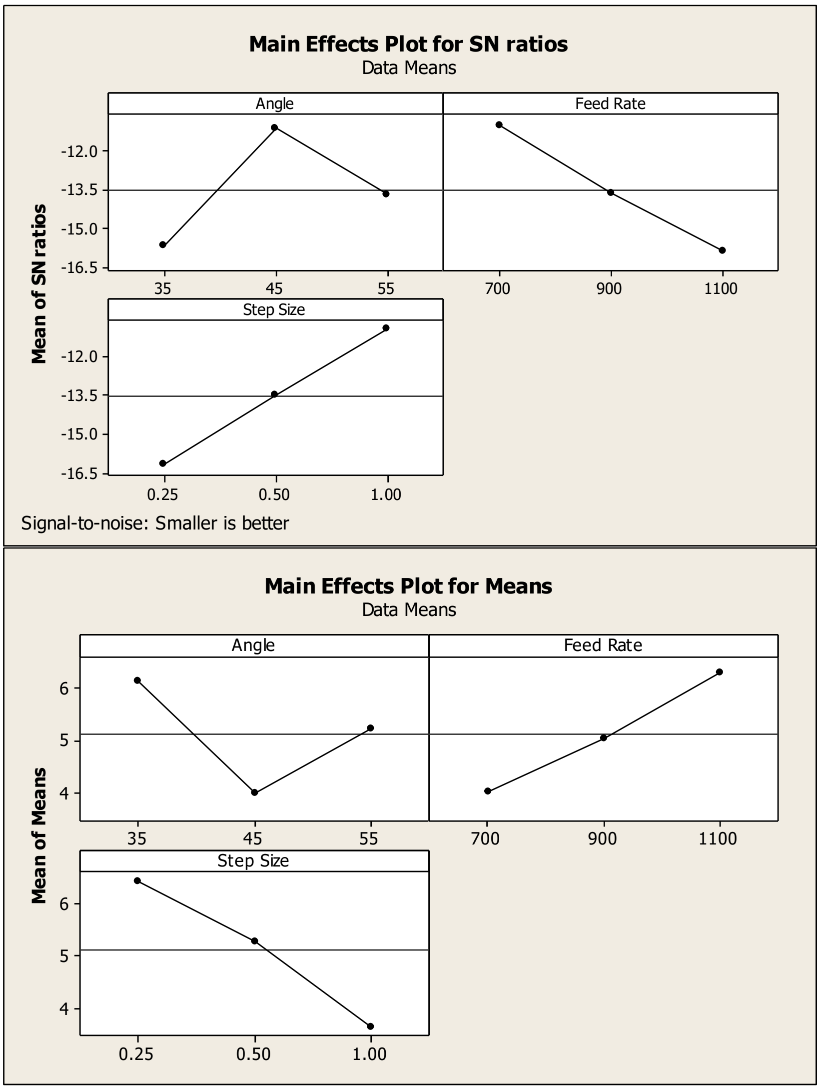

Figure 4.17: Response graph for S/N ratios and means for surface roughness

From the response graph of mean of means (surface roughness) in Figure 4.17, it can be observed that the lowest mean surface roughness recorded for different wall angles was at 45º. Furthermore, the surface roughness will increase along with rising feed rate. While an increase in step size will produce a smoother surface of aluminium sheet.

Table 4.41: Response table for S/N ratio of surface roughness (smaller is better)

Level	Angle	Feed Rate	Step Size
1	-15.69	-11.02	-16.14
2	-11.15	-13.64	-13.50
3	-13.73	-15.89	-10.92
Delta	4.54	4.87	5.22
Rank	3	2	1

Table 4.42: Response table for means (surface roughness)

Level	Angle	Feed Rate	Step Size
1	6.136	4.024	6.434
2	3.991	5.045	5.275
3	5.236	6.294	3.653
Delta	2.145	2.270	2.780
Rank	3	2	1

Table 4.44 and Table 4.45 displayed the response table for S/N ratios and means of surface roughness. The delta ranks represented the significance of the parameters to the response. For the optimisation of parameters to obtain the minimum surface roughness, each parameters with lowest value of mean surface roughness was taken. For example in Table 4.45, the parameters with lowest mean of means are level 2 wall angle (45º), level 1 feed rate (700 mm/min), and level 3 step size (1.00 mm), in which these are the optimized parameters for minimum surface roughness of aluminium sheet.

Detailed observation was done by analysing the mean surface roughness of each corner in the pyramid frustum. Figure 4.18 revealed the response graph for S/N ratios and means for surface roughness of R5.

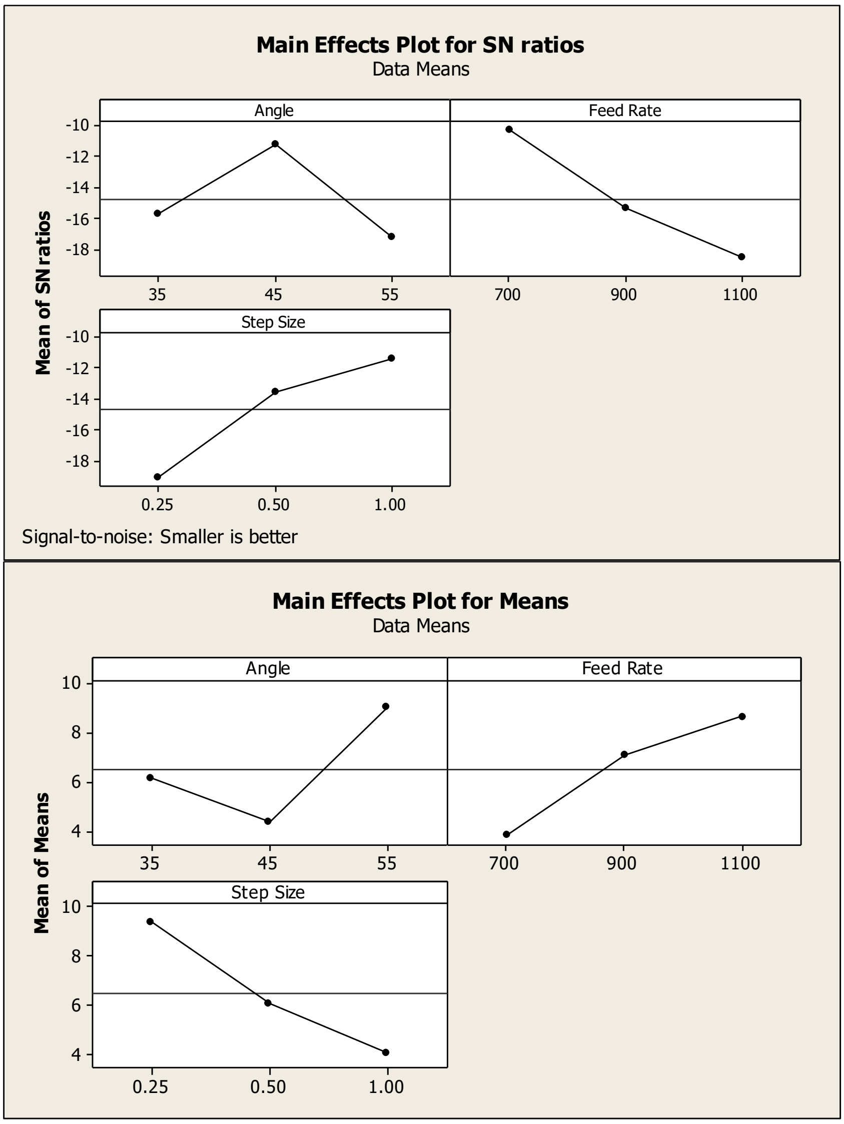

Figure 4.18: Response graph for S/N ratios and means for surface roughness of R5

From the figure above, it can be concluded that wall angle of 45º formed the lowest mean surface roughness of R5. Besides that, an increase in surface roughness of R5 was formed when the feed rate is increased or when the step size is decreased.

Table 4.43: Response table for S/N ratio of surface roughness of R5 (smaller is better)

Level	Angle	Feed Rate	Step Size
1	-15.68	-10.26	-19.11
2	-11.22	-15.37	-13.57
3	-17.24	-18.50	-11.45
Delta	6.03	8.24	7.65
Rank	3	1	2

Table 4.44: Response table for means (surface roughness of R5)

Level	Angle	Feed Rate	Step Size
1	6.142	3.819	9.382
2	4.355	7.074	6.080
3	9.035	8.639	4.071
Delta	4.680	4.821	5.311
Rank	3	2	1

Table 4.46 and Table 4.47 showed the response table for S/N ratio and means for surface roughness of R5 respectively. Table 4.47 concluded that the lowest mean surface roughness of R5 was obtained at level 2 wall angle (45º), level 1 feed rate (700 mm/min), and level 3 step size (1.00 mm). These are the optimised parameters for minimum surface roughness of R5.

Figure 4.19 showed the response graph of S/N ratios and means for surface roughness of R10.

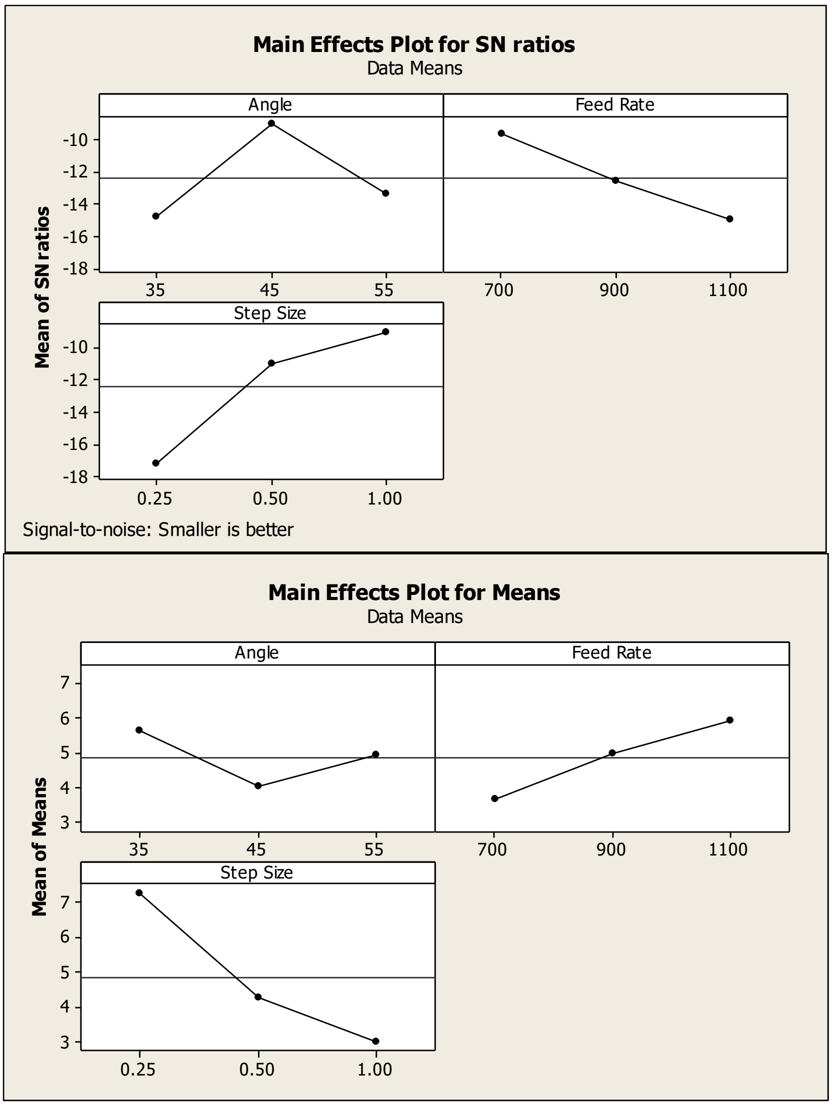

Figure 4.19: Response graph for S/N ratios and means for surface roughness of R10

The response graph of mean of means (surface roughness of R10) showed that the minimum mean surface roughness can be obtained at wall angle of 45º. Besides, the surface roughness increases when the feed rate increases. However, increasing step size will lead to declining of surface roughness.

Table 4.45: Response table for S/N ratio of surface roughness of R10 (smaller is better)

Level	Angle	Feed Rate	Step Size
1	-14.801	-9.702	-17.151
2	-9.060	-12.613	-11.029
3	-13.399	-14.945	-9.079
Delta	5.741	5.243	8.072
Rank	2	3	1

Table 4.46: Response table for means (surface roughness of R10)

Level	Angle	Feed Rate	Step Size
1	5.615	3.645	7.274
2	3.996	4.970	4.247
3	4.907	5.904	2.998
Delta	1.619	2.259	4.276
Rank	3	2	1

Table 4.48 and Table 4.49 showed the response table for S/N ratios and means for surface roughness of R10 respectively. According to Table 4.49, the lowest mean surface roughness of R10 can be observed at level 2 wall angle (45º), level 1 feed rate (700 mm/min), and level 3 step size (1.00 mm) which formed the optimised parameters for minimum surface roughness of R10.

Figure 4.20 revealed the response graph for S/N ratios and means for surface roughness of R15.

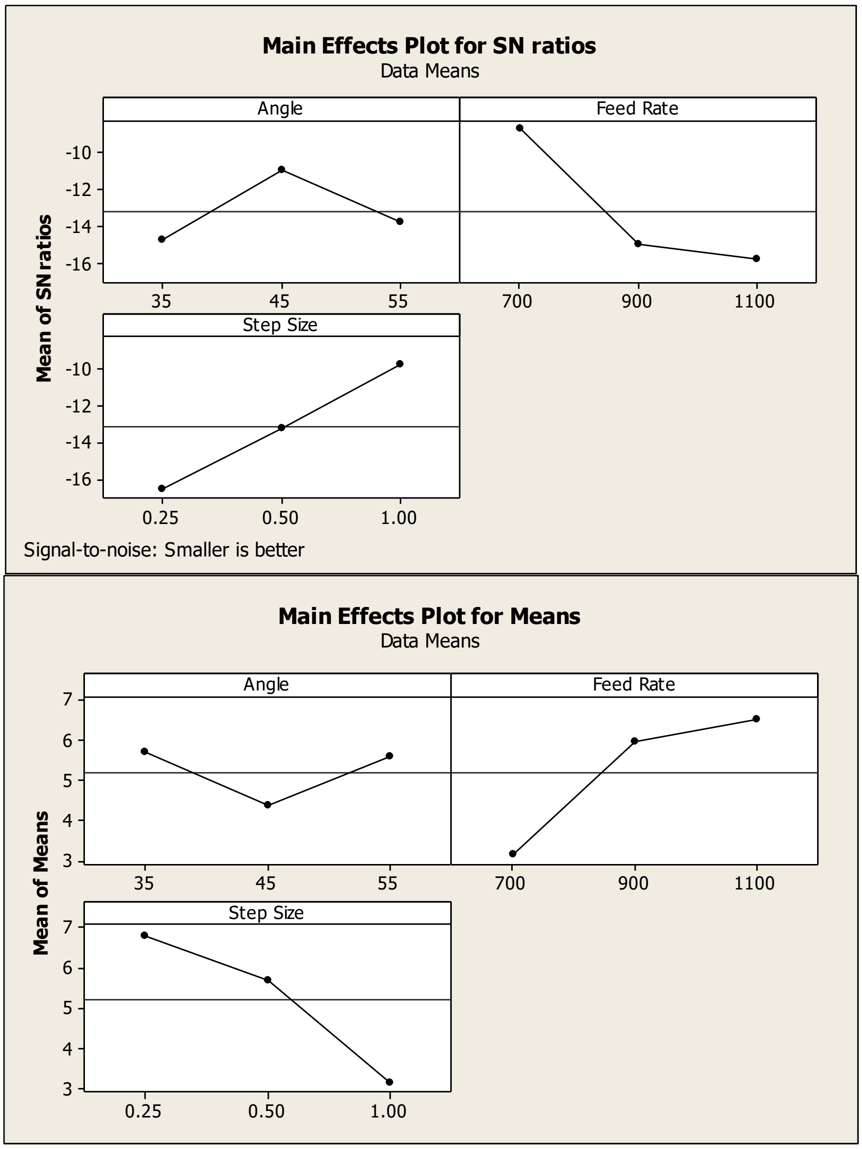

Figure 4.20: Response graph for S/N ratios and means for surface roughness of R15

As seen in response graph of mean of means (surface roughness of R15), the optimum wall angle for minimum mean surface roughness can be obtained at 45°. While the increasing of feed rate and decreasing of step size will increase the mean surface roughness of R15.

Table 4.47: Response table for S/N ratio of surface roughness of R15 (smaller is better)

Level	Angle	Feed Rate	Step Size
1	-14.740	-8.724	-16.539
2	-10.940	-14.988	-13.199
3	-13.819	-15.788	-9.762
Delta	3.799	7.064	6.777
Rank	3	1	2

Table 4.48: Response table for means of surface roughness of R15

Level	Angle	Feed Rate	Step Size
1	5.695	3.152	6.790
2	4.350	5.959	5.682
3	5.572	6.506	3.146
Delta	1.345	3.354	3.644
Rank	3	2	1

The response table for S/N ratios and means for surface roughness of R15 was shown in Table 4.50 and Table 4.51 respectively. It can be concluded from Table 4.51 that the lowest mean surface roughness of R15 can be obtained at level 2 wall angle (45º), level 1 feed rate (700 mm/min), and level 3 step size (1.00 mm). These are the optimised parameters for minimum surface roughness of R15.

The response graph for S/N ratios and means for surface roughness of R20 was displayed in Figure 4.21.

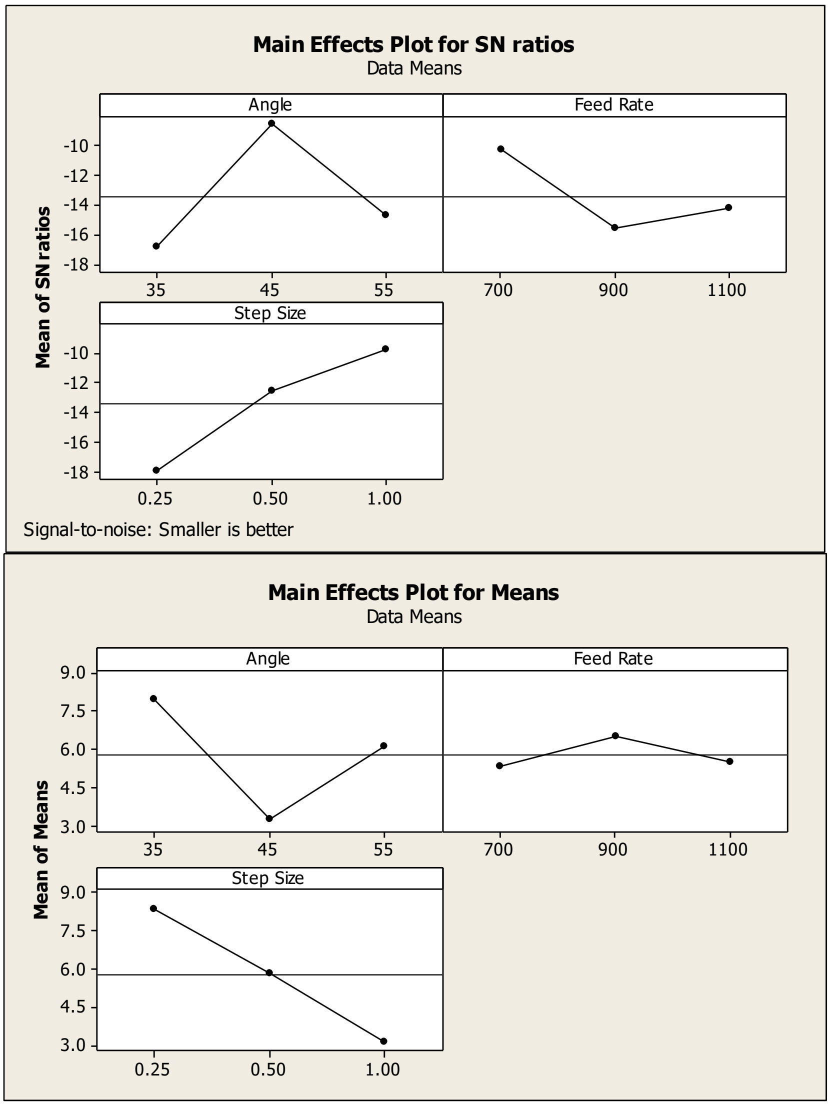

Figure 4.21: Response graph for S/N ratios and means for surface roughness of R20

From the observation of response graph of mean of means (surface roughness of R20), 45º is the optimum wall angle to obtain minimum mean surface roughness of R20. Besides, growth in step size will lead to decline of surface roughness. However, the result for feed rate showed a different pattern as compared with the previous graphs, where the surface roughness drops at 1100 mm/min instead of increasing. The lowest mean surface roughness can be observed at 700 mm/min.

Table 4.49: Response table for S/N ratio of surface roughness of R20 (smaller is better)

Level	Angle	Feed Rate	Step Size
1	-16.855	-10.340	-17.907
2	-8.635	-15.617	-12.503
3	-14.715	-14.248	-9.795
Delta	8.220	5.277	8.113
Rank	1	3	2

Table 4.50: Response table for means of surface roughness of R20

Level	Angle	Feed Rate	Step Size
1	7.956	5.294	8.342
2	3.240	6.503	5.844
3	6.099	5.498	3.108
Delta	4.715	1.208	5.234
Rank	2	3	1

Table 4.52 showed the response table for S/N ratio of surface roughness of R20, and Table 4.53 showed the response table for means of surface roughness of R20. As stated in Table 4.53, the least mean surface roughness can be seen at level 2 wall angle (45º), level 1 feed rate (700 mm/min), and level 3 step size (1.00 mm).

4.3.5 Parameters Optimisation for Uniform Thickness Reduction

Figure 4.22 displayed the response graph for S/N ratios and means for thickness uniformity of aluminium sheet.

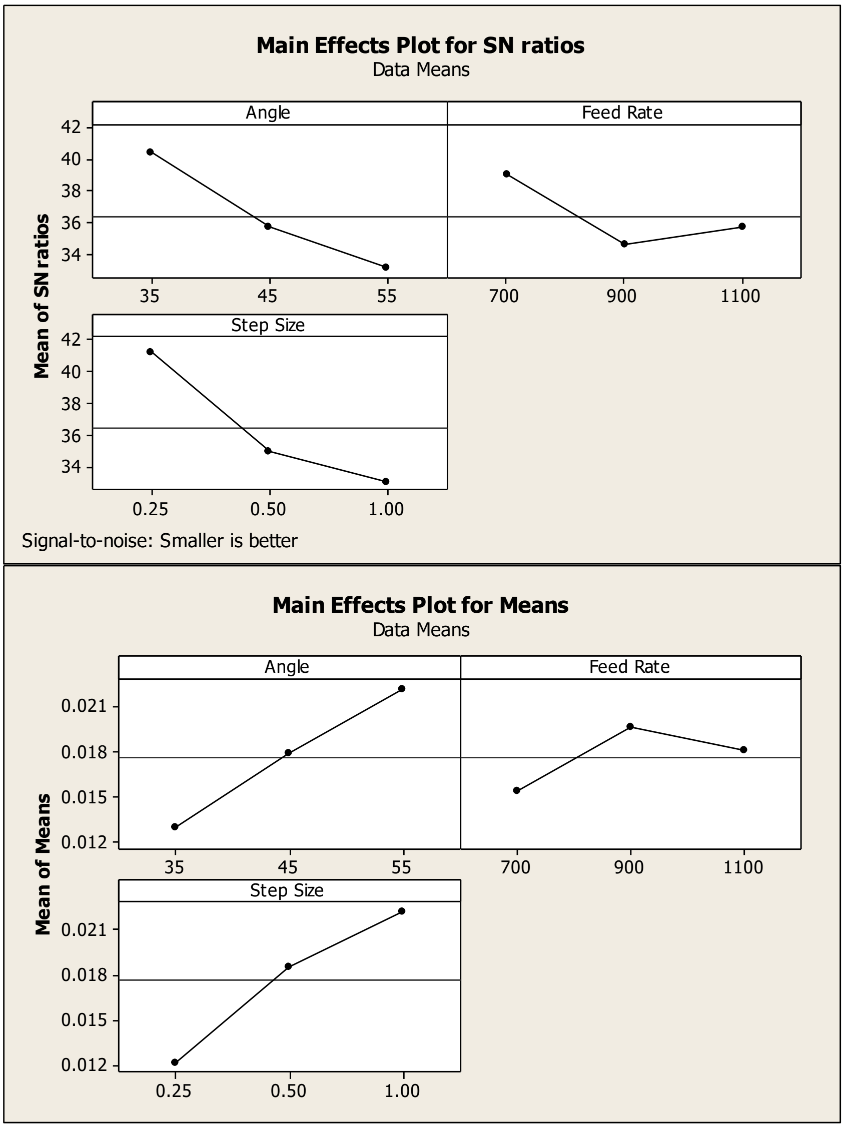

Figure 4.22: Response graph for S/N ratios and means for thickness uniformity

From the response graph of mean of means (thickness uniformity), increase in wall angle and step size caused the thickness of aluminium sheet less uniform. On the other hand, the thickness uniformity decreased at 900 mm/min and rose at 1100 mm/min.

Table 4.51: Response table for S/N ratio of thickness uniformity (smaller is better)

Level	Angle	Feed Rate	Step Size
1	40.40	38.99	41.18
2	35.72	34.59	35.01
3	33.14	35.68	33.08
Delta	7.26	4.40	8.10
Rank	2	3	1

Table 4.52: Response table for means (thickness uniformity)

Level	Angle	Feed Rate	Step Size
1	0.01293	0.01530	0.01217
2	0.01787	0.01960	0.01850
3	0.02210	0.01800	0.2223
Delta	0.00917	0.00430	0.01007
Rank	2	3	1

Table 4.54 and Table 4.55 displayed the response table for S/N ratios and means for thickness uniformity. The value was stated in the form of standard deviation, therefore a lower value represents better uniformity. It can be concluded from Table 4.55 that the best thickness uniformity can be acquired at level 1 wall angle (35°), level 1 feed rate (700 mm/min), and level 1 step size (0.25 mm), in which these are the parameters for Experiment 1.

4.3.7 Confirmation Test

A confirmation test was carried out to verify the results of parameters optimisation. The optimised parameters for surface roughness and thickness uniformity was summarised in Table 4.58. However, the optimised parameters for thickness uniformity was exactly same with Experiment 1, therefore a confirmation test was not required. The result of average surface roughness with optimised parameters was revealed in Table 4.50.

Table 4.53: Optimised parameters for each outcome

Optimisation	Angle	Feed Rate (mm/min)	Step Size (mm)
Surface Roughness	45º	700	1.00
Thickness Uniformity	35º	700	0.25

Table 4.54: Average surface roughness of aluminium sheet for optimised parameters

	Surface Roughness (µm)			
	Trial 1	**Trial 2**	**Trial 3**	**Average**
Area A	1.160	1.637	1.747	1.515
Area B	1.962	1.587	1.884	1.811
Area C	1.475	1.631	1.830	1.645
Area D	1.327	2.222	1.866	1.805
R5	0.931	1.048	0.677	0.885
R10	1.316	1.587	1.789	1.564
R15	2.307	2.430	2.133	2.290
R20	2.245	1.973	2.149	2.122
			Overall	1.705

By using the regression equations as stated in Eq. (4.2) to Eq. (4.6) for the optimised parameters, the predicted value of surface roughness was calculated and used to compare with the actual surface roughness in the confirmation test. The results were shown in Table 4.60.

Table 4.55: Comparison of actual surface roughness with the predicted value

Area	**Surface Roughness (μm)**			**Error (%)**
	Prediction	**Actual**	**Difference**	
Overall	2.469	1.705	0.764	30.9437
R5	1.332	0.885	0.447	33.5586
R10	1.525	1.564	0.039	2.5574
R15	1.491	2.290	0.799	53.5882
R20	2.85	2.122	0.728	25.5439

From Table 4.60, it can be observed that the difference between the predicted and actual surface roughness of aluminium sheet showed a relatively high error percentage except for area R5.

4.4 Discussions

4.4.1 Surface Roughness

Durante et al (2009) had proposed that the presence or absence of tool rotation will affects the value of surface roughness within the range of 10%. Initially, these experiments was intended to carry out with a spindle speed of 1500 rpm as suggested by Echrif and Hrairi (2014) where they produced the best result for surface roughness. Unfortunately, major scratching was found on the surface of the aluminium sheet with the indicated spindle speed in these experiments, causing undesirable surface finish to be produced. Therefore, the surface roughness test was neglected. One of the surface of the aluminium sheet with 1500 rpm spindle speed was shown in Figure 4.23.

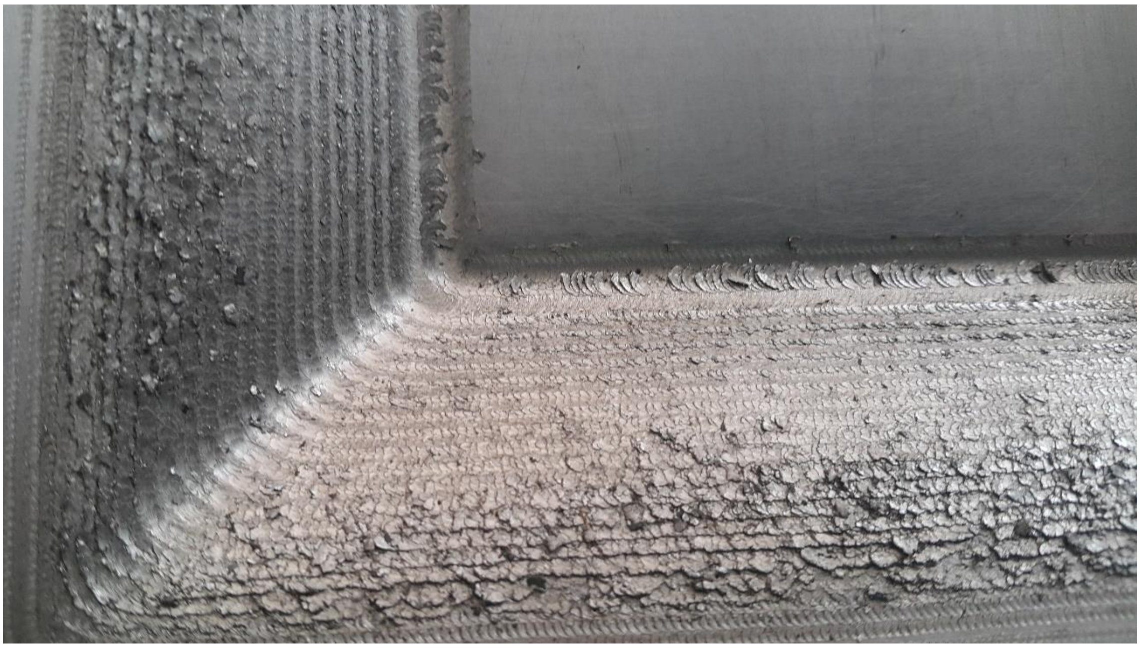

Figure 4.23: Surface of aluminium sheet with 1500 rpm spindle speed

In order to eliminate or reduce the unwanted scratches on the aluminium sheet surface, tool rotation was disabled for all experiments. In addition, lubricant was applied to the tip of forming tool in the beginning of each experiment. The scratches were greatly reduced and better surface finish was produced. It was believed that tool rotation generated more friction and surface contact between the tool and sheet, moreover no lubrication was involved, and hence it caused rough scratching to occur along the sheet.

The surface roughness of aluminium sheet with optimised parameters appeared to be the lowest as compared with all the previous experiments. However, it showed a significant amount of error percentage relative to the predicted value using regression equations. This is because the regression equations have an R-squared value ranged from 45.3% to 75.3% only, in which it could represents the probability that an actual value tally with the prediction obtained from the regression equation. In other words, this was also known as the confidence level. Thus, it was expected to have an error percentage ranged from 24.7% to 54.7%. However, only the result for R10 showed a notable low value of error percentage as compared with the others which is way below the error range.

4.4.2 Thickness Uniformity

The thickness uniformity of aluminium sheet was measured in term of standard deviation of the thickness, where a lower value indicates that the thicknesses are closer to the mean, therefore it means a more uniform thickness. It was observed from the analysis of results that increasing of step size and wall angle will reduce the thickness uniformity, where the former parameter influenced the most to the thickness uniformity followed by the latter one.

Besides that, Figure 4.15 clearly revealed that the surface roughness and thickness uniformity were varied inversely. This finding has proved that better surface roughness does not come along with uniform thickness reduction, which can be explained by the effect of surface waviness as proposed by Echrif and Hrairi (2014). In addition, step size played an important role in the formation of surface waviness as illustrated in Figure 4.24.

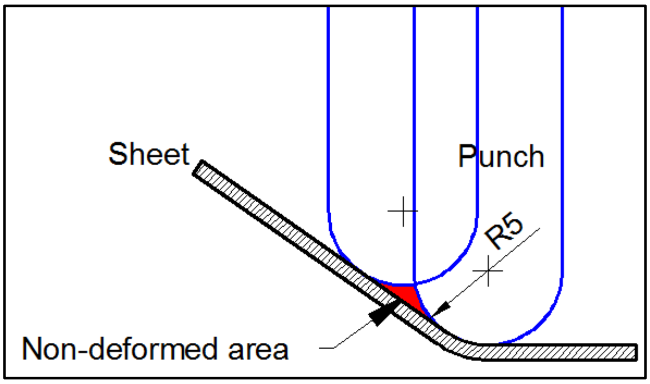

Figure 4.24: Formation of surface waviness in ISF

As seen in Figure 4.24, the highlighted red area is the region where the sheet is not deformed during ISF due to the gap of punch between the paths which did not contact the sheet. A lower step size will reduce the size of the surface waviness and lead to better surface roughness, but the number of non-deformed area will increased, which caused the sheet thickness to be less uniform. On the other hand, forming tool with larger diameter can help to decrease the size of surface waviness.

Figure 4.25 showed the interface of Precision Plotter software associated with the video profile measuring system to observe the cross section of the aluminium sheets.

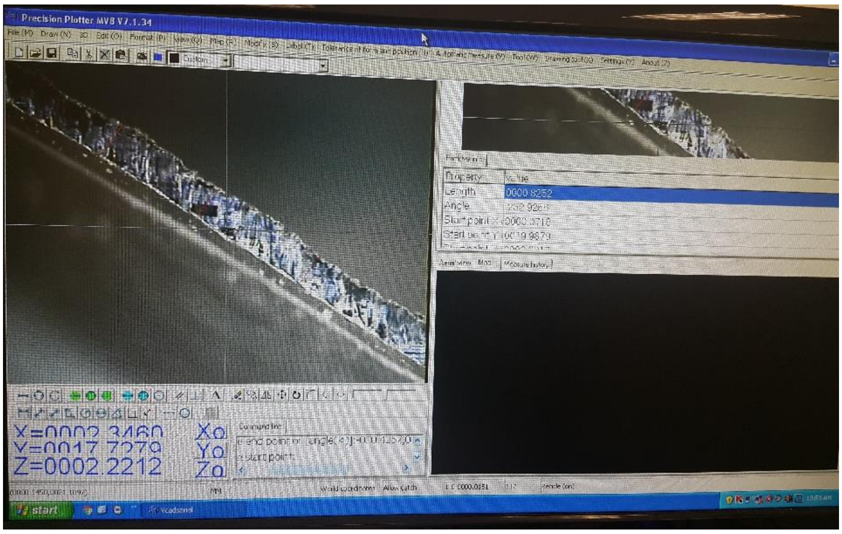

Figure 4.25: Interface of Precision Plotter software

CHAPTER 5

CONCLUSIONS AND RECOMMENDATIONS

5.1 Conclusions

In this project, the optimised parameters for minimum surface roughness and uniform thickness reduction in ISF has been determined via Taguchi analysis. From the design of experiments, the optimum parameters for minimum surface roughness was 45º wall angle, 700 mm/min feed rate, and 1.00 mm step size. On the other hand, uniform thickness of aluminium sheet was optimised at 35º wall angle, 700 mm/min feed rate, and 0.25 mm step size.

Besides that, the effect of each parameters to the surface roughness and thickness uniformity has been investigated. Increase in step size and decrease in feed rate will improve the surface roughness of aluminium sheet in ISF. While decrease in wall angle and step size will produce a sheet with better thickness uniformity. According to the results of ANOVA, step size was the most significant parameter to both the surface roughness and thickness uniformity of aluminium sheet.

5.2 Recommendations

They are a few recommendations that can be done to improve the outcome of this project in the future. Firstly, the blank holder along with the clamping device in this project did not provide a uniform clamping force to the aluminium sheet, which caused the force to concentrate on the left side and right side of the sheet only. While it is still unknown whether it will affect the surface roughness or thickness reduction or not, the geometric accuracy was noticeably affected as seen in this project due to the springback effect of the sheet. The sides with concentrated clamping force will have less springback effect after the ISF process, and it can only be observed after the blank holder was removed. Therefore, a blank holder with uniform clamping force such as metal plates with screws is highly recommended to improve the geometric accuracy of aluminium sheet in ISF.

Another recommendation for this project is the thickness measurement of aluminium sheet. Due to the limitation of tools, the thickness of aluminium sheet in this project was investigated using the video profile measurement system and measured manually using point-to-point method in the Precision Plotter software. Although the measurement have a precision up to 3 decimal places, it might not be accurate due to parallax error as the aluminium sheet might not in an absolute upright position, and the points chosen might not be on the exact actual position. Hence, a point micrometer is a recommended tool in measuring the thickness of aluminium sheet for improved accuracies.

Last but not least, the predictability of the surface roughness and thickness uniformity could be improved by increase the number of experiments. For the best result, a full-factorial run for the design of experiments is highly recommended to obtain a better regression fit of results.

REFERENCES

This thesis is prepared based on the following references;

Ambrogio, G., Cozza, V., Filice, L., & Micari, F. (2007). An analytical model for improving precision in single point incremental forming. *Journal of Materials Processing Technology*, *191*(1-3), 92–95.

Duflou, J., Tunçkol, Y., Szekeres, A., & Vanherck, P. (2007). Experimental study on force measurements for single point incremental forming. *Journal of Materials Processing Technology*, *189*(1-3), 65–72.

Durante, M., Formisano, A., Langella, A., & Capece Minutolo, F. M. (2009). The influence of tool rotation on an incremental forming process. *Journal of Materials Processing Technology*, *209*(9), 4621–4626.

Emmens, W. C., Sebastiani, G., & van den Boogaard, a. H. (2010). The technology of Incremental Sheet Forming-A brief review of the history. *Journal of Materials Processing Technology*, *210*(8), 981–997.

Hamilton, K., & Jeswiet, J. (2010). Manufacturing Technology Single point incremental forming at high feed rates and rotational speeds : Surface and structural consequences. *CIRP Annals - Manufacturing Technology*, *59*(1), 311–314.

Han, F., Mo, J. H., Qi, H. W., Long, R. F., Cui, X. H., & Li, Z. W. (2013). Springback prediction for incremental sheet forming based on FEM-PSONN technology. *Transactions of Nonferrous Metals Society of China (English Edition)*, *23*(4), 1061–1071.

Jackson, K., & Allwood, J. (2009). The mechanics of incremental sheet forming. *Journal of Materials Processing Technology*, *209*(3), 1158–1174.

Jeswiet, J., Micari, F., Hirt, G., Bramley, A., Duflou, J., & Allwood, J. (2005). Asymmetric Single Point Incremental Forming of Sheet Metal. *CIRP Annals - Manufacturing Technology*, *54*(2), 88–114.

Kim, Y. . H., & Park, J. . J. (2002). Effect of process parameters on formability in incremental forming of sheet metal. *Journal of Materials Processing Technology*, *130-131*(3), 42–46.

Malwad, D. S., & Nandedkar, V. M. (2014). Deformation Mechanism Analysis of Single Point Incremental Sheet Metal Forming. *Procedia Materials Science*, *6*(Icmpc), 1505–1510.

Oleksik, V. (2014). Influence of Geometrical Parameters, Wall Angle and Part Shape on Thickness Reduction of Single Point Incremental Forming. *Procedia Engineering, 81*, 2280–2285.

Park, J.-J., & Kim, Y.-H. (2003). Fundamental studies on the incremental sheet metal forming technique. *Journal of Materials Processing Technology*, *140*(1-3), 447–453.

Pohlak, M., Majak, J., & Küttner, R. (2007). Manufacturability and limitations in incremental sheet forming. *Proceedings of the Estonian Academy of Sciences (Engineering)*, *13*(2), 129–138.

Strano, M. (2005). Technological representation of forming limits for negative incremental forming of thin aluminum sheets. *Journal of Manufacturing Processes*, *7*(2), 122–129.

APPENDIX A1

Gantt Chart of FYP 1

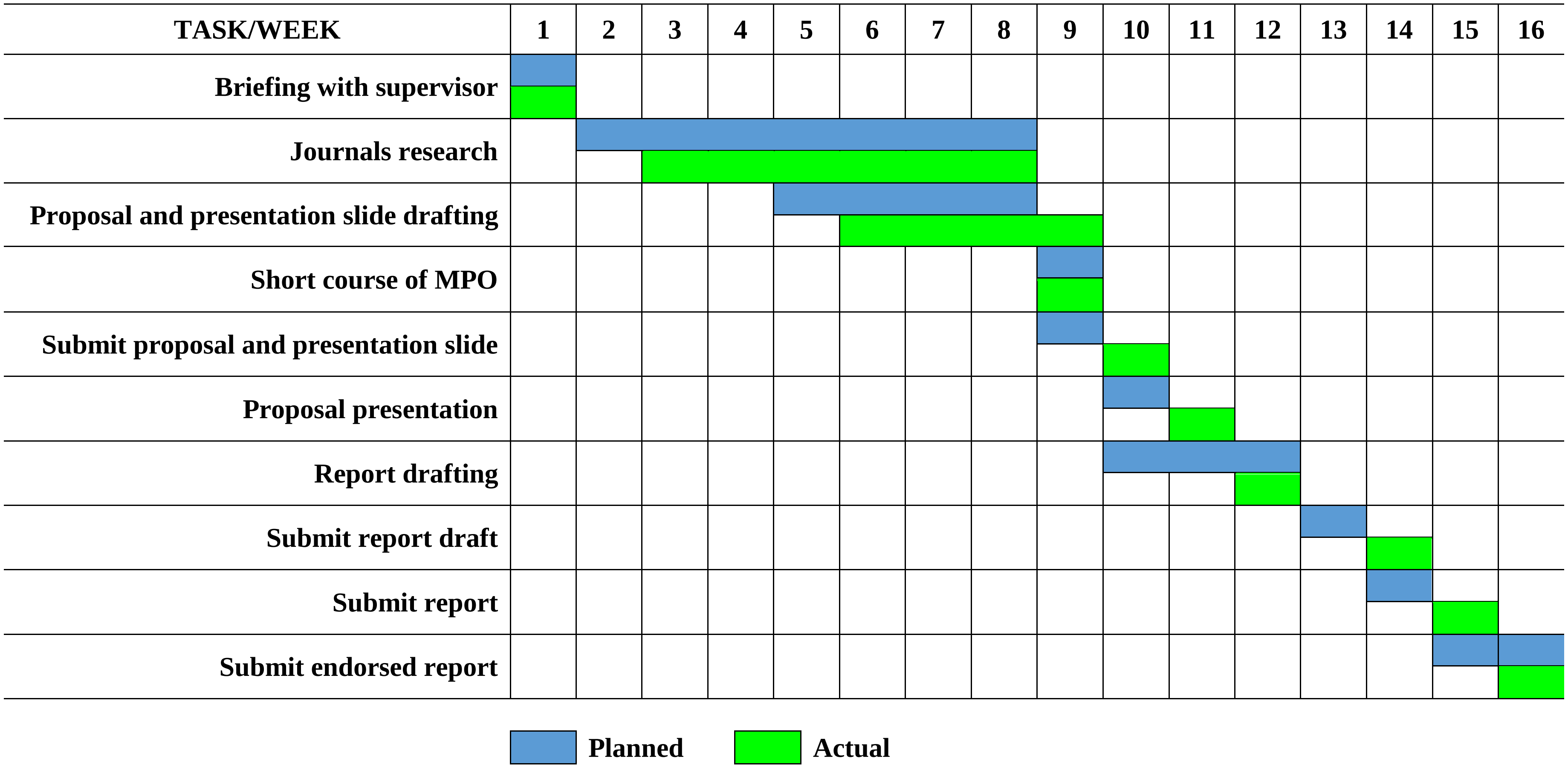

Appendix A2

Gantt Chart of FYP 2

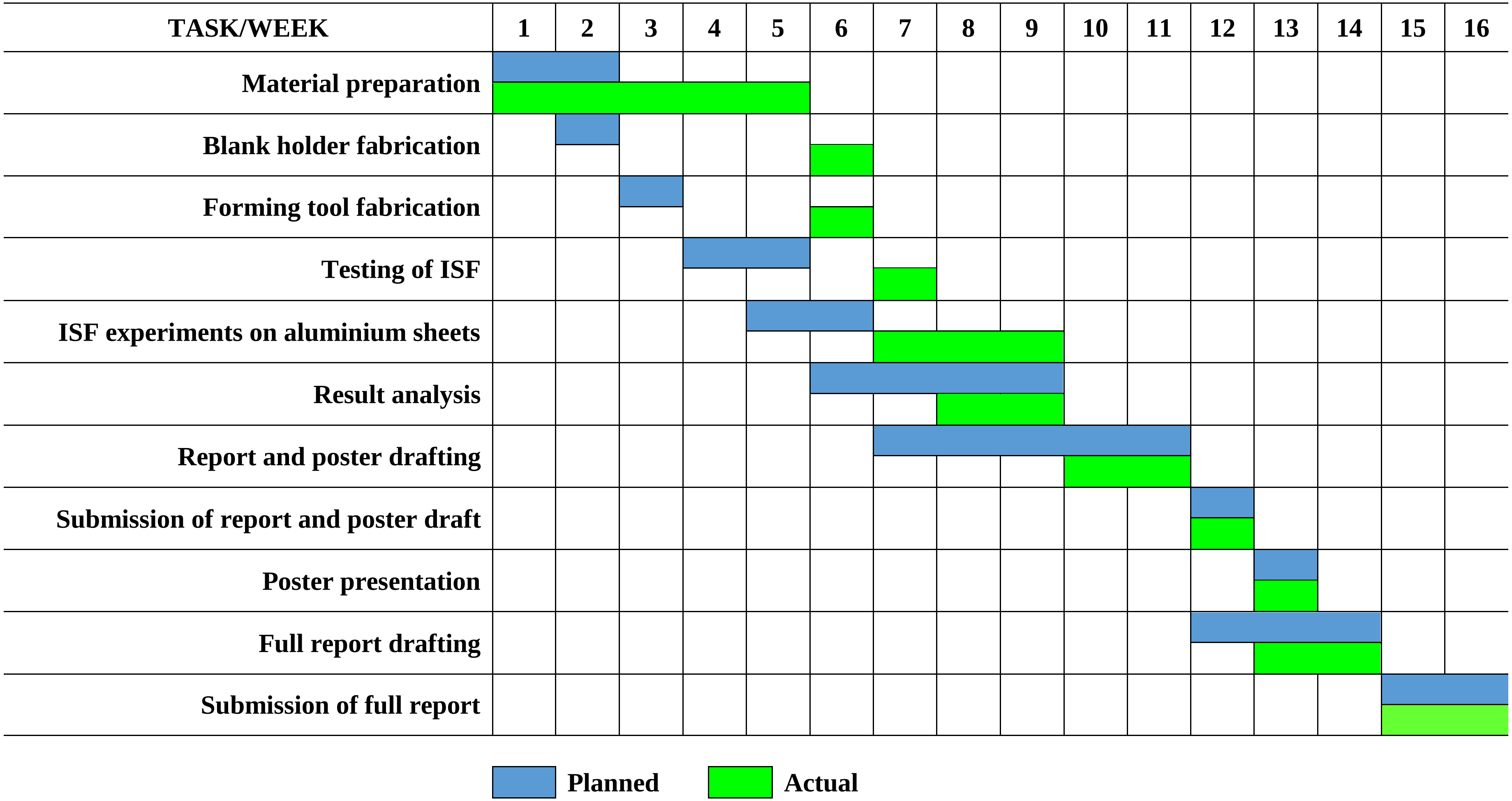

Appendix B1

G-code of optimum parameters for minimum surface roughness

```
%
O1990
N1 G90 G54 X0 Y0 Z100
N2 G21 T1 M5
N3 G0 X39.019 Y173.408
N4 G43 Z50. H1
N5 Z9.
N6 G1 Z-1. F300.
N7 X36.022 Y172.759 F700.
N8 X33.826 Y171.875
N9 X32.026 Y170.77
N10 X30.726 Y169.67
N11 X29.455 Y168.27
N12 X27.886 Y165.679
N13 X27.05 Y163.35
N14 X26.424 Y159.839
N15 X26.402 Y157.992
N16 X26.329 Y63.133
N17 X26.401 Y31.534
N18 X26.543 Y29.825
N19 X26.937 Y28.683
N20 X27.73 Y27.626
N21 X28.971 Y26.769
N22 X30.596 Y26.405
N23 X64.779 Y26.329
N24 X164.919 Y26.401
N25 X167.091 Y26.564
N26 X169.076 Y27.095
N27 X170.378 Y27.786
N28 X171.931 Y29.247
N29 X172.893 Y30.888
N30 X173.389 Y32.53
N31 X173.601 Y34.929
N32 X173.671 Y129.787
N33 X173.597 Y161.488
N34 X173.412 Y164.211
N35 X172.843 Y166.543
N36 X172.037 Y168.313
N37 X170.993 Y169.826
N38 X168.85 Y171.716
N39 X166.518 Y172.849
N40 X163.553 Y173.537
N41 X161.473 Y173.599
N42 X71.928 Y173.671
N43 X42.272 Y173.6
N44 X39.019 Y173.408
N45 Z9. F1000.
N46 G0 Z50.
N47 X38.775 Y171.206
N48 Z9.9
N49 G1 Z-.1 F300.
N50 Z-2.
N51 X36.668 Y170.751 F700.
N52 X34.803 Y170.04
N53 X33.164 Y169.072
N54 X31.901 Y167.98
N55 X30.684 Y166.489
N56 X29.802 Y164.866
N57 X29.098 Y162.77
N58 X28.65 Y160.218
N59 X28.551 Y158.15
N60 X28.495 Y148.111
N61 X28.55 Y31.078
N62 X28.813 Y29.6
N63 X29.411 Y28.911
N64 X31.059 Y28.551
N65 X154.263 Y28.495
N66 X165.416 Y28.555
N67 X168.446 Y29.107
N68 X169.184 Y29.472
N69 X170.154 Y30.295
N70 X171.078 Y31.928
N71 X171.444 Y34.36
N72 X171.505 Y44.809
N73 X171.451 Y161.433
N74 X171.283 Y163.955
N75 X170.909 Y165.716
N76 X170.189 Y167.402
N77 X169.058 Y168.896
N78 X167.286 Y170.252
N79 X165.989 Y170.79
N80 X163.982 Y171.277
N81 X161.476 Y171.451
N82 X152.261 Y171.504
N83 X42.272 Y171.451
N84 X38.775 Y171.206
N85 Z8. F1000.
N86 G0 Z50.
N87 X39.622 Y169.855
N88 Z9.195
```

```
N89 G1 Z-.805 F300.
N90 Z-3.
N91 X37.134 Y169.317 F700.
N92 X35.748 Y168.812
N93 X34.048 Y167.831
N94 X32.96 Y166.879
N95 X31.949 Y165.637
N96 X31.189 Y164.245
N97 X30.205 Y161.065
N98 X29.953 Y159.169
N99 X29.916 Y82.222
N100 X29.955 Y31.484
N101 X30.196 Y30.206
N102 X30.794 Y29.926
N103 X31.874 Y29.955
N104 X84.672 Y29.916
N105 X164.797 Y29.955
N106 X165.692 Y29.944
N107 X168.299 Y30.713
N108 X169.254 Y31.635
N109 X169.774 Y32.873
N110 X170.046 Y34.978
N111 X170.084 Y110.8
N112 X170.045 Y161.436
N113 X169.852 Y163.645
N114 X169.58 Y164.814
N115 X168.89 Y166.609
N116 X167.522 Y168.257
N117 X166.49 Y168.955
N118 X164.376 Y169.725
N119 X162.538 Y170.044
N120 X90.35 Y170.084
N121 X42.393 Y170.045
N122 X39.622 Y169.855
N123 Z7. F1000.
N124 G0 Z50.
N125 X39.677 Y168.639
N126 Z8.562
N127 G1 Z-1.438 F300.
N128 Z-4.
N129 X38.119 Y168.302 F700.
N130 X36.821 Y167.817
N131 X35.033 Y166.816
N132 X33.941 Y165.864
N133 X33.026 Y164.745
N134 X32.182 Y163.232
N135 X31.637 Y161.682
N136 X31.3 Y159.87
N137 X31.208 Y158.213
N138 X31.161 Y139.48
N139 X31.21 Y31.244
N140 X31.509 Y31.206
N141 X145.302 Y31.161
N142 X164.904 Y31.206
N143 X166.982 Y31.553
N144 X167.73 Y32.022
N145 X168.54 Y33.22
N146 X168.79 Y34.809
N147 X168.839 Y53.44
N148 X168.794 Y161.37
N149 X168.53 Y163.973
N150 X167.904 Y165.577
N151 X167.236 Y166.558
N152 X166.464 Y167.312
N153 X165.536 Y167.93
N154 X163.522 Y168.62
N155 X161.487 Y168.793
N156 X144.193 Y168.838
N157 X42.284 Y168.794
N158 X39.677 Y168.639
N159 Z6. F1000.
N160 G0 Z50.
N161 X40.787 Y167.651
N162 Z7.893
N163 G1 Z-2.107 F300.
N164 Z-5.
N165 X38.94 Y167.252 F700.
N166 X37.749 Y166.79
N167 X36.018 Y165.801
N168 X34.106 Y163.853
N169 X33.227 Y162.333
N170 X32.697 Y160.888
N171 X32.311 Y158.963
N172 X32.217 Y157.408
N173 X32.212 Y32.279
N174 X32.377 Y32.212
N175 X164.354 Y32.213
N176 X166.03 Y32.575
N177 X166.575 Y32.898
N178 X167.502 Y34.121
N179 X167.786 Y35.615
N180 X167.787 Y160.846
N181 X167.513 Y163.037
N182 X166.918 Y164.545
N183 X166.255 Y165.528
N184 X164.707 Y166.83
N185 X162.606 Y167.603
N186 X160.621 Y167.788
N187 X42.835
N188 X40.787 Y167.651
```

```
N189 Z5. F1000.
N190 G0 Z50.
N191 X41.853 Y166.654
N192 Z8.084
N193 G1 Z-1.916 F300.
N194 Z-6.
N195 X39.802 Y166.211 F700.
N196 X38.68 Y165.763
N197 X37.002 Y164.787
N198 X35.087 Y162.838
N199 X34.278 Y161.435
N200 X33.722 Y159.984
N201 X33.338 Y158.162
N202 X33.213 Y156.396
N203 X33.212 Y33.314
N204 X33.216 Y33.212
N205 X163.3
N206 X164.088 Y33.281
N207 X165.4 Y33.769
N208 X166.407 Y34.907
N209 X166.783 Y36.524
N210 X166.784 Y160.015
N211 X166.666 Y161.319
N212 X166.314 Y162.675
N213 X165.212 Y164.586
N214 X163.754 Y165.805
N215 X161.689 Y166.586
N216 X159.782 Y166.788
N217 X43.888
N218 X41.853 Y166.654
N219 Z4. F1000.
N220 G0 Z50.
N221 X42.93 Y165.66
N222 Z7.809
N223 G1 Z-2.192 F300.
N224 Z-7.
N225 X40.688 Y165.174 F700.
N226 X39.615 Y164.738
N227 X37.985 Y163.771
N228 X36.167 Y161.946
N229 X35.266 Y160.421
N230 X34.63 Y158.646
N231 X34.215 Y155.487
N232 X34.212 Y34.246
N233 X34.528 Y34.212
N234 X162.247
N235 X163.562 Y34.394
N236 X164.619 Y34.93
N237 X165.514 Y36.147
N238 X165.785 Y37.536
N239 X165.783 Y159.082
N240 X165.53 Y160.971
N241 X164.857 Y162.667
N242 X164.161 Y163.642
N243 X162.799 Y164.78
N244 X160.769 Y165.569
N245 X158.935 Y165.786
N246 X44.449 Y165.783
N247 X42.93 Y165.66
N248 Z3. F1000.
N249 G0 Z50.
N250 X44.022 Y164.668
N251 Z8.069
N252 G1 Z-1.931 F300.
N253 Z-8.
N254 X41.589 Y164.142 F700.
N255 X40.554 Y163.713
N256 X38.76 Y162.609
N257 X37.252 Y161.055
N258 X36.319 Y159.523
N259 X35.654 Y157.742
N260 X35.217 Y154.578
N261 X35.212 Y35.281
N262 X35.367 Y35.212
N263 X161.194
N264 X162.755 Y35.448
N265 X163.64 Y35.946
N266 X164.516 Y37.159
N267 X164.785 Y38.547
N268 X164.788 Y157.741
N269 X164.777 Y158.25
N270 X164.266 Y160.8
N271 X163.187 Y162.613
N272 X161.955 Y163.677
N273 X159.848 Y164.551
N274 X158.082 Y164.783
N275 X45.499
N276 X44.022 Y164.668
N277 Z2. F1000.
N278 G0 Z50.
N279 X45.132 Y163.68
N280 Z7.768
N281 G1 Z-2.232 F300.
N282 Z-9.
N283 X42.501 Y163.111 F700.
N284 X41.126 Y162.507
N285 X38.999 Y160.921
N286 X37.824 Y159.439
N287 X36.85 Y157.387
N288 X36.397 Y155.55
```

N289 X36.213 Y153.259
N290 X36.212 Y36.214
N291 X36.68 Y36.212
N292 X160.141
N293 X161.821 Y36.473
N294 X162.662 Y36.962
N295 X163.477 Y38.059
N296 X163.787 Y39.661
N297 X163.788 Y156.707
N298 X163.648 Y158.416
N299 X163.242 Y159.863
N300 X162.138 Y161.67
N301 X160.494 Y162.951
N302 X158.926 Y163.533
N303 X156.791 Y163.787
N304 X47.047 Y163.788
N305 X45.132 Y163.68
N306 Z1. F1000.
N307 G0 Z50.
N308 X46.262 Y162.697
N309 Z8.022
N310 G1 Z-1.978 F300.
N311 Z-10.
N312 X43.421 Y162.082 F700.
N313 X42.439 Y161.665
N314 X40.724 Y160.578
N315 X39.319 Y159.149
N316 X38.361 Y157.612
N317 X37.412 Y154.644
N318 X37.214 Y152.35
N319 X37.212 Y37.249
N320 X37.519 Y37.212
N321 X159.088
N322 X160.885 Y37.499
N323 X161.682 Y37.978
N324 X162.483 Y39.072
N325 X162.787 Y40.673
N326 X162.788 Y155.774
N327 X162.763 Y156.485
N328 X162.326 Y158.641
N329 X161.574 Y160.116
N330 X160.041 Y161.626
N331 X158.001 Y162.515
N332 X155.935 Y162.784
N333 X47.608 Y162.783
N334 X46.262 Y162.697
N335 Z0 F1000.
N336 G0 Z50.
N337 X46.248 Y161.568
N338 Z7.923
N339 G1 Z-2.077 F300.
N340 Z-11.
N341 X45.663 Y161.442 F700.
N342 X43.06 Y160.47
N343 X40.963 Y158.891
N344 X39.351 Y156.598
N345 X38.428 Y153.738
N346 X38.215 Y151.339
N347 X38.212 Y38.283
N348 X38.358 Y38.212
N349 X158.036
N350 X159.941 Y38.522
N351 X160.699 Y38.993
N352 X161.488 Y40.085
N353 X161.784 Y41.581
N354 X161.788 Y154.739
N355 X161.756 Y155.551
N356 X161.301 Y157.703
N357 X160.533 Y159.174
N358 X159.078 Y160.599
N359 X157.076 Y161.496
N360 X154.64 Y161.788
N361 X48.667 Y161.785
N362 X46.248 Y161.568
N363 Z-1. F1000.
N364 G0 Z50.
N365 X47.473 Y160.605
N366 Z8.076
N367 G1 Z-1.924 F300.
N368 Z-12.
N369 X46.477 Y160.39 F700.
N370 X44.028 Y159.451
N371 X41.95 Y157.876
N372 X40.404 Y155.7
N373 X39.444 Y152.833
N374 X39.215 Y150.327
N375 X39.212 Y39.216
N376 X39.67 Y39.212
N377 X157.478 Y39.217
N378 X158.987 Y39.544
N379 X159.542 Y39.868
N380 X160.443 Y40.984
N381 X160.784 Y42.593
N382 X160.788 Y153.704
N383 X160.743 Y154.718
N384 X160.276 Y156.765
N385 X159.492 Y158.233
N386 X158.226 Y159.494
N387 X156.148 Y160.477
N388 X153.799 Y160.787

```
N389 X49.73
N390 X47.473 Y160.605
N391 Z-2. F1000.
N392 G0 Z50.
N393 X48.599 Y159.621
N394 Z7.845
N395 G1 Z-2.155 F300.
N396 Z-13.
N397 X47.332 Y159.347 F700.
N398 X44.998 Y158.433
N399 X42.938 Y156.862
N400 X41.396 Y154.687
N401 X40.463 Y151.927
N402 X40.214 Y149.316
N403 X40.212 Y40.251
N404 X40.509 Y40.212
N405 X156.418 Y40.216
N406 X158.031 Y40.565
N407 X158.563 Y40.884
N408 X159.449 Y41.997
N409 X159.784 Y43.604
N410 X159.788 Y152.772
N411 X159.725 Y153.884
N412 X159.217 Y155.923
N413 X158.09 Y157.725
N414 X156.536 Y158.924
N415 X155.219 Y159.457
N416 X152.488 Y159.788
N417 X50.786
N418 X48.599 Y159.621
N419 Z-3. F1000.
N420 G0 Z50.
N421 X49.76 Y158.645
N422 Z8.065
N423 G1 Z-1.935 F300.
N424 Z-14.
N425 X48.216 Y158.311 F700.
N426 X45.968 Y157.415
N427 X43.925 Y155.848
N428 X42.449 Y153.789
N429 X41.483 Y151.023
N430 X41.214 Y148.304
N431 X41.212 Y41.285
N432 X41.349 Y41.212
N433 X155.356 Y41.214
N434 X157.071 Y41.585
N435 X157.584 Y41.9
N436 X158.456 Y43.01
N437 X158.784 Y44.615
N438 X158.788 Y151.737
N439 X158.717 Y152.95
N440 X158.189 Y154.984
N441 X157.036 Y156.781
N442 X155.454 Y157.973
N443 X154.289 Y158.438
N444 X151.649 Y158.788
N445 X51.839
N446 X49.76 Y158.645
N447 Z-4. F1000.
N448 G0 Z50.
N449 X50.969 Y157.679
N450 Z7.756
N451 G1 Z-2.244 F300.
N452 Z-15.
N453 X49.122 Y157.279 F700.
N454 X47.248 Y156.567
N455 X45.038 Y154.963
N456 X43.442 Y152.776
N457 X42.527 Y150.225
N458 X42.214 Y147.293
N459 X42.212 Y42.218
N460 X42.661 Y42.212
N461 X154.297
N462 X155.532 Y42.377
N463 X156.767 Y43.054
N464 X157.552 Y44.247
N465 X157.785 Y45.627
N466 X157.786 Y150.804
N467 X157.611 Y152.608
N468 X156.786 Y154.783
N469 X155.437 Y156.333
N470 X153.357 Y157.418
N471 X150.806 Y157.787
N472 X52.892 Y157.788
N473 X50.969 Y157.679
N474 Z-5. F1000.
N475 G0 Z50.
N476 X52.022 Y156.679
N477 Z8.034
N478 G1 Z-1.966 F300.
N479 Z-16.
N480 X50.044 Y156.251 F700.
N481 X48.215 Y155.548
N482 X46.021 Y153.948
N483 X44.496 Y151.879
N484 X43.548 Y149.321
N485 X43.214 Y146.281
N486 X43.212 Y43.253
N487 X43.5 Y43.212
N488 X153.244
```

```
N489 X153.874 Y43.247
N490 X155.424 Y43.786
N491 X156.414 Y44.921
N492 X156.785 Y46.639
N493 X156.788 Y149.77
N494 X156.685 Y151.18
N495 X156.095 Y153.201
N496 X155.089 Y154.723
N497 X153.534 Y155.921
N498 X152.424 Y156.397
N499 X149.498 Y156.788
N500 X53.945
N501 X52.022 Y156.679
N502 Z-6. F1000.
N503 G0 Z50.
N504 X53.034 Y155.67
N505 Z7.761
N506 G1 Z-2.239 F300.
N507 Z-17.
N508 X50.978 Y155.225 F700.
N509 X49.183 Y154.53
N510 X47.005 Y152.933
N511 X45.489 Y150.866
N512 X44.57 Y148.416
N513 X44.213 Y145.27
N514 X44.212 Y44.287
N515 X44.339 Y44.212
N516 X152.191
N517 X153.741 Y44.445
N518 X154.451 Y44.804
N519 X155.42 Y45.934
N520 X155.786 Y47.65
N521 X155.788 Y148.735
N522 X155.661 Y150.345
N523 X155.063 Y152.262
N524 X154.039 Y153.779
N525 X152.456 Y154.972
N526 X151.29 Y155.436
N527 X148.659 Y155.788
N528 X54.998
N529 X53.034 Y155.67
N530 Z-7. F1000.
N531 G0 Z50.
N532 X54.047 Y154.661
N533 Z8.053
N534 G1 Z-1.947 F300.
N535 Z-18.
N536 X51.922 Y154.201 F700.
N537 X50.477 Y153.684
N538 X48.568 Y152.453
N539 X46.752 Y150.321
N540 X45.593 Y147.512
N541 X45.213 Y144.258
N542 X45.212 Y45.22
N543 X45.651 Y45.212
N544 X151.138
N545 X152.799 Y45.469
N546 X153.664 Y45.964
N547 X154.478 Y47.06
N548 X154.786 Y48.662
N549 Y147.802
N550 X154.647 Y149.409
N551 X153.992 Y151.416
N552 X153.215 Y152.578
N553 X151.494 Y153.945
N554 X150.553 Y154.356
N555 X147.813 Y154.786
N556 X56.051 Y154.788
N557 X54.047 Y154.661
N558 Z-8. F1000.
N559 G0 Z50.
N560 X55.06 Y153.652
N561 Z7.78
N562 G1 Z-2.22 F300.
N563 Z-19.
N564 X52.875 Y153.18 F700.
N565 X51.431 Y152.663
N566 X49.395 Y151.302
N567 X47.746 Y149.308
N568 X46.707 Y146.935
N569 X46.33 Y145.114
N570 X46.212 Y143.247
N571 Y46.255
N572 X46.49 Y46.212
N573 X150.085
N574 X151.855 Y46.493
N575 X152.683 Y46.979
N576 X153.483 Y48.073
N577 X153.787 Y49.673
N578 X153.788 Y146.768
N579 X153.619 Y148.573
N580 X152.959 Y150.477
N581 X152.165 Y151.635
N582 X150.412 Y152.995
N583 X148.312 Y153.666
N584 X146.507 Y153.788
N585 X57.104
N586 X55.06 Y153.652
N587 Z-9. F1000.
N588 G0 Z50.
```

N589 X55.291 Y152.577
N590 Z8.046
N591 G1 Z-1.954 F300.
N592 Z-20.
N593 X52.387 Y151.642 F700.
N594 X50.382 Y150.287
N595 X48.74 Y148.295
N596 X47.704 Y145.923
N597 X47.346 Y144.208
N598 X47.217 Y142.339
N599 X47.212 Y47.289
N600 X47.33 Y47.212
N601 X149.032
N602 X150.91 Y47.517
N603 X151.522 Y47.853
N604 X152.38 Y48.858
N605 X152.788 Y50.685
N606 X152.783 Y145.834
N607 X152.603 Y147.637
N608 X151.923 Y149.536
N609 X151.114 Y150.691
N610 X149.456 Y151.97
N611 X147.4 Y152.65
N612 X145.668 Y152.788
N613 X58.157
N614 X55.291 Y152.577
N615 Z-10. F1000.
N616 G0 Z50.
N617 X56.27 Y151.561
N618 Z7.906
N619 G1 Z-2.094 F300.
N620 Z-21.
N621 X53.346 Y150.621 F700.
N622 X51.214 Y149.137
N623 X49.734 Y147.283
N624 X48.736 Y145.02
N625 X48.327 Y143.09
N626 X48.217 Y141.327
N627 X48.212 Y48.222
N628 X48.642 Y48.212
N629 X147.979
N630 X149.965 Y48.54
N631 X150.543 Y48.869
N632 X151.388 Y49.871
N633 X151.788 Y51.696
N634 X151.786 Y144.8
N635 X151.571 Y146.8
N636 X150.845 Y148.689
N637 X150.061 Y149.747
N638 X148.493 Y150.943
N639 X146.472 Y151.631
N640 X144.818 Y151.785
N641 X58.729 Y151.786
N642 X56.27 Y151.561
N643 Z-11. F1000.
N644 G0 Z50.
N645 X57.246 Y150.544
N646 Z8.068
N647 G1 Z-1.932 F300.
N648 Z-22.
N649 X54.314 Y149.603 F700.
N650 X52.213 Y148.126
N651 X50.729 Y146.27
N652 X49.729 Y144.007
N653 X49.339 Y142.184
N654 X49.217 Y140.316
N655 X49.212 Y49.257
N656 X49.481 Y49.212
N657 X146.926
N658 X149.018 Y49.563
N659 X149.875 Y50.157
N660 X150.579 Y51.333
N661 X150.788 Y52.708
N662 Y143.766
N663 X150.553 Y145.864
N664 X149.808 Y147.749
N665 X149.008 Y148.803
N666 X147.415 Y149.994
N667 X145.32 Y150.666
N668 X143.517 Y150.788
N669 X59.79
N670 X57.246 Y150.544
N671 Z-12. F1000.
N672 G0 Z50.
N673 X58.061 Y149.493
N674 Z7.997
N675 G1 Z-2.003 F300.
N676 Z-23.
N677 X55.274 Y148.583 F700.
N678 X53.049 Y146.976
N679 X51.782 Y145.372
N680 X51.055 Y143.783
N681 X50.583 Y142.248
N682 X50.317 Y139.837
N683 X50.342 Y73.135
N684 X50.315 Y50.416
N685 X50.318 Y50.314
N686 X74.57 Y50.342
N687 X146.817 Y50.314
N688 X148.074 Y50.586

```
N689 X148.584 Y50.901
N690 X149.399 Y51.896
N691 X149.683 Y53.083
N692 X149.68 Y107.103
N693 X149.688 Y143.323
N694 X149.551 Y144.726
N695 X148.773 Y146.809
N696 X147.955 Y147.86
N697 X146.71 Y148.818
N698 X145.478 Y149.37
N699 X143.164 Y149.688
N700 X60.384
N701 X58.061 Y149.493
N702 Z-13. F1000.
N703 G0 Z50.
N704 M30
%
```

Appendix B2

G-code of optimum parameters for uniform thickness reduction

```
%
O1991
N1 G90 G54 X0 Y0 Z100
N2 G21 T1 M5
N3 G0 X36.505 Y171.841
N4 G43 Z50. H1
N5 Z9.75
N6 G1 Z-.25 F300.
N7 X33.938 Y171.286 F700.
N8 X32.239 Y170.509
N9 X30.521 Y169.114
N10 X29.222 Y167.299
N11 X28.373 Y165.069
N12 X28.14 Y163.484
N13 X28.034 Y161.005
N14 X27.974 Y40.98
N15 X28.033 Y30.454
N16 X27.981 Y29.318
N17 X28.271 Y28.664
N18 X28.619 Y28.228
N19 X30.555 Y28.033
N20 X155.636 Y27.974
N21 X166.307 Y28.031
N22 X168.043 Y28.1
N23 X169.766 Y28.472
N24 X170.54 Y28.947
N25 X171.451 Y30.064
N26 X171.799 Y31.061
N27 X171.969 Y33.246
N28 X172.026 Y153.271
N29 X171.967 Y163.796
N30 X171.851 Y166.124
N31 X171.426 Y167.874
N32 X170.791 Y169.169
N33 X169.722 Y170.37
N34 X168.095 Y171.348
N35 X166.442 Y171.809
N36 X163.864 Y171.968
N37 X154.191 Y172.024
N38 X38.965 Y171.964
N39 X36.505 Y171.841
N40 Z9.75 F1000.
N41 G0 Z50.
N42 X36.431 Y171.313
N43 Z9.872
N44 G1 Z-.128 F300.
N45 Z-.5
N46 X34.018 Y170.689 F700.
N47 X32.525 Y169.957
N48 X30.74 Y168.445
N49 X29.824 Y167.122
N50 X28.834 Y164.657
N51 X28.525 Y162.748
N52 X28.459 Y59.194
N53 X28.527 Y30.459
N54 X28.461 Y29.524
N55 X28.804 Y28.984
N56 X29.225 Y28.564
N57 X30.475 Y28.527
N58 X136.591 Y28.459
N59 X166.231 Y28.526
N60 X167.656 Y28.63
N61 X169.561 Y29.042
N62 X170.789 Y30.126
N63 X171.324 Y31.367
N64 X171.477 Y33.242
N65 X171.541 Y135.056
N66 X171.473 Y163.791
N67 X171.32 Y166.112
N68 X170.88 Y167.653
N69 X169.775 Y169.46
N70 X168.211 Y170.657
N71 X165.945 Y171.395
N72 X163.473 Y171.474
N73 X136.35 Y171.541
N74 X39.061 Y171.473
N75 X36.431 Y171.313
N76 Z9.5 F1000.
N77 G0 Z50.
N78 X36.967 Y170.815
N79 Z9.709
N80 G1 Z-.291 F300.
N81 Z-.75
N82 X34.798 Y170.346 F700.
N83 X32.528 Y169.344
N84 X31.041 Y167.999
N85 X30.278 Y166.811
```

N86 X29.294 Y164.245
N87 X28.992 Y162.44
N88 X28.938 Y77.509
N89 X28.993 Y30.457
N90 X28.941 Y29.73
N91 X29.385 Y29.11
N92 X30.736 Y28.993
N93 X117.522 Y28.938
N94 X166.497 Y28.993
N95 X168.298 Y29.178
N96 X169.796 Y29.809
N97 X170.646 Y31.016
N98 X171.023 Y32.53
N99 X171.011 Y33.243
N100 X171.062 Y116.741
N101 X171.007 Y163.793
N102 X170.803 Y166.
N103 X169.877 Y168.46
N104 X169.271 Y169.249
N105 X167.862 Y170.172
N106 X165.863 Y170.865
N107 X163.681 Y171.007
N108 X118.994 Y171.062
N109 X39.273 Y171.007
N110 X36.967 Y170.815
N111 Z9.25 F1000.
N112 G0 Z50.
N113 X36.965 Y170.303
N114 Z9.499
N115 G1 Z-.501 F300.
N116 Z-1.
N117 X34.571 Y169.786 F700.
N118 X32.707 Y168.871
N119 X31.426 Y167.673
N120 X30.267 Y165.581
N121 X29.461 Y162.132
N122 X29.459 Y161.006
N123 X29.411 Y95.721
N124 X29.459 Y30.456
N125 X29.42 Y29.936
N126 X29.666 Y29.58
N127 X30.526 Y29.459
N128 X98.423 Y29.411
N129 X166.285 Y29.459
N130 X169.363 Y30.124
N131 X170.021 Y30.881
N132 X170.563 Y32.737
N133 X170.545 Y33.245
N134 X170.589 Y98.529
N135 X170.541 Y163.794
N136 X170.334 Y165.284
N137 X169.95 Y167.145
N138 X169.482 Y168.169
N139 X168.241 Y169.436
N140 X166.43 Y170.169
N141 X163.907 Y170.544
N142 X101.67 Y170.589
N143 X39.485 Y170.541
N144 X36.965 Y170.303
N145 Z9. F1000.
N146 G0 Z50.
N147 X36.239 Y169.737
N148 Z9.258
N149 G1 Z-.742 F300.
N150 Z-1.25
N151 X35.436 Y169.563 F700.
N152 X33.113 Y168.549
N153 X31.692 Y167.219
N154 X31.02 Y166.153
N155 X30.33 Y164.162
N156 X29.924 Y161.005
N157 X29.876 Y114.033
N158 X29.925 Y30.454
N159 X29.901 Y30.142
N160 X30.181 Y29.896
N161 X30.786 Y29.925
N162 X79.286 Y29.876
N163 X166.548 Y29.925
N164 X168.936 Y30.441
N165 X169.652 Y31.21
N166 X170.079 Y33.246
N167 X170.124 Y80.217
N168 X170.075 Y163.796
N169 X169.755 Y166.182
N170 X169.137 Y167.788
N171 X167.912 Y169.058
N172 X166.278 Y169.727
N173 X163.63 Y170.075
N174 X84.383 Y170.124
N175 X39.222 Y170.075
N176 X36.239 Y169.737
N177 Z8.75 F1000.
N178 G0 Z50.
N179 X37.456 Y169.489
N180 Z9.031
N181 G1 Z-.969 F300.
N182 Z-1.5
N183 X35.017 Y168.961 F700.

```
N184 X33.532 Y168.231
N185 X32.074 Y166.892
N186 X31.394 Y165.824
N187 X30.893 Y164.591
N188 X30.565 Y163.087
N189 X30.39 Y161.003
N190 X30.331 Y132.241
N191 X30.391 Y30.453
N192 X30.576 Y30.391
N193 X60.106 Y30.332
N194 X166.337 Y30.391
N195 X168.509 Y30.758
N196 X169.277 Y31.538
N197 X169.614 Y33.248
N198 X169.669 Y62.01
N199 X169.609 Y163.798
N200 X169.44 Y165.603
N201 X168.743 Y167.498
N202 X167.583 Y168.679
N203 X165.762 Y169.411
N204 X163.848 Y169.611
N205 X66.67 Y169.669
N206 X39.436 Y169.61
N207 X37.456 Y169.489
N208 Z8.5 F1000.
N209 G0 Z50.
N210 X37.529 Y169.095
N211 Z8.833
N212 G1 Z-1.167 F300.
N213 Z-1.75
N214 X35.477 Y168.651 F700.
N215 X33.724 Y167.761
N216 X32.46 Y166.567
N217 X31.768 Y165.496
N218 X31.258 Y164.26
N219 X30.83 Y161.61
N220 X30.775 Y150.548
N221 X30.823 Y30.853
N222 X31.141 Y30.82
N223 X41.342 Y30.775
N224 X166.915 Y30.823
N225 X168.083 Y31.075
N226 X168.903 Y31.866
N227 X169.176 Y32.949
N228 X169.225 Y43.702
N229 X169.174 Y164.317
N230 X168.81 Y166.285
N231 X167.847 Y167.816
N232 X166.439 Y168.739
N233 X164.199 Y169.175
N234 X49.481 Y169.225
N235 X38.344 Y169.169
N236 X37.529 Y169.095
N237 Z8.25 F1000.
N238 G0 Z50.
N239 X37.641 Y168.71
N240 Z8.614
N241 G1 Z-1.386 F300.
N242 Z-2.
N243 X35.978 Y168.351 F700.
N244 X34.126 Y167.438
N245 X32.846 Y166.241
N246 X32.142 Y165.168
N247 X31.624 Y163.93
N248 X31.288 Y162.425
N249 X31.18 Y160.867
N250 X31.176 Y31.237
N251 X31.37 Y31.176
N252 X166.185
N253 X167.658 Y31.392
N254 X168.528 Y32.195
N255 X168.819 Y33.383
N256 X168.824 Y163.628
N257 X168.73 Y164.835
N258 X168.057 Y166.736
N259 X166.823 Y168.004
N260 X165.161 Y168.667
N261 X163.52 Y168.824
N262 X39.585
N263 X37.641 Y168.71
N264 Z8. F1000.
N265 G0 Z50.
N266 X37.816 Y168.339
N267 Z8.428
N268 G1 Z-1.572 F300.
N269 Z-2.25
N270 X35.944 Y167.832 F700.
N271 X34.536 Y167.118
N272 X33.232 Y165.915
N273 X32.444 Y164.722
N274 X31.99 Y163.6
N275 X31.537 Y160.535
N276 X31.533 Y31.621
N277 X31.602 Y31.533
N278 X165.943
N279 X167.517 Y31.874
N280 X168.225 Y32.641
N281 X168.467 Y33.818
```

N282 X168.466 Y163.346
N283 X168.113 Y165.52
N284 X167.17 Y167.056
N285 X165.658 Y168.059
N286 X163.288 Y168.467
N287 X39.826
N288 X37.816 Y168.339
N289 Z7.75 F1000.
N290 G0 Z50.
N291 X38.723 Y168.024
N292 Z8.21
N293 G1 Z-1.79 F300.
N294 Z-2.5
N295 X36.402 Y167.521 F700.
N296 X34.955 Y166.799
N297 X33.499 Y165.461
N298 X32.816 Y164.393
N299 X32.355 Y163.27
N300 X31.893 Y160.203
N301 X31.89 Y31.903
N302 X32.307 Y31.89
N303 X165.702
N304 X167.092 Y32.191
N305 X167.853 Y32.97
N306 X168.109 Y34.15
N307 X168.11 Y162.962
N308 X167.763 Y165.137
N309 X166.759 Y166.762
N310 X165.34 Y167.683
N311 X163.044 Y168.107
N312 X40.068 Y168.11
N313 X38.723 Y168.024
N314 Z7.5 F1000.
N315 G0 Z50.
N316 X38.899 Y167.652
N317 Z7.982
N318 G1 Z-2.018 F300.
N319 Z-2.75
N320 X36.858 Y167.211 F700.
N321 X35.143 Y166.328
N322 X33.88 Y165.134
N323 X32.721 Y162.94
N324 X32.25 Y159.871
N325 X32.247 Y32.287
N326 X32.538 Y32.247
N327 X165.461
N328 X166.667 Y32.508
N329 X167.478 Y33.298
N330 X167.751 Y34.482
N331 X167.752 Y162.68
N332 X167.642 Y163.884
N333 X166.976 Y165.684
N334 X165.836 Y166.869
N335 X164.055 Y167.609
N336 X162.352 Y167.753
N337 X40.309
N338 X38.899 Y167.652
N339 Z7.25 F1000.
N340 G0 Z50.
N341 X39.07 Y167.28
N342 Z7.775
N343 G1 Z-2.225 F300.
N344 Z-3.
N345 X37.391 Y166.917 F700.
N346 X35.55 Y166.007
N347 X34.266 Y164.809
N348 X33.087 Y162.61
N349 X32.606 Y159.539
N350 X32.604 Y32.671
N351 X32.77 Y32.604
N352 X164.746
N353 X166.243 Y32.826
N354 X167.103 Y33.626
N355 X167.392 Y34.814
N356 X167.395 Y162.296
N357 X167.29 Y163.501
N358 X166.633 Y165.302
N359 X165.401 Y166.571
N360 X163.753 Y167.237
N361 X162.12 Y167.396
N362 X40.548 Y167.395
N363 X39.07 Y167.28
N364 Z7. F1000.
N365 G0 Z50.
N366 X39.235 Y166.906
N367 Z7.701
N368 G1 Z-2.299 F300.
N369 Z-3.25
N370 X37.335 Y166.393 F700.
N371 X35.959 Y165.686
N372 X34.652 Y164.483
N373 X33.938 Y163.408
N374 X33.348 Y161.95
N375 X32.963 Y159.207
N376 X32.961 Y33.055
N377 X33.001 Y32.961
N378 X164.505
N379 X166.098 Y33.306

N380 X166.798 Y34.071
N381 X167.034 Y35.145
N382 X167.037 Y162.014
N383 X166.687 Y164.086
N384 X165.747 Y165.622
N385 X164.24 Y166.626
N386 X161.888 Y167.039
N387 X40.779 Y167.036
N388 X39.235 Y166.906
N389 Z6.75 F1000.
N390 G0 Z50.
N391 X40.179 Y166.599
N392 Z7.54
N393 G1 Z-2.46 F300.
N394 Z-3.5
N395 X37.789 Y166.082 F700.
N396 X36.628 Y165.524
N397 X35.038 Y164.157
N398 X34.245 Y162.962
N399 X33.711 Y161.619
N400 X33.32 Y158.875
N401 X33.318 Y33.337
N402 X33.706 Y33.318
N403 X164.263
N404 X165.674 Y33.624
N405 X166.427 Y34.4
N406 X166.681 Y35.581
N407 X166.682 Y161.425
N408 X166.337 Y163.704
N409 X165.337 Y165.329
N410 X163.922 Y166.251
N411 X161.649 Y166.68
N412 X41.506 Y166.682
N413 X40.179 Y166.599
N414 Z6.5 F1000.
N415 G0 Z50.
N416 X40.345 Y166.226
N417 Z7.313
N418 G1 Z-2.687 F300.
N419 Z-3.75
N420 X38.251 Y165.773 F700.
N421 X36.565 Y164.897
N422 X35.306 Y163.704
N423 X34.614 Y162.633
N424 X34.076 Y161.289
N425 X33.678 Y158.543
N426 X33.676 Y33.721
N427 X33.938 Y33.675
N428 X164.022
N429 X165.251 Y33.941
N430 X166.054 Y34.729
N431 X166.324 Y35.913
N432 X166.322 Y161.347
N433 X166.215 Y162.45
N434 X165.551 Y164.25
N435 X164.418 Y165.437
N436 X162.645 Y166.179
N437 X160.952 Y166.325
N438 X41.748
N439 X40.345 Y166.226
N440 Z6.25 F1000.
N441 G0 Z50.
N442 X40.504 Y165.851
N443 Z7.09
N444 G1 Z-2.91 F300.
N445 Z-4.
N446 X38.807 Y165.484 F700.
N447 X36.974 Y164.576
N448 X35.687 Y163.377
N449 X34.985 Y162.304
N450 X34.412 Y160.85
N451 X34.036 Y158.211
N452 X34.033 Y34.105
N453 X34.169 Y34.033
N454 X163.8 Y34.037
N455 X164.828 Y34.259
N456 X165.679 Y35.057
N457 X165.965 Y36.244
N458 X165.967 Y160.759
N459 X165.86 Y162.066
N460 X165.208 Y163.869
N461 X164.088 Y165.059
N462 X162.346 Y165.807
N463 X160.721 Y165.967
N464 X41.985
N465 X40.504 Y165.851
N466 Z6. F1000.
N467 G0 Z50.
N468 X40.658 Y165.475
N469 Z6.897
N470 G1 Z-3.103 F300.
N471 Z-4.25
N472 X38.728 Y164.955 F700.
N473 X36.831 Y163.829
N474 X35.36 Y161.976
N475 X34.774 Y160.519
N476 X34.393 Y157.879
N477 X34.39 Y34.489

```
N478 X34.401 Y34.39
N479 X163.066
N480 X164.679 Y34.738
N481 X165.37 Y35.502
N482 X165.607 Y36.576
N483 Y160.681
N484 X165.262 Y162.653
N485 X164.246 Y164.274
N486 X162.822 Y165.194
N487 X160.487 Y165.61
N488 X42.219 Y165.608
N489 X40.658 Y165.475
N490 Z5.75 F1000.
N491 G0 Z50.
N492 X41.644 Y165.177
N493 Z6.799
N494 G1 Z-3.201 F300.
N495 Z-4.5
N496 X39.177 Y164.643 F700.
N497 X37.231 Y163.506
N498 X35.734 Y161.648
N499 X35.138 Y160.189
N500 X34.751 Y157.547
N501 X34.747 Y34.771
N502 X35.106 Y34.747
N503 X162.825
N504 X164.256 Y35.056
N505 X165. Y35.831
N506 X165.249 Y36.908
N507 X165.253 Y159.991
N508 X164.912 Y162.27
N509 X163.914 Y163.896
N510 X162.504 Y164.818
N511 X160.25 Y165.252
N512 X42.451 Y165.249
N513 X41.644 Y165.177
N514 Z5.5 F1000.
N515 G0 Z50.
N516 X41.798 Y164.801
N517 Z6.675
N518 G1 Z-3.325 F300.
N519 Z-4.75
N520 X39.678 Y164.342 F700.
N521 X37.99 Y163.466
N522 X36.637 Y162.15
N523 X35.609 Y160.188
N524 X35.242 Y158.676
N525 X35.104 Y156.907
N526 Y35.155
N527 X35.337 Y35.104
N528 X162.583
N529 X163.834 Y35.374
N530 X164.629 Y36.16
N531 X164.896 Y37.343
N532 Y149.58
N533 X164.891 Y160.015
N534 X164.77 Y161.114
N535 X164.127 Y162.816
N536 X163. Y164.005
N537 X161.23 Y164.747
N538 X159.553 Y164.896
N539 X43.186
N540 X41.798 Y164.801
N541 Z5.25 F1000.
N542 G0 Z50.
N543 X41.945 Y164.423
N544 Z6.463
N545 G1 Z-3.537 F300.
N546 Z-5.
N547 X40.227 Y164.052 F700.
N548 X38.398 Y163.145
N549 X37.114 Y161.946
N550 X36.415 Y160.874
N551 X35.839 Y159.419
N552 X35.462 Y156.575
N553 X35.461 Y35.54
N554 X35.569 Y35.461
N555 X162.349 Y35.462
N556 X163.409 Y35.692
N557 X164.254 Y36.488
N558 X164.538 Y37.675
N559 X164.539 Y159.325
N560 X164.419 Y160.731
N561 X163.784 Y162.435
N562 X162.67 Y163.627
N563 X160.936 Y164.377
N564 X159.321 Y164.539
N565 X43.422 Y164.538
N566 X41.945 Y164.423
N567 Z5. F1000.
N568 G0 Z50.
N569 X42.085 Y164.044
N570 Z6.499
N571 G1 Z-3.501 F300.
N572 Z-5.25
N573 X40.121 Y163.517 F700.
N574 X38.256 Y162.398
N575 X36.785 Y160.545
```

N576 X36.201 Y159.088
N577 X35.819 Y156.243
N578 X35.818 Y35.821
N579 X36.274 Y35.818
N580 X161.627
N581 X163.26 Y36.171
N582 X163.879 Y36.816
N583 X164.18 Y38.007
N584 X164.182 Y158.94
N585 X163.836 Y161.219
N586 X162.824 Y162.841
N587 X161.404 Y163.762
N588 X159.085 Y164.181
N589 X43.653 Y164.179
N590 X42.085 Y164.044
N591 Z4.75 F1000.
N592 G0 Z50.
N593 X43.121 Y163.757
N594 Z6.859
N595 G1 Z-3.141 F300.
N596 Z-5.5
N597 X40.566 Y163.204 F700.
N598 X39.221 Y162.504
N599 X37.687 Y161.047
N600 X36.709 Y159.198
N601 X36.306 Y157.576
N602 X36.175 Y155.809
N603 Y36.206
N604 X36.505 Y36.175
N605 X161.386
N606 X162.838 Y36.489
N607 X163.574 Y37.262
N608 X163.822 Y38.339
N609 X163.825 Y158.659
N610 X163.486 Y160.836
N611 X162.49 Y162.462
N612 X161.086 Y163.386
N613 X158.846 Y163.823
N614 X44.384 Y163.825
N615 X43.121 Y163.757
N616 Z4.5 F1000.
N617 G0 Z50.
N618 X43.262 Y163.378
N619 Z6.76
N620 G1 Z-3.24 F300.
N621 Z-5.75
N622 X41.107 Y162.912 F700.
N623 X39.415 Y162.034
N624 X38.062 Y160.719
N625 X37.076 Y158.868
N626 X36.666 Y157.245
N627 X36.533 Y155.477
N628 X36.532 Y36.59
N629 X36.737 Y36.532
N630 X161.145
N631 X162.416 Y36.807
N632 X163.202 Y37.591
N633 X163.468 Y38.774
N634 Y158.274
N635 X163.343 Y159.68
N636 X162.702 Y161.383
N637 X161.578 Y162.572
N638 X160.028 Y163.26
N639 X158.153 Y163.468
N640 X44.625
N641 X43.262 Y163.378
N642 Z4.25 F1000.
N643 G0 Z50.
N644 X43.394 Y162.997
N645 Z6.733
N646 G1 Z-3.267 F300.
N647 Z-6.
N648 X41.071 Y162.393 F700.
N649 X39.283 Y161.29
N650 X37.905 Y159.559
N651 X37.265 Y157.989
N652 X36.89 Y155.145
N653 X36.889 Y36.974
N654 X36.968 Y36.889
N655 X160.909 Y36.89
N656 X161.989 Y37.124
N657 X162.83 Y37.919
N658 X163.11 Y39.105
N659 X163.111 Y157.89
N660 X162.989 Y159.296
N661 X162.359 Y161.002
N662 X161.252 Y162.195
N663 X159.52 Y162.945
N664 X157.921 Y163.111
N665 X45.339
N666 X43.394 Y162.997
N667 Z4. F1000.
N668 G0 Z50.
N669 X43.518 Y162.615
N670 Z6.61
N671 G1 Z-3.39 F300.
N672 Z-6.25
N673 X41.515 Y162.079 F700.

```
N674 X39.682 Y160.967
N675 X38.28 Y159.231
N676 X37.628 Y157.658
N677 X37.248 Y154.813
N678 X37.246 Y37.256
N679 X37.673 Y37.246
N680 X160.189
N681 X161.84 Y37.603
N682 X162.454 Y38.247
N683 X162.753 Y39.437
N684 X162.754 Y157.506
N685 X162.41 Y159.785
N686 X161.401 Y161.408
N687 X159.986 Y162.33
N688 X157.683 Y162.753
N689 X45.087 Y162.75
N690 X43.518 Y162.615
N691 Z3.75 F1000.
N692 G0 Z50.
N693 X44.612 Y162.34
N694 Z6.306
N695 G1 Z-3.694 F300.
N696 Z-6.5
N697 X41.583 Y161.583 F700.
N698 X39.926 Y160.508
N699 X38.585 Y158.786
N700 X37.994 Y157.328
N701 X37.603 Y154.378
N702 Y37.64
N703 X37.905 Y37.603
N704 X159.947
N705 X161.419 Y37.921
N706 X162.147 Y38.692
N707 X162.395 Y39.769
N708 X162.397 Y157.224
N709 X162.381 Y157.732
N710 X161.951 Y159.686
N711 X161.066 Y161.029
N712 X159.668 Y161.954
N713 X157.441 Y162.393
N714 X45.822 Y162.397
N715 X44.612 Y162.34
N716 Z3.5 F1000.
N717 G0 Z50.
N718 X44.738 Y161.958
N719 Z6.231
N720 G1 Z-3.769 F300.
N721 Z-6.75
N722 X42.027 Y161.269 F700.
N723 X40.313 Y160.182
N724 X38.956 Y158.456
N725 X38.329 Y156.889
N726 X37.961 Y154.046
N727 X37.96 Y38.024
N728 X38.136 Y37.96
N729 X159.706
N730 X160.999 Y38.24
N731 X161.775 Y39.021
N732 X162.036 Y40.101
N733 X162.04 Y156.84
N734 X161.896 Y158.344
N735 X161.277 Y159.949
N736 X160.26 Y161.059
N737 X158.618 Y161.829
N738 X156.754 Y162.04
N739 X46.064
N740 X44.738 Y161.958
N741 Z3.25 F1000.
N742 G0 Z50.
N743 X44.853 Y161.574
N744 Z6.173
N745 G1 Z-3.827 F300.
N746 Z-7.
N747 X42.469 Y160.956 F700.
N748 X40.708 Y159.859
N749 X39.328 Y158.128
N750 X38.692 Y156.558
N751 X38.319 Y153.715
N752 X38.317 Y38.408
N753 X38.368 Y38.317
N754 X159.472 Y38.318
N755 X160.569 Y38.556
N756 X161.404 Y39.35
N757 X161.682 Y40.536
N758 X161.683 Y156.456
N759 X161.546 Y157.961
N760 X160.934 Y159.568
N761 X159.828 Y160.761
N762 X158.313 Y161.457
N763 X156.522 Y161.683
N764 X46.299 Y161.682
N765 X44.853 Y161.574
N766 Z3. F1000.
N767 G0 Z50.
N768 X44.959 Y161.187
N769 Z6.111
N770 G1 Z-3.889 F300.
N771 Z-7.25
```

N772 X42.909 Y160.642 F700.
N773 X41.107 Y159.536
N774 X39.702 Y157.799
N775 X39.056 Y156.227
N776 X38.677 Y153.383
N777 X38.674 Y38.69
N778 X39.073 Y38.674
N779 X158.75
N780 X160.419 Y39.035
N781 X161.03 Y39.679
N782 X161.324 Y40.868
N783 X161.326 Y156.072
N784 X161.308 Y156.682
N785 X160.872 Y158.634
N786 X159.979 Y159.975
N787 X158.568 Y160.898
N788 X156.279 Y161.324
N789 X47.019 Y161.326
N790 X44.959 Y161.187
N791 Z2.75 F1000.
N792 G0 Z50.
N793 X45.053 Y160.798
N794 Z6.046
N795 G1 Z-3.954 F300.
N796 Z-7.5
N797 X42.989 Y160.147 F700.
N798 X41.348 Y159.076
N799 X40.077 Y157.471
N800 X39.422 Y155.897
N801 X39.031 Y152.948
N802 Y39.074
N803 X39.304 Y39.031
N804 X158.509
N805 X159.513 Y39.146
N806 X160.492 Y39.767
N807 X160.966 Y41.2
N808 X160.969 Y155.79
N809 X160.821 Y157.293
N810 X160.193 Y158.896
N811 X159.172 Y160.005
N812 X157.512 Y160.772
N813 X155.586 Y160.969
N814 X47.261
N815 X45.053 Y160.798
N816 Z2.5 F1000.
N817 G0 Z50.
N818 X46.23 Y160.541
N819 Z6.768
N820 G1 Z-3.232 F300.
N821 Z-7.75
N822 X43.429 Y159.833 F700.
N823 X41.736 Y158.751
N824 X40.452 Y157.143
N825 X39.756 Y155.458
N826 X39.389 Y152.616
N827 X39.388 Y39.458
N828 X39.536 Y39.388
N829 X158.267
N830 X159.581 Y39.672
N831 X160.348 Y40.452
N832 X160.609 Y41.532
N833 X160.612 Y155.406
N834 X160.47 Y156.91
N835 X159.852 Y158.515
N836 X158.841 Y159.627
N837 X157.208 Y160.399
N838 X155.354 Y160.612
N839 X47.502
N840 X46.23 Y160.541
N841 Z2.25 F1000.
N842 G0 Z50.
N843 X46.326 Y160.153
N844 Z6.769
N845 G1 Z-3.231 F300.
N846 Z-8.
N847 X43.868 Y159.519 F700.
N848 X42.134 Y158.428
N849 X40.757 Y156.697
N850 X40.119 Y155.127
N851 X39.747 Y152.284
N852 X39.745 Y39.843
N853 X39.768 Y39.745
N854 X158.033 Y39.747
N855 X159.149 Y39.988
N856 X159.976 Y40.781
N857 X160.25 Y41.863
N858 X160.255 Y155.022
N859 X160.117 Y156.526
N860 X159.51 Y158.134
N861 X158.51 Y159.248
N862 X156.902 Y160.026
N863 X155.119 Y160.254
N864 X47.738
N865 X46.326 Y160.153
N866 Z2. F1000.
N867 G0 Z50.
N868 X46.409 Y159.762
N869 Z6.769

```
N870 G1 Z-3.231 F300.
N871 Z-8.25
N872 X45.026 Y159.463 F700.
N873 X43.956 Y159.026
N874 X42.384 Y157.97
N875 X41.128 Y156.368
N876 X40.484 Y154.797
N877 X40.105 Y151.952
N878 X40.102 Y40.124
N879 X40.472 Y40.102
N880 X157.312
N881 X158.999 Y40.467
N882 X159.605 Y41.11
N883 X159.896 Y42.298
N884 X159.898 Y154.637
N885 X159.746 Y156.242
N886 X159.165 Y157.753
N887 X158.077 Y158.95
N888 X156.597 Y159.653
N889 X154.874 Y159.894
N890 X48.458 Y159.898
N891 X46.409 Y159.762
N892 Z1.75 F1000.
N893 G0 Z50.
N894 X46.479 Y159.367
N895 Z6.769
N896 G1 Z-3.231 F300.
N897 Z-8.5
N898 X44.394 Y158.712 F700.
N899 X42.771 Y157.645
N900 X41.5 Y156.04
N901 X40.851 Y154.467
N902 X40.459 Y151.518
N903 Y40.509
N904 X40.704 Y40.459
N905 X157.07
N906 X158.58 Y40.786
N907 X159.229 Y41.438
N908 X159.538 Y42.63
N909 X159.541 Y154.356
N910 X159.395 Y155.859
N911 X158.768 Y157.462
N912 X157.751 Y158.573
N913 X156.094 Y159.34
N914 X154.186 Y159.541
N915 X48.7
N916 X46.479 Y159.367
N917 Z1.5 F1000.
N918 G0 Z50.
N919 X47.745 Y159.13
N920 Z6.325
N921 G1 Z-3.675 F300.
N922 Z-8.75
N923 X44.831 Y158.397 F700.
N924 X43.162 Y157.32
N925 X41.875 Y155.712
N926 X41.183 Y154.027
N927 X40.817 Y151.186
N928 X40.816 Y40.893
N929 X40.936 Y40.816
N930 X156.829
N931 X158.162 Y41.105
N932 X158.921 Y41.883
N933 X159.18 Y42.962
N934 X159.184 Y153.971
N935 X159.021 Y155.573
N936 X158.427 Y157.082
N937 X157.422 Y158.195
N938 X155.797 Y158.969
N939 X153.954 Y159.184
N940 X48.941
N941 X47.745 Y159.13
N942 Z1.25 F1000.
N943 G0 Z50.
N944 X47.817 Y158.736
N945 Z6.294
N946 G1 Z-3.706 F300.
N947 Z-9.
N948 X45.27 Y158.083 F700.
N949 X43.559 Y156.997
N950 X42.25 Y155.383
N951 X41.546 Y153.696
N952 X41.176 Y150.854
N953 X41.173 Y41.175
N954 X41.64 Y41.173
N955 X156.595 Y41.175
N956 X157.728 Y41.42
N957 X158.549 Y42.211
N958 X158.822 Y43.294
N959 X158.827 Y153.587
N960 X158.672 Y155.191
N961 X158.085 Y156.701
N962 X157.091 Y157.816
N963 X155.491 Y158.595
N964 X153.716 Y158.825
N965 X49.178 Y158.826
N966 X47.817 Y158.736
N967 Z1. F1000.
```

```
N968 G0 Z50.
N969 X47.873 Y158.339
N970 Z6.273
N971 G1 Z-3.727 F300.
N972 Z-9.25
N973 X46.45 Y158.031 F700.
N974 X45.364 Y157.592
N975 X43.806 Y156.538
N976 X42.625 Y155.055
N977 X41.912 Y153.366
N978 X41.534 Y150.522
N979 X41.53 Y41.559
N980 X41.872 Y41.53
N981 X155.873
N982 X157.578 Y41.899
N983 X158.177 Y42.54
N984 X158.467 Y43.728
N985 X158.47 Y153.305
N986 X158.319 Y154.807
N987 X157.741 Y156.319
N988 X156.759 Y157.437
N989 X155.185 Y158.222
N990 X153.469 Y158.465
N991 X49.897 Y158.47
N992 X47.873 Y158.339
N993 Z.75 F1000.
N994 G0 Z50.
N995 X47.913 Y157.938
N996 Z6.272
N997 G1 Z-3.728 F300.
N998 Z-9.5
N999 X45.8 Y157.277 F700.
N1000 X44.193 Y156.213
N1001 X42.929 Y154.609
N1002 X42.247 Y152.927
N1003 X41.888 Y150.087
N1004 X41.887 Y41.943
N1005 X42.104 Y41.887
N1006 X155.632
N1007 X157.161 Y42.218
N1008 X157.804 Y42.869
N1009 X158.109 Y44.06
N1010 X158.113 Y152.921
N1011 X157.946 Y154.522
N1012 X157.343 Y156.029
N1013 X156.428 Y157.059
N1014 X154.879 Y157.849
N1015 X152.786 Y158.113
N1016 X50.138
N1017 X47.913 Y157.938
N1018 Z.5 F1000.
N1019 G0 Z50.
N1020 X49.217 Y157.709
N1021 Z6.472
N1022 G1 Z-3.528 F300.
N1023 Z-9.75
N1024 X46.234 Y156.961 F700.
N1025 X44.588 Y155.889
N1026 X43.3 Y154.28
N1027 X42.61 Y152.596
N1028 X42.246 Y149.755
N1029 X42.244 Y42.327
N1030 X42.335 Y42.244
N1031 X155.39
N1032 X156.744 Y42.537
N1033 X157.428 Y43.197
N1034 X157.752 Y44.392
N1035 X157.756 Y152.537
N1036 X157.596 Y154.14
N1037 X157.002 Y155.648
N1038 X155.999 Y156.761
N1039 X154.378 Y157.536
N1040 X152.555 Y157.756
N1041 X50.38
N1042 X49.217 Y157.709
N1043 Z.25 F1000.
N1044 G0 Z50.
N1045 X49.333 Y157.325
N1046 Z6.753
N1047 G1 Z-3.247 F300.
N1048 Z-10.
N1049 X47.36 Y156.898 F700.
N1050 X46.339 Y156.472
N1051 X44.842 Y155.432
N1052 X43.673 Y153.952
N1053 X42.974 Y152.266
N1054 X42.604 Y149.424
N1055 X42.601 Y42.609
N1056 X43.04 Y42.601
N1057 X155.156 Y42.603
N1058 X156.308 Y42.852
N1059 X157.122 Y43.642
N1060 X157.394 Y44.724
N1061 X157.399 Y152.153
N1062 X157.243 Y153.756
N1063 X156.66 Y155.267
N1064 X155.672 Y156.383
N1065 X154.08 Y157.165
```

N1066 X152.312 Y157.396
N1067 X50.618 Y157.398
N1068 X49.333 Y157.325
N1069 Z0 F1000.
N1070 G0 Z50.
N1071 X49.356 Y156.92
N1072 Z6.772
N1073 G1 Z-3.228 F300.
N1074 Z-10.25
N1075 X47.875 Y156.6 F700.
N1076 X46.773 Y156.157
N1077 X45.229 Y155.107
N1078 X44.048 Y153.624
N1079 X43.341 Y151.936
N1080 X42.962 Y149.092
N1081 X42.958 Y42.993
N1082 X43.271 Y42.958
N1083 X154.434
N1084 X156.157 Y43.331
N1085 X156.75 Y43.971
N1086 X157.039 Y45.159
N1087 X157.042 Y151.871
N1088 X156.871 Y153.471
N1089 X156.316 Y154.886
N1090 X155.34 Y156.005
N1091 X153.773 Y156.791
N1092 X151.619 Y157.042
N1093 X51.335
N1094 X49.356 Y156.92
N1095 Z-.25 F1000.
N1096 G0 Z50.
N1097 X49.358 Y156.512
N1098 Z6.794
N1099 G1 Z-3.206 F300.
N1100 Z-10.5
N1101 X47.205 Y155.841 F700.
N1102 X45.617 Y154.782
N1103 X44.423 Y153.296
N1104 X43.674 Y151.497
N1105 X43.316 Y148.657
N1106 Y43.377
N1107 X43.503 Y43.316
N1108 X154.193 Y43.315
N1109 X155.741 Y43.65
N1110 X156.378 Y44.3
N1111 X156.684 Y45.594
N1112 X156.685 Y151.487
N1113 X156.52 Y153.088
N1114 X155.918 Y154.595
N1115 X155.008 Y155.626
N1116 X153.466 Y156.418
N1117 X151.387 Y156.685
N1118 X51.577
N1119 X49.358 Y156.512
N1120 Z-.5 F1000.
N1121 G0 Z50.
N1122 X50.621 Y156.273
N1123 Z6.494
N1124 G1 Z-3.506 F300.
N1125 Z-10.75
N1126 X47.659 Y155.53 F700.
N1127 X46.013 Y154.458
N1128 X44.729 Y152.85
N1129 X44.037 Y151.166
N1130 X43.674 Y148.325
N1131 X43.673 Y43.761
N1132 X43.735 Y43.673
N1133 X153.952
N1134 X155.325 Y43.97
N1135 X156.003 Y44.628
N1136 X156.323 Y45.822
N1137 X156.327 Y151.103
N1138 X156.167 Y152.705
N1139 X155.577 Y154.214
N1140 X154.676 Y155.247
N1141 X153.159 Y156.045
N1142 X151.155 Y156.327
N1143 X51.818
N1144 X50.621 Y156.273
N1145 Z-.75 F1000.
N1146 G0 Z50.
N1147 X50.813 Y155.906
N1148 Z6.386
N1149 G1 Z-3.614 F300.
N1150 Z-11.
N1151 X48.177 Y155.233 F700.
N1152 X46.566 Y154.271
N1153 X45.101 Y152.522
N1154 X44.402 Y150.836
N1155 X44.032 Y147.993
N1156 X44.03 Y44.043
N1157 X44.439 Y44.03
N1158 X153.716 Y44.031
N1159 X154.887 Y44.284
N1160 X155.695 Y45.073
N1161 X155.968 Y46.257
N1162 X155.97 Y150.719
N1163 X155.796 Y152.42

N1164 X155.236 Y153.834
N1165 X154.246 Y154.95
N1166 X152.66 Y155.732
N1167 X150.907 Y155.967
N1168 X52.06 Y155.97
N1169 X50.813 Y155.906
N1170 Z-1. F1000.
N1171 G0 Z50.
N1172 X50.854 Y155.505
N1173 Z6.387
N1174 G1 Z-3.613 F300.
N1175 Z-11.25
N1176 X49.303 Y155.169 F700.
N1177 X48.181 Y154.722
N1178 X46.652 Y153.675
N1179 X45.473 Y152.193
N1180 X44.769 Y150.506
N1181 X44.391 Y147.661
N1182 X44.387 Y44.427
N1183 X44.671 Y44.387
N1184 X152.996
N1185 X154.736 Y44.763
N1186 X155.323 Y45.401
N1187 X155.61 Y46.589
N1188 X155.613 Y150.437
N1189 X155.444 Y152.037
N1190 X154.891 Y153.452
N1191 X153.919 Y154.572
N1192 X152.361 Y155.361
N1193 X150.219 Y155.613
N1194 X52.774
N1195 X50.854 Y155.505
N1196 Z-1.25 F1000.
N1197 G0 Z50.
N1198 X50.811 Y155.087
N1199 Z6.444
N1200 G1 Z-3.556 F300.
N1201 Z-11.5
N1202 X48.611 Y154.406 F700.
N1203 X47.043 Y153.351
N1204 X45.847 Y151.864
N1205 X45.101 Y150.066
N1206 X44.744 Y147.226
N1207 Y44.812
N1208 X44.903 Y44.744
N1209 X152.754
N1210 X154.32 Y45.082
N1211 X154.95 Y45.73
N1212 X155.256 Y47.024
N1213 Y150.053
N1214 X155.069 Y151.752
N1215 X154.547 Y153.071
N1216 X153.588 Y154.194
N1217 X152.054 Y154.987
N1218 X149.987 Y155.256
N1219 X53.015
N1220 X50.811 Y155.087
N1221 Z-1.5 F1000.
N1222 G0 Z50.
N1223 X52.015 Y154.835
N1224 Z5.795
N1225 G1 Z-4.205 F300.
N1226 Z-11.75
N1227 X49.117 Y154.106 F700.
N1228 X47.594 Y153.163
N1229 X46.222 Y151.536
N1230 X45.464 Y149.735
N1231 X45.102 Y146.894
N1232 X45.101 Y45.196
N1233 X45.134 Y45.101
N1234 X152.513
N1235 X153.905 Y45.402
N1236 X154.578 Y46.059
N1237 X154.898 Y47.356
N1238 X154.899 Y149.668
N1239 X154.72 Y151.369
N1240 X154.152 Y152.781
N1241 X153.256 Y153.815
N1242 X151.745 Y154.614
N1243 X149.753 Y154.899
N1244 X53.257
N1245 X52.015 Y154.835
N1246 Z-1.75 F1000.
N1247 G0 Z50.
N1248 X52.202 Y154.467
N1249 Z5.561
N1250 G1 Z-4.439 F300.
N1251 Z-12.
N1252 X49.631 Y153.808 F700.
N1253 X47.991 Y152.84
N1254 X46.597 Y151.208
N1255 X45.831 Y149.405
N1256 X45.461 Y146.563
N1257 X45.458 Y45.478
N1258 X45.839 Y45.458
N1259 X152.276 Y45.459
N1260 X153.466 Y45.716
N1261 X154.12 Y46.267

N1262 X154.54 Y47.688
N1263 X154.542 Y149.387
N1264 X154.474 Y150.395
N1265 X154.048 Y151.94
N1266 X153.199 Y153.189
N1267 X151.794 Y154.112
N1268 X149.501 Y154.537
N1269 X53.498 Y154.542
N1270 X52.202 Y154.467
N1271 Z-2. F1000.
N1272 G0 Z50.
N1273 X52.381 Y154.096
N1274 Z6.735
N1275 G1 Z-3.265 F300.
N1276 Z-12.25
N1277 X50.732 Y153.739 F700.
N1278 X49.589 Y153.288
N1279 X48.075 Y152.244
N1280 X46.902 Y150.762
N1281 X46.198 Y149.075
N1282 X45.819 Y146.231
N1283 X45.815 Y45.862
N1284 X46.071 Y45.815
N1285 X151.557
N1286 X153.314 Y46.195
N1287 X153.896 Y46.832
N1288 X154.182 Y48.019
N1289 X154.185 Y149.002
N1290 X154.109 Y150.111
N1291 X153.467 Y152.019
N1292 X152.493 Y153.138
N1293 X150.94 Y153.928
N1294 X148.819 Y154.185
N1295 X54.213
N1296 X52.381 Y154.096
N1297 Z-2.25 F1000.
N1298 G0 Z50.
N1299 X52.288 Y153.667
N1300 Z6.758
N1301 G1 Z-3.242 F300.
N1302 Z-12.5
N1303 X50.065 Y152.981 F700.
N1304 X48.622 Y152.055
N1305 X47.275 Y150.434
N1306 X46.528 Y148.635
N1307 X46.172 Y145.796
N1308 Y46.246
N1309 X46.302 Y46.172
N1310 X151.316
N1311 X152.9 Y46.514
N1312 X153.523 Y47.161
N1313 X153.828 Y48.454
N1314 Y148.618
N1315 X153.753 Y149.728
N1316 X153.123 Y151.637
N1317 X152.165 Y152.76
N1318 X150.641 Y153.556
N1319 X148.588 Y153.828
N1320 X54.454
N1321 X52.288 Y153.667
N1322 Z-2.5 F1000.
N1323 G0 Z50.
N1324 X53.415 Y153.399
N1325 Z6.698
N1326 G1 Z-3.302 F300.
N1327 Z-12.75
N1328 X50.576 Y152.683 F700.
N1329 X49.016 Y151.731
N1330 X47.647 Y150.105
N1331 X46.892 Y148.305
N1332 X46.53 Y145.464
N1333 X46.529 Y46.63
N1334 X46.534 Y46.529
N1335 X151.074
N1336 X152.484 Y46.834
N1337 X153.15 Y47.489
N1338 X153.47 Y48.786
N1339 X153.469 Y148.336
N1340 X153.388 Y149.444
N1341 X152.925 Y150.981
N1342 X151.836 Y152.382
N1343 X150.332 Y153.182
N1344 X148.348 Y153.469
N1345 X54.695 Y153.471
N1346 X53.415 Y153.399
N1347 Z-2.75 F1000.
N1348 G0 Z50.
N1349 X53.597 Y153.029
N1350 Z6.61
N1351 G1 Z-3.39 F300.
N1352 Z-13.
N1353 X51.085 Y152.383 F700.
N1354 X49.421 Y151.41
N1355 X48.021 Y149.777
N1356 X47.259 Y147.975
N1357 X46.889 Y145.132
N1358 X46.886 Y46.912
N1359 X47.239 Y46.886

N1360 X150.836 Y46.887
N1361 X152.044 Y47.148
N1362 X152.776 Y47.818
N1363 X153.112 Y49.118
N1364 X153.114 Y147.952
N1365 X153.032 Y149.06
N1366 X152.581 Y150.6
N1367 X151.504 Y152.003
N1368 X150.023 Y152.809
N1369 X147.651 Y153.114
N1370 X54.937
N1371 X53.597 Y153.029
N1372 Z-3. F1000.
N1373 G0 Z50.
N1374 X53.777 Y152.659
N1375 Z6.485
N1376 G1 Z-3.515 F300.
N1377 Z-13.25
N1378 X52.162 Y152.309 F700.
N1379 X51.02 Y151.858
N1380 X49.651 Y150.948
N1381 X48.397 Y149.449
N1382 X47.627 Y147.645
N1383 X47.248 Y144.801
N1384 X47.243 Y47.296
N1385 X47.47 Y47.243
N1386 X150.118
N1387 X151.597 Y47.46
N1388 X152.317 Y48.025
N1389 X152.754 Y49.45
N1390 X152.757 Y147.568
N1391 X152.667 Y148.776
N1392 X152.235 Y150.218
N1393 X151.171 Y151.625
N1394 X149.519 Y152.495
N1395 X147.42 Y152.757
N1396 X55.651
N1397 X53.777 Y152.659
N1398 Z-3.25 F1000.
N1399 G0 Z50.
N1400 X53.826 Y152.26
N1401 Z6.511
N1402 G1 Z-3.489 F300.
N1403 Z-13.5
N1404 X51.528 Y151.558 F700.
N1405 X50.045 Y150.624
N1406 X48.703 Y149.003
N1407 X47.955 Y147.205
N1408 X47.6 Y144.365
N1409 Y47.68
N1410 X47.702 Y47.6
N1411 X149.877
N1412 X151.095 Y47.761
N1413 X152.023 Y48.473
N1414 X152.4 Y49.885
N1415 Y147.184
N1416 X152.311 Y148.392
N1417 X151.845 Y149.929
N1418 X150.839 Y151.246
N1419 X149.219 Y152.123
N1420 X147.188 Y152.4
N1421 X55.893
N1422 X53.826 Y152.26
N1423 Z-3.5 F1000.
N1424 G0 Z50.
N1425 X54.82 Y151.963
N1426 Z6.132
N1427 G1 Z-3.868 F300.
N1428 Z-13.75
N1429 X52.035 Y151.259 F700.
N1430 X50.447 Y150.301
N1431 X49.076 Y148.675
N1432 X48.32 Y146.874
N1433 X47.958 Y144.034
N1434 X47.957 Y47.962
N1435 X48.406 Y47.957
N1436 X149.636
N1437 X151.06 Y48.265
N1438 X151.787 Y49.036
N1439 X152.042 Y50.217
N1440 X152.041 Y146.902
N1441 X151.945 Y148.109
N1442 X151.501 Y149.547
N1443 X150.411 Y150.949
N1444 X148.918 Y151.751
N1445 X146.943 Y152.04
N1446 X56.134 Y152.043
N1447 X54.82 Y151.963
N1448 Z-3.75 F1000.
N1449 G0 Z50.
N1450 X54.996 Y151.592
N1451 Z5.997
N1452 G1 Z-4.003 F300.
N1453 Z-14.
N1454 X53.097 Y151.181 F700.
N1455 X51.982 Y150.736
N1456 X50.681 Y149.84
N1457 X49.449 Y148.346

N1458 X48.688 Y146.545
N1459 X48.317 Y143.702
N1460 X48.314 Y48.346
N1461 X48.638 Y48.314
N1462 X149.395
N1463 X150.623 Y48.58
N1464 X151.35 Y49.249
N1465 X151.683 Y50.548
N1466 X151.686 Y146.518
N1467 X151.38 Y148.6
N1468 X150.585 Y150.065
N1469 X149.262 Y151.109
N1470 X147.961 Y151.544
N1471 X146.252 Y151.686
N1472 X56.375
N1473 X54.996 Y151.592
N1474 Z-4. F1000.
N1475 G0 Z50.
N1476 X55.166 Y151.22
N1477 Z5.837
N1478 G1 Z-4.163 F300.
N1479 Z-14.25
N1480 X53.594 Y150.88 F700.
N1481 X52.487 Y150.436
N1482 X51.074 Y149.516
N1483 X49.822 Y148.018
N1484 X49.019 Y146.105
N1485 X48.676 Y143.37
N1486 X48.671 Y48.73
N1487 X48.87 Y48.671
N1488 X148.68
N1489 X150.178 Y48.893
N1490 X150.974 Y49.577
N1491 X151.325 Y50.88
N1492 X151.329 Y146.134
N1493 X151.223 Y147.441
N1494 X150.765 Y148.877
N1495 X149.75 Y150.192
N1496 X148.299 Y151.003
N1497 X146.02 Y151.329
N1498 X57.09
N1499 X55.166 Y151.22
N1500 Z-4.25 F1000.
N1501 G0 Z50.
N1502 X55.333 Y150.847
N1503 Z6.327
N1504 G1 Z-3.673 F300.
N1505 Z-14.5
N1506 X54.09 Y150.578 F700.
N1507 X52.991 Y150.136
N1508 X51.473 Y149.193
N1509 X50.197 Y147.689
N1510 X49.382 Y145.774
N1511 X49.028 Y142.935
N1512 Y49.115
N1513 X49.101 Y49.028
N1514 X148.438
N1515 X149.686 Y49.196
N1516 X150.597 Y49.904
N1517 X150.972 Y51.315
N1518 Y145.75
N1519 X150.867 Y147.057
N1520 X150.421 Y148.495
N1521 X149.418 Y149.813
N1522 X147.796 Y150.69
N1523 X145.789 Y150.972
N1524 X57.331
N1525 X55.333 Y150.847
N1526 Z-4.5 F1000.
N1527 G0 Z50.
N1528 X56.216 Y150.526
N1529 Z6.854
N1530 G1 Z-3.146 F300.
N1531 Z-14.75
N1532 X54.038 Y150.055 F700.
N1533 X52.97 Y149.619
N1534 X51.877 Y148.871
N1535 X50.573 Y147.362
N1536 X49.749 Y145.444
N1537 X49.386 Y142.603
N1538 X49.385 Y49.396
N1539 X49.806 Y49.385
N1540 X148.197
N1541 X149.636 Y49.696
N1542 X150.361 Y50.467
N1543 X150.613 Y51.647
N1544 X150.614 Y145.468
N1545 X150.501 Y146.773
N1546 X150.073 Y148.113
N1547 X149.085 Y149.434
N1548 X147.495 Y150.318
N1549 X145.537 Y150.61
N1550 X57.573 Y150.615
N1551 X56.216 Y150.526
N1552 Z-4.75 F1000.
N1553 G0 Z50.
N1554 X56.382 Y150.153
N1555 Z6.728

N1556 G1 Z-3.272 F300.
N1557 Z-15.
N1558 X54.534 Y149.753 F700.
N1559 X53.452 Y149.314
N1560 X52.105 Y148.409
N1561 X50.948 Y147.034
N1562 X50.117 Y145.114
N1563 X49.745 Y142.272
N1564 X49.742 Y49.781
N1565 X50.038 Y49.742
N1566 X147.956
N1567 X149.201 Y50.012
N1568 X149.922 Y50.679
N1569 X150.255 Y51.979
N1570 X150.258 Y145.084
N1571 X149.954 Y147.166
N1572 X149.157 Y148.631
N1573 X147.837 Y149.676
N1574 X146.544 Y150.112
N1575 X144.852 Y150.258
N1576 X57.814
N1577 X56.382 Y150.153
N1578 Z-5. F1000.
N1579 G0 Z50.
N1580 X56.544 Y149.779
N1581 Z6.698
N1582 G1 Z-3.302 F300.
N1583 Z-15.25
N1584 X55.028 Y149.451 F700.
N1585 X53.266 Y148.66
N1586 X51.572 Y147.066
N1587 X50.446 Y144.674
N1588 X50.099 Y141.837
N1589 Y50.165
N1590 X50.269 Y50.099
N1591 X147.241
N1592 X148.759 Y50.325
N1593 X149.549 Y51.008
N1594 X149.897 Y52.311
N1595 X149.901 Y144.699
N1596 X149.778 Y146.105
N1597 X149.34 Y147.443
N1598 X148.593 Y148.509
N1599 X146.885 Y149.572
N1600 X144.621 Y149.901
N1601 X58.529
N1602 X56.544 Y149.779
N1603 Z-5.25 F1000.
N1604 G0 Z50.
N1605 X56.702 Y149.403
N1606 Z6.653
N1607 G1 Z-3.347 F300.
N1608 Z-15.5
N1609 X55.52 Y149.148 F700.
N1610 X53.45 Y148.188
N1611 X51.858 Y146.616
N1612 X50.81 Y144.343
N1613 X50.456 Y141.505
N1614 Y50.549
N1615 X50.501 Y50.456
N1616 X147.
N1617 X148.275 Y50.63
N1618 X149.171 Y51.335
N1619 X149.544 Y52.746
N1620 X149.541 Y144.417
N1621 X149.421 Y145.721
N1622 X148.993 Y147.061
N1623 X148.257 Y148.129
N1624 X146.574 Y149.198
N1625 X144.388 Y149.543
N1626 X58.77 Y149.544
N1627 X56.702 Y149.403
N1628 Z-5.5 F1000.
N1629 G0 Z50.
N1630 X56.464 Y148.943
N1631 Z6.617
N1632 G1 Z-3.383 F300.
N1633 Z-15.75
N1634 X54.423 Y148.194 F700.
N1635 X53.136 Y147.302
N1636 X52.236 Y146.289
N1637 X51.178 Y144.014
N1638 X50.815 Y141.173
N1639 X50.813 Y50.831
N1640 X51.206 Y50.813
N1641 X146.758
N1642 X148.213 Y51.128
N1643 X148.934 Y51.898
N1644 X149.185 Y53.077
N1645 X149.186 Y144.033
N1646 X148.877 Y146.115
N1647 X148.07 Y147.577
N1648 X146.737 Y148.619
N1649 X145.428 Y149.052
N1650 X143.684 Y149.187
N1651 X59.011
N1652 X56.464 Y148.943
N1653 Z-5.75 F1000.

```
N1654 G0 Z50.
N1655 X57.764 Y148.712
N1656 Z6.312
N1657 G1 Z-3.688 F300.
N1658 Z-16.
N1659 X55.973 Y148.325 F700.
N1660 X54.923 Y147.893
N1661 X53.529 Y146.978
N1662 X52.373 Y145.602
N1663 X51.546 Y143.684
N1664 X51.174 Y140.841
N1665 X51.17 Y51.215
N1666 X51.437 Y51.17
N1667 X146.517
N1668 X147.78 Y51.443
N1669 X148.561 Y52.226
N1670 X148.827 Y53.409
N1671 X148.83 Y143.649
N1672 X148.528 Y145.733
N1673 X147.664 Y147.285
N1674 X146.41 Y148.242
N1675 X145.127 Y148.68
N1676 X143.453 Y148.83
N1677 X59.253
N1678 X57.764 Y148.712
N1679 Z-6. F1000.
N1680 G0 Z50.
N1681 X57.917 Y148.336
N1682 Z6.203
N1683 G1 Z-3.797 F300.
N1684 Z-16.25
N1685 X56.463 Y148.022 F700.
N1686 X54.69 Y147.229
N1687 X52.907 Y145.513
N1688 X51.873 Y143.243
N1689 X51.527 Y140.406
N1690 Y51.599
N1691 X51.669 Y51.527
N1692 X145.803
N1693 X147.34 Y51.758
N1694 X148.039 Y52.318
N1695 X148.468 Y53.741
N1696 X148.473 Y143.265
N1697 X148.331 Y144.769
N1698 X147.912 Y146.009
N1699 X147.086 Y147.16
N1700 X145.467 Y148.14
N1701 X143.221 Y148.473
N1702 X59.967
N1703 X57.917 Y148.336
N1704 Z-6.25 F1000.
N1705 G0 Z50.
N1706 X58.064 Y147.959
N1707 Z6.12
N1708 G1 Z-3.88 F300.
N1709 Z-16.5
N1710 X56.951 Y147.718 F700.
N1711 X54.874 Y146.757
N1712 X53.284 Y145.185
N1713 X52.239 Y142.913
N1714 X51.884 Y140.074
N1715 Y51.983
N1716 X51.901 Y51.884
N1717 X145.561
N1718 X147.215 Y52.242
N1719 X147.877 Y52.999
N1720 X148.115 Y54.176
N1721 X148.113 Y142.983
N1722 X147.799 Y145.063
N1723 X146.913 Y146.611
N1724 X145.159 Y147.766
N1725 X142.982 Y148.114
N1726 X60.209 Y148.116
N1727 X58.064 Y147.959
N1728 Z-6.5 F1000.
N1729 G0 Z50.
N1730 X58.103 Y147.558
N1731 Z6.122
N1732 G1 Z-3.878 F300.
N1733 Z-16.75
N1734 X55.897 Y146.774 F700.
N1735 X54.56 Y145.871
N1736 X53.664 Y144.859
N1737 X52.607 Y142.584
N1738 X52.243 Y139.742
N1739 X52.241 Y52.265
N1740 X52.605 Y52.241
N1741 X145.32
N1742 X146.789 Y52.559
N1743 X147.507 Y53.328
N1744 X147.757 Y54.508
N1745 X147.758 Y142.599
N1746 X147.451 Y144.681
N1747 X146.578 Y146.232
N1748 X145.31 Y147.185
N1749 X144.011 Y147.62
N1750 X142.285 Y147.759
N1751 X60.45
```

N1752 X58.103 Y147.558
N1753 Z-6.75 F1000.
N1754 G0 Z50.
N1755 X59.141 Y147.271
N1756 Z6.736
N1757 G1 Z-3.264 F300.
N1758 Z-17.
N1759 X57.412 Y146.897 F700.
N1760 X55.697 Y146.117
N1761 X54.046 Y144.532
N1762 X52.936 Y142.143
N1763 X52.602 Y139.411
N1764 X52.598 Y52.649
N1765 X52.837 Y52.598
N1766 X145.078
N1767 X146.358 Y52.875
N1768 X146.991 Y53.421
N1769 X147.399 Y54.84
N1770 X147.402 Y142.215
N1771 X147.102 Y144.299
N1772 X146.237 Y145.851
N1773 X144.982 Y146.807
N1774 X143.71 Y147.248
N1775 X142.053 Y147.402
N1776 X60.691
N1777 X59.141 Y147.271
N1778 Z-7. F1000.
N1779 G0 Z50.
N1780 X59.283 Y146.892
N1781 Z6.752
N1782 G1 Z-3.248 F300.
N1783 Z-17.25
N1784 X57.899 Y146.593 F700.
N1785 X56.114 Y145.798
N1786 X54.333 Y144.082
N1787 X53.3 Y141.813
N1788 X52.955 Y138.976
N1789 X52.956 Y53.033
N1790 X53.068 Y52.956
N1791 X144.364 Y52.955
N1792 X145.921 Y53.19
N1793 X146.613 Y53.749
N1794 X147.04 Y55.171
N1795 X147.045 Y141.831
N1796 X146.883 Y143.433
N1797 X146.443 Y144.668
N1798 X145.827 Y145.558
N1799 X144.224 Y146.643
N1800 X141.822 Y147.045
N1801 X61.406
N1802 X59.283 Y146.892
N1803 Z-7.25 F1000.
N1804 G0 Z50.
N1805 X59.42 Y146.513
N1806 Z6.756
N1807 G1 Z-3.244 F300.
N1808 Z-17.5
N1809 X58.384 Y146.289 F700.
N1810 X56.298 Y145.326
N1811 X54.71 Y143.755
N1812 X53.668 Y141.483
N1813 X53.313 Y138.644
N1814 Y53.315
N1815 X53.773 Y53.313
N1816 X144.123
N1817 X145.793 Y53.674
N1818 X146.45 Y54.43
N1819 X146.687 Y55.607
N1820 X146.685 Y141.548
N1821 X146.372 Y143.629
N1822 X145.49 Y145.178
N1823 X143.739 Y146.334
N1824 X141.575 Y146.684
N1825 X61.647 Y146.687
N1826 X59.42 Y146.513
N1827 Z-7.5 F1000.
N1828 G0 Z50.
N1829 X59.551 Y146.132
N1830 Z6.751
N1831 G1 Z-3.249 F300.
N1832 Z-17.75
N1833 X57.37 Y145.353 F700.
N1834 X55.99 Y144.441
N1835 X55.092 Y143.428
N1836 X54.036 Y141.153
N1837 X53.671 Y138.312
N1838 X53.67 Y53.699
N1839 X54.005 Y53.67
N1840 X143.881
N1841 X145.365 Y53.991
N1842 X146.08 Y54.759
N1843 X146.329 Y55.938
N1844 X146.33 Y141.165
N1845 X146.025 Y143.247
N1846 X145.149 Y144.797
N1847 X143.882 Y145.751
N1848 X142.595 Y146.189
N1849 X140.885 Y146.33

N1850 X61.889
N1851 X59.551 Y146.132
N1852 Z-7.75 F1000.
N1853 G0 Z50.
N1854 X60.513 Y145.828
N1855 Z6.573
N1856 G1 Z-3.427 F300.
N1857 Z-18.
N1858 X58.853 Y145.469 F700.
N1859 X57.119 Y144.685
N1860 X55.382 Y142.979
N1861 X54.364 Y140.713
N1862 X54.03 Y137.98
N1863 X54.027 Y54.084
N1864 X54.236 Y54.027
N1865 X143.64
N1866 X144.936 Y54.307
N1867 X145.708 Y55.088
N1868 X145.97 Y56.27
N1869 X145.973 Y140.781
N1870 X145.802 Y142.38
N1871 X145.363 Y143.616
N1872 X144.74 Y144.504
N1873 X143.438 Y145.45
N1874 X142.07 Y145.871
N1875 X140.654 Y145.973
N1876 X62.13
N1877 X60.513 Y145.828
N1878 Z-8. F1000.
N1879 G0 Z50.
N1880 X60.643 Y145.447
N1881 Z6.508
N1882 G1 Z-3.492 F300.
N1883 Z-18.25
N1884 X59.336 Y145.164 F700.
N1885 X57.537 Y144.366
N1886 X55.759 Y142.651
N1887 X54.728 Y140.382
N1888 X54.384 Y137.545
N1889 Y54.468
N1890 X54.468 Y54.384
N1891 X142.925
N1892 X144.502 Y54.622
N1893 X145.187 Y55.18
N1894 X145.612 Y56.602
N1895 Y140.498
N1896 X145.433 Y142.096
N1897 X145.016 Y143.234
N1898 X144.402 Y144.124
N1899 X142.806 Y145.211
N1900 X140.422 Y145.616
N1901 X62.844
N1902 X60.643 Y145.447
N1903 Z-8.25 F1000.
N1904 G0 Z50.
N1905 X60.767 Y145.065
N1906 Z6.445
N1907 G1 Z-3.555 F300.
N1908 Z-18.5
N1909 X59.817 Y144.859 F700.
N1910 X57.722 Y143.895
N1911 X56.138 Y142.324
N1912 X55.097 Y140.053
N1913 X54.741 Y137.213
N1914 Y54.75
N1915 X55.173 Y54.741
N1916 X142.684
N1917 X144.369 Y55.105
N1918 X145.023 Y55.861
N1919 X145.259 Y57.037
N1920 X145.257 Y140.114
N1921 X144.945 Y142.195
N1922 X144.061 Y143.743
N1923 X142.494 Y144.837
N1924 X140.168 Y145.254
N1925 X63.086 Y145.259
N1926 X60.767 Y145.065
N1927 Z-8.5 F1000.
N1928 G0 Z50.
N1929 X60.884 Y144.681
N1930 Z6.326
N1931 G1 Z-3.674 F300.
N1932 Z-18.75
N1933 X58.371 Y143.728 F700.
N1934 X57.423 Y143.011
N1935 X56.521 Y141.998
N1936 X55.466 Y139.723
N1937 X55.099 Y136.881
N1938 X55.098 Y55.134
N1939 X55.404 Y55.098
N1940 X142.442
N1941 X143.941 Y55.422
N1942 X144.653 Y56.19
N1943 X144.901 Y57.369
N1944 X144.902 Y139.73
N1945 X144.708 Y141.428
N1946 X144.281 Y142.563
N1947 X143.653 Y143.45

N1948 X142.337 Y144.394
N1949 X141.178 Y144.757
N1950 X139.486 Y144.902
N1951 X63.327
N1952 X60.884 Y144.681
N1953 Z-8.75 F1000.
N1954 G0 Z50.
N1955 X61.877 Y144.384
N1956 Z6.616
N1957 G1 Z-3.384 F300.
N1958 Z-19.
N1959 X60.294 Y144.042 F700.
N1960 X58.849 Y143.422
N1961 X57.658 Y142.551
N1962 X56.808 Y141.548
N1963 X55.791 Y139.282
N1964 X55.458 Y136.55
N1965 X55.455 Y55.518
N1966 X55.636 Y55.455
N1967 X142.201
N1968 X143.514 Y55.739
N1969 X144.281 Y56.519
N1970 X144.542 Y57.7
N1971 X144.545 Y139.346
N1972 X144.351 Y141.044
N1973 X143.934 Y142.181
N1974 X143.314 Y143.07
N1975 X142.01 Y144.016
N1976 X140.658 Y144.44
N1977 X139.254 Y144.545
N1978 X63.569
N1979 X61.877 Y144.384
N1980 Z-9. F1000.
N1981 G0 Z50.
N1982 X61.994 Y144.
N1983 Z6.668
N1984 G1 Z-3.332 F300.
N1985 Z-19.25
N1986 X60.774 Y143.736 F700.
N1987 X58.959 Y142.934
N1988 X57.185 Y141.22
N1989 X56.157 Y138.952
N1990 X55.812 Y136.115
N1991 Y55.902
N1992 X55.868 Y55.812
N1993 X141.487
N1994 X143.082 Y56.055
N1995 X143.761 Y56.611
N1996 X144.184 Y58.032
N1997 Y139.064
N1998 X143.982 Y140.759
N1999 X143.587 Y141.799
N2000 X142.973 Y142.69
N2001 X141.682 Y143.638
N2002 X140.365 Y144.069
N2003 X139.022 Y144.188
N2004 X64.283
N2005 X61.994 Y144.
N2006 Z-9.25 F1000.
N2007 G0 Z50.
N2008 X62.104 Y143.615
N2009 Z6.711
N2010 G1 Z-3.289 F300.
N2011 Z-19.5
N2012 X61.252 Y143.43 F700.
N2013 X59.374 Y142.615
N2014 X58.454 Y141.904
N2015 X57.567 Y140.894
N2016 X56.526 Y138.623
N2017 X56.169 Y135.783
N2018 Y56.184
N2019 X56.572 Y56.169
N2020 X141.245
N2021 X142.943 Y56.536
N2022 X143.597 Y57.291
N2023 X143.831 Y58.467
N2024 X143.83 Y138.68
N2025 X143.626 Y140.375
N2026 X143.2 Y141.511
N2027 X142.566 Y142.397
N2028 X141.235 Y143.337
N2029 X140.063 Y143.697
N2030 X138.318 Y143.831
N2031 X64.524
N2032 X62.104 Y143.615
N2033 Z-9.5 F1000.
N2034 G0 Z50.
N2035 X62.207 Y143.228
N2036 Z6.744
N2037 G1 Z-3.256 F300.
N2038 Z-19.75
N2039 X59.842 Y142.307 F700.
N2040 X58.693 Y141.444
N2041 X57.949 Y140.567
N2042 X56.895 Y138.293
N2043 X56.527 Y135.451
N2044 X56.526 Y56.568
N2045 X56.804 Y56.526

N2046 X141.004
N2047 X142.517 Y56.853
N2048 X143.226 Y57.62
N2049 X143.473 Y58.799
N2050 X143.474 Y138.296
N2051 X143.256 Y140.091
N2052 X142.853 Y141.129
N2053 X142.226 Y142.016
N2054 X140.91 Y142.959
N2055 X139.76 Y143.325
N2056 X138.086 Y143.474
N2057 X64.766
N2058 X62.207 Y143.228
N2059 Z-9.75 F1000.
N2060 G0 Z50.
N2061 X63.234 Y142.938
N2062 Z6.806
N2063 G1 Z-3.194 F300.
N2064 Z-20.
N2065 X61.736 Y142.614 F700.
N2066 X60.33 Y142.003
N2067 X59.084 Y141.12
N2068 X58.234 Y140.117
N2069 X57.218 Y137.851
N2070 X56.886 Y135.12
N2071 X56.883 Y56.952
N2072 X57.036 Y56.883
N2073 X140.762
N2074 X142.092 Y57.171
N2075 X142.855 Y57.949
N2076 X143.114 Y59.131
N2077 X143.117 Y137.912
N2078 X142.899 Y139.707
N2079 X142.463 Y140.84
N2080 X141.885 Y141.636
N2081 X140.582 Y142.582
N2082 X139.246 Y143.009
N2083 X137.854 Y143.117
N2084 X65.007
N2085 X63.234 Y142.938
N2086 Z-10. F1000.
N2087 G0 Z50.
N2088 X63.336 Y142.551
N2089 Z6.729
N2090 G1 Z-3.271 F300.
N2091 Z-20.25
N2092 X62.213 Y142.308 F700.
N2093 X60.381 Y141.503
N2094 X59.485 Y140.797
N2095 X58.612 Y139.79
N2096 X57.586 Y137.522
N2097 X57.24 Y134.684
N2098 Y57.336
N2099 X57.267 Y57.24
N2100 X140.048
N2101 X141.663 Y57.487
N2102 X142.481 Y58.278
N2103 X142.755 Y59.462
N2104 X142.756 Y137.629
N2105 X142.53 Y139.422
N2106 X142.118 Y140.458
N2107 X141.478 Y141.343
N2108 X140.132 Y142.28
N2109 X138.949 Y142.638
N2110 X137.616 Y142.759
N2111 X65.227 Y142.755
N2112 X63.336 Y142.551
N2113 Z-10.25 F1000.
N2114 G0 Z50.
N2115 X63.429 Y142.162
N2116 Z6.716
N2117 G1 Z-3.284 F300.
N2118 Z-20.5
N2119 X62.688 Y142.002 F700.
N2120 X60.839 Y141.192
N2121 X59.728 Y140.338
N2122 X58.995 Y139.464
N2123 X57.956 Y137.192
N2124 X57.597 Y134.352
N2125 Y57.618
N2126 X57.972 Y57.597
N2127 X139.807
N2128 X141.518 Y57.967
N2129 X142.169 Y58.722
N2130 X142.403 Y59.898
N2131 X142.402 Y137.246
N2132 X142.173 Y139.038
N2133 X141.771 Y140.076
N2134 X141.138 Y140.962
N2135 X139.809 Y141.903
N2136 X138.646 Y142.265
N2137 X136.918 Y142.403
N2138 X65.963
N2139 X63.429 Y142.162
N2140 Z-10.5 F1000.
N2141 G0 Z50.
N2142 X63.515 Y141.771
N2143 Z6.601

N2144 G1 Z-3.399 F300.
N2145 Z-20.75
N2146 X61.325 Y140.888 F700.
N2147 X60.118 Y140.013
N2148 X59.283 Y139.014
N2149 X58.282 Y136.751
N2150 X57.955 Y134.021
N2151 X57.954 Y58.002
N2152 X58.203 Y57.954
N2153 X139.565
N2154 X141.093 Y58.285
N2155 X141.799 Y59.051
N2156 X142.045 Y60.23
N2157 X142.046 Y136.862
N2158 X141.803 Y138.753
N2159 X141.381 Y139.787
N2160 X140.726 Y140.669
N2161 X139.481 Y141.525
N2162 X138.342 Y141.893
N2163 X136.687 Y142.046
N2164 X66.205
N2165 X63.515 Y141.771
N2166 Z-10.75 F1000.
N2167 G0 Z50.
N2168 X64.581 Y141.49
N2169 Z6.339
N2170 G1 Z-3.661 F300.
N2171 Z-21.
N2172 X63.179 Y141.187 F700.
N2173 X61.81 Y140.584
N2174 X60.518 Y139.691
N2175 X59.66 Y138.687
N2176 X58.646 Y136.421
N2177 X58.314 Y133.689
N2178 X58.311 Y58.387
N2179 X58.435 Y58.311
N2180 X139.324
N2181 X140.67 Y58.602
N2182 X141.428 Y59.38
N2183 X141.686 Y60.561
N2184 X141.689 Y136.478
N2185 X141.446 Y138.369
N2186 X141.036 Y139.406
N2187 X140.39 Y140.289
N2188 X139.153 Y141.147
N2189 X137.834 Y141.578
N2190 X136.455 Y141.689
N2191 X66.446
N2192 X64.581 Y141.49
N2193 Z-11. F1000.
N2194 G0 Z50.
N2195 X64.665 Y141.099
N2196 Z6.298
N2197 G1 Z-3.702 F300.
N2198 Z-21.25
N2199 X63.653 Y140.88 F700.
N2200 X61.84 Y140.079
N2201 X60.918 Y139.368
N2202 X60.041 Y138.36
N2203 X59.016 Y136.092
N2204 X58.668 Y133.254
N2205 Y58.668
N2206 X59.14
N2207 X139.104 Y58.673
N2208 X140.243 Y58.919
N2209 X141.054 Y59.708
N2210 X141.327 Y60.893
N2211 X141.329 Y136.195
N2212 X141.076 Y138.084
N2213 X140.643 Y139.116
N2214 X140.049 Y139.909
N2215 X138.708 Y140.846
N2216 X137.532 Y141.206
N2217 X136.209 Y141.329
N2218 X66.675
N2219 X64.665 Y141.099
N2220 Z-11.25 F1000.
N2221 G0 Z50.
N2222 X64.74 Y140.706
N2223 Z6.459
N2224 G1 Z-3.541 F300.
N2225 Z-21.5
N2226 X62.324 Y139.774 F700.
N2227 X61.153 Y138.907
N2228 X60.424 Y138.033
N2229 X59.385 Y135.762
N2230 X59.025 Y132.922
N2231 Y59.053
N2232 X59.371 Y59.025
N2233 X138.368
N2234 X140.092 Y59.398
N2235 X140.74 Y60.152
N2236 X140.975 Y61.328
N2237 Y135.812
N2238 X140.719 Y137.7
N2239 X140.3 Y138.735
N2240 X139.638 Y139.615
N2241 X138.38 Y140.468

```
N2242 X137.229 Y140.833
N2243 X135.519 Y140.975
N2244 X67.402
N2245 X64.74 Y140.706
N2246 Z-11.5 F1000.
N2247 G0 Z50.
N2248 X64.806 Y140.311
N2249 Z6.139
N2250 G1 Z-3.861 F300.
N2251 Z-21.75
N2252 X62.808 Y139.47 F700.
N2253 X61.551 Y138.584
N2254 X60.709 Y137.583
N2255 X59.709 Y135.321
N2256 X59.382 Y132.59
N2257 Y59.437
N2258 X59.603 Y59.382
N2259 X138.127
N2260 X139.67 Y59.716
N2261 X140.371 Y60.482
N2262 X140.617 Y61.66
N2263 X140.618 Y135.427
N2264 X140.349 Y137.416
N2265 X139.954 Y138.353
N2266 X139.301 Y139.235
N2267 X138.052 Y140.09
N2268 X136.925 Y140.46
N2269 X135.287 Y140.618
N2270 X67.643
N2271 X64.806 Y140.311
N2272 Z-11.75 F1000.
N2273 G0 Z50.
N2274 X65.917 Y140.04
N2275 Z6.758
N2276 G1 Z-3.242 F300.
N2277 Z-22.
N2278 X64.622 Y139.76 F700.
N2279 X62.845 Y138.966
N2280 X61.951 Y138.261
N2281 X61.087 Y137.256
N2282 X60.075 Y134.991
N2283 X59.742 Y132.259
N2284 X59.739 Y59.821
N2285 X59.835 Y59.739
N2286 X137.885
N2287 X139.248 Y60.034
N2288 X140.002 Y60.811
N2289 X140.258 Y61.992
N2290 X140.261 Y135.043
N2291 X139.992 Y137.031
N2292 X139.607 Y137.971
N2293 X138.96 Y138.855
N2294 X137.608 Y139.79
N2295 X136.419 Y140.147
N2296 X135.055 Y140.261
N2297 X67.885
N2298 X65.917 Y140.04
N2299 Z-12. F1000.
N2300 G0 Z50.
N2301 X65.981 Y139.644
N2302 Z6.78
N2303 G1 Z-3.22 F300.
N2304 Z-22.25
N2305 X65.093 Y139.452 F700.
N2306 X63.328 Y138.661
N2307 X62.189 Y137.801
N2308 X61.47 Y136.929
N2309 X60.445 Y134.662
N2310 X60.096 Y131.824
N2311 Y60.103
N2312 X60.539 Y60.096
N2313 X137.662 Y60.1
N2314 X138.823 Y60.351
N2315 X139.627 Y61.139
N2316 X139.899 Y62.323
N2317 X139.901 Y134.761
N2318 X139.621 Y136.747
N2319 X139.218 Y137.683
N2320 X138.549 Y138.561
N2321 X137.279 Y139.412
N2322 X136.115 Y139.774
N2323 X134.801 Y139.899
N2324 X68.125 Y139.904
N2325 X65.981 Y139.644
N2326 Z-12.25 F1000.
N2327 G0 Z50.
N2328 X66.064 Y139.253
N2329 Z6.798
N2330 G1 Z-3.202 F300.
N2331 Z-22.5
N2332 X65.456 Y139.122 F700.
N2333 X63.791 Y138.352
N2334 X62.585 Y137.477
N2335 X61.853 Y136.603
N2336 X60.836 Y134.439
N2337 X60.492 Y131.807
N2338 X60.504 Y77.584
N2339 X60.493 Y60.495
```

```
N2340 X60.956 Y60.493
N2341 X78.507 Y60.504
N2342 X137.584 Y60.493
N2343 X138.364 Y60.661
N2344 X138.852 Y60.972
N2345 X139.435 Y61.916
N2346 X139.503 Y62.34
N2347 X139.508 Y62.443
N2348 X139.494 Y115.541
N2349 X139.507 Y134.676
N2350 X139.265 Y136.363
N2351 X138.872 Y137.301
N2352 X138.212 Y138.181
N2353 X136.951 Y139.034
N2354 X136.053 Y139.351
N2355 X134.412 Y139.508
N2356 X101.564 Y139.463
N2357 X68.189 Y139.508
N2358 X66.064 Y139.253
N2359 Z-12.5 F1000.
N2360 G0 Z50.
N2361 X66.13 Y138.756
N2362 Z7.054
N2363 G1 Z-2.946 F300.
N2364 Z-22.75
N2365 X64.784 Y138.26 F700.
N2366 X63.252 Y137.315
N2367 X61.942 Y135.701
N2368 X61.383 Y134.148
N2369 X61.034 Y131.822
N2370 X61.05 Y120.776
N2371 X61.035 Y61.124
N2372 X61.093 Y61.035
N2373 X125.498 Y61.05
N2374 X137.218 Y61.027
N2375 X137.754 Y61.041
N2376 X138.537 Y61.415
N2377 X138.966 Y62.326
N2378 X138.973 Y62.43
N2379 X138.949 Y73.372
N2380 X138.966 Y134.661
N2381 X138.773 Y136.154
N2382 X138.416 Y136.998
N2383 X137.819 Y137.789
N2384 X136.515 Y138.633
N2385 X134.74 Y138.965
N2386 X125.208 Y138.949
N2387 X68.52 Y138.966
N2388 X66.13 Y138.756
N2389 Z-12.75 F1000.
N2390 G0 Z50.
N2391 X66.455 Y137.394
N2392 Z8.306
N2393 G1 Z-1.694 F300.
N2394 Z-23.
N2395 X65.05 Y136.885 F700.
N2396 X64.037 Y136.155
N2397 X63.096 Y134.928
N2398 X62.626 Y133.599
N2399 X62.429 Y131.817
N2400 Y62.653
N2401 X62.808 Y62.429
N2402 X137.074
N2403 X137.571 Y62.638
N2404 Y134.666
N2405 X137.431 Y135.761
N2406 X136.866 Y136.765
N2407 X136.09 Y137.313
N2408 X134.447 Y137.571
N2409 X68.222
N2410 X66.455 Y137.394
N2411 Z-13. F1000.
N2412 G0 Z50.
N2413 M30
%
```